

APPLICATION OF SURFACE ELECTROMYOGRAPHY BASED PATTERN RECOGNITION FOR EFFICIENT CONTROL OF UPPER LIMB PROSTHESES

Thesis

Submitted in partial fulfillment of the requirements for the degree of

DOCTOR OF PHILOSOPHY

by

OMKAR S POWAR



DEPARTMENT OF ELECTRICAL AND ELECTRONICS ENGINEERING,

NATIONAL INSTITUTE OF TECHNOLOGY KARNATAKA,

SURATHKAL, MANGALORE -575025

MARCH, 2020

To my dear Lord Swami Koragajja, my strength, and savior

To my mother Shashikala and father Sairam, my inspiration

To my beloved sister Pooja

DECLARATION

by the Ph.D. Research Scholar

I hereby *declare* that the Research Thesis entitled “**Application of Surface Electromyography based Pattern Recognition for Efficient Control of Upper Limb Protheses**” which is being submitted to the **National Institute of Technology Karnataka, Surathkal** in partial fulfillment of the requirement for the award of the Degree of **Doctor of Philosophy in Electrical and Electronics Engineering** is a *bonafide report of the research work carried out by me*. The material contained in this Research Thesis has not been submitted to any University or Institution for the award of any degree.

.....

Omkar S Powar, 158037EE15FV11

Department of Electrical and Electronics Engineering

Place: NITK-Surathkal

Date:

CERTIFICATE

This is to *certify* that the Research Thesis entitled “**Application of Surface Electromyography based Pattern Recognition for Efficient Control of Upper Limb Prostheses**” submitted by **Omkar S Powar** (Register Number: EE15FV11) as the record of the research work carried out by him, is *accepted as the Research Thesis submission* in partial fulfillment of the requirements for the award of degree of **Doctor of Philosophy**.

Dr. Krishnan C. M. C
(Research Guide)

Dr. Shubhanga K. N
(Chairman-DRPC, EEE dept.)

Acknowledgements

First, I would like to thank God, who endowed me with strength, confidence, and determination to finish this Ph.D. research.

It is my pleasure to thank my supervisor *Dr. Krishnan CMC*, for all the direction, opportunities, thoughts, encouragement, patience, advice, and the assistance you have presented me. You have been a source of inspiration that helped me to achieve research goals. The skills of you have helped me to give the best from me and for letting me develop my ideas.

I thank *National Institute of Technology Karnataka (NITK)* for the great experience and knowledge you gave me. I acknowledge your support by granting me the “*Visvesvaraya Ph.D. Scheme for Electronics and IT*” scholarship.

I wish to thank my research progress assessment committee (RPAC) members *Dr. Sharaon Figarado, Dr. Deepu, and Dr. Nagendrappa*, for their constructive feedback and guidance. Thanks also go to *Dr. Vinatha U* and *Dr. Venkatesaperumal*, former HODs for providing the necessary resources in the department to carry out my research. Also, I would like to thank present HOD, *Dr. Shubanga*, for his thought-provoking ideas and suggestions. I also thank all the faculties of the EEE department for their valuable support. I also wish to thank the non-teaching staff of the EEE department, especially, *K.M. Naik, Umesh, Arun Kumar Shetty, Basavarajaiah, Karunakar .B .S, Kasturi Rohidas, Ratnakar, and Gangadhar* for providing necessary support in conducting experimentation. I am truly indebted to *Dr. Panduranga Vittal K, and Dhaneesh* for their support in carrying out my research work.

I wish to acknowledge the support of researchers in the department who provided me their EMG data. I want to thank my colleagues at NITK for their support, valuable inputs, and constant encouragement.

Special appreciations must go to my parents *Sairam Powar* and *Shashikala K* for their moral and emotional support and also pursue higher education. I would also like to thank my sister, *Pooja S*, who was always there to support me and to ease my concentration on research. I am very grateful for the encouragement and support of *Dr. Lakshminarayana Bhatta* and *Dr. Vijay Kumar Guna* from *CIIRC, Jyothy Institute of Technology*, who motivated me to pursue Ph.D. Finally, I would like to thank *Kishore, Lohith, Prassana, Vinay, Anurag, Raghu*, and *Divakar* from *Drone Technologies* for their technical help and guidance throughout my Ph.D. study. I thank my dearest friends *Mr. Kaushikraj* and *Mr. Prasad Kunder*, who was there at all times to support me.

Mangalore, September 2019

Omkar S Powar

Abstract

The main aim of the hand prostheses is to help people restore human hand functions using artificial limbs. Electromyogram (EMG) signals have been used as a control signal, and this control scheme is referred to as Myoelectric Control (MEC). The conventional prostheses use a proportional control scheme based on the amplitude of the EMG signal. However, these schemes cannot achieve more than two degrees of freedom. This limited functionality is the key reason for the rejection of prosthesis by the amputees. If additional degrees of freedom are required, then Pattern Recognition (PR) based MEC offers favorable control.

This research work aims at improving the classification accuracy of surface EMG driven pattern recognition (PR) system. Many factors affect the classification efficiency of PR based MEC. Significant challenges and practical limitations need to be addressed before making the PR scheme commercially available. The goal is to tackle these problems and to provide a solution using novel strategies developed in this research work.

Surface Electromyogram (sEMG) signals are contaminated with a wide variety of noise, and this causes problems in PR. Noise sources such as power-line interference, motion artifact, ambient noise, characteristic instability of the signal, and noise due to electronic and recording equipment could be present in the sEMG signal. Noises can be decreased but cannot be removed totally by using high-quality equipment and intelligent circuits. Conventional filtering methods are commonly used to remove noise. But, if the noise from the recording instrument lies in the usable frequency range, it becomes hard to eliminate noise using conventional filters. In the pre-processing of sEMG signals, the challenge lies in the suppression of noise associated with the measurement and signal conditioning. The first contribution of the thesis is overcoming this limitation by proposing a novel pre-processing method. The method differentiates the original sEMG from noise using higher order statistics such as kurtosis, which is the fourth moment of distribution. The effectiveness of the method is demonstrated in terms of the improvement in PR performance. A significant number of studies have been performed on the various stages

of sEMG-based PR. There have been problems during the clinical implementation of the system even though the previous studies have reported a high classification accuracy of more than 90%. PR has shown great promise in predefined settings in laboratory conditions. The real-time factors which affect the performance have to be taken into consideration for PR to be commercially available. There are various other factors that also affect the performance of the PR system, such as variation in limb position, variation in forearm orientation, variation in electrode position, variation in force level, and change in the characteristics of the sEMG signal. It is becoming crucial to test the PR with these various factors due to the difference between ideal laboratory conditions and practical application of the MEC prostheses. The second contribution of the thesis is to address the robustness aspect of the PR-based control by developing a novel classification scheme that can function well under such changing conditions. Specifically, the focus was given to variations in force levels and wrist orientations. The proposed scheme achieved a significant improvement in classification accuracy when compared to the traditional method. To demonstrate that this research can be translated to clinical applications, study has been conducted on sEMG data set of upper limb amputees. This distinguishes the study from most of the previous studies done on non-amputee subjects.

The findings of this work could improve the quality of life of amputees with better interaction to the outer world.

Contents

Acknowledgement	i
Abstract	iii
List of figures	x
List of tables	xiv
Acronyms and Abbreviations	xv
1 Introduction	1
1.1 Background	1
1.2 History and present day prostheses	2
1.3 Amputation Statistics and Prostheses Rejection	3
1.4 sEMG driven Prosthetic arm	5
1.5 Methods of Prostheses Control	6
1.5.1 Body powered control	6
1.5.2 ON/ OFF Control	7
1.5.3 Proportional control	8
1.5.4 Pattern Recognition Based MEC Control	8
1.6 Challenges with MEC	10
1.7 Research Objectives	11
1.8 Thesis Structure	12
1.9 Summary	14
2 Background and Literature Survey	15
2.1 Introduction	15
2.2 sEMG Signal Generation, Characteristics, Measurements and Signal conditioning	15
2.2.1 sEMG Signal Generation	15
2.2.2 sEMG Characteristics	17

2.2.3	sEMG Measurements	17
2.2.4	sEMG Signal Conditioning	18
2.3	Windowing	18
2.3.1	Disjoint Windowing Scheme	20
2.3.2	Overlapped Windowing Scheme	20
2.3.3	Controller Delay	21
2.4	Feature Extraction	23
2.4.1	Time domain features	23
2.4.2	Frequency domain features	24
2.4.3	Time-Frequency domain features	24
2.5	Dimensionality Reduction	25
2.5.1	Feature projection	26
2.5.2	Feature Selection	27
2.6	Classification Techniques	28
2.7	Literature review on Pre-processing of sEMG signal	29
2.7.1	Noise in sEMG signal	29
2.7.1.1	Inherent Noise in the Electrode	30
2.7.1.2	Movement Artifact	30
2.7.1.3	Electromagnetic Noise	30
2.7.1.4	Cross Talk	30
2.7.1.5	Internal Noise	31
2.7.1.6	Electrocardiographic (ECG) Artifacts	31
2.7.2	Methods for pre-processing	31
2.7.2.1	Autoregressive Modeling (AR) and Autoregressive Moving Average Modeling (ARMA)	31
2.7.2.2	Empirical Mode Decomposition (EMD)	32
2.7.2.3	Cyclostationary Analysis	32
2.7.2.4	Cepstrum Analysis	33
2.7.2.5	Independent Component Analysis (ICA)	33
2.7.2.6	Higher Order Statistics (HOS)	34
2.7.2.7	Wavelet Transform	34
2.8	Literature review on factors affecting the robustness of myoelectric pattern recognition	35
2.8.1	Force Level Variation	36

2.8.2	Wrist Level orientation	37
2.8.3	Electrode Shift	39
2.8.4	Variation in Position of Limb	39
2.9	Summary	40
3	A Novel Pre-processing Procedure for Enhanced Feature Extraction and Characterization of sEMG Signals	41
3.1	Introduction	41
3.2	Material and Data collection	42
3.3	Methodology	44
3.3.1	Conventional filtering methods from the literature	44
3.3.1.1	Weiner filter	44
3.3.1.2	Spectral Subtraction (SS) Approach	45
3.3.1.3	Butterworth Filter	46
3.3.2	Novel method used for pre-processing	47
3.3.2.1	Minimum Entropy Deconvolution (MED)	47
3.3.2.2	Minimum Entropy Deconvolution with convolution ad- justment (MEDA)	49
3.3.3	Feature extraction	50
3.3.4	Dimensionality reduction and Classification	50
3.3.4.1	Greedy stepwise	52
3.3.4.2	Best First	52
3.3.4.3	Linear Forward Selection	53
3.3.4.4	Particle Swarm Optimization	53
3.4	Results and Discussion on the previously used filters from literature .	54
3.4.1	Comparison of filters without dimensionality reduction	54
3.4.2	Comparison of filters with dimensionality reduction	55
3.4.3	Confusion matrix	56
3.4.4	Performance comparison in terms of processing time	58
3.4.5	Discussion	58
3.5	Results and Discussion on novel MEDA filter	58
3.5.1	Impact of MEDA on classification accuracy	60
3.5.1.1	Average confusion matrix for the classification of eight hand movements	63

3.5.2	Performance of MEDA with reduced feature set	66
3.5.3	Effect of window size on accuracy	68
3.5.4	Performance Comparison with other noise reducing method	68
3.6	Summary	69
4	Reducing the Effect of Force Variation and Wrist Orientation on Pattern Recognition of Myoelectric Hand Prostheses Control	71
4.1	Introduction	71
4.1.1	Study on Force Level Variation	72
4.1.2	Study on the changes in Wrist Orientation	74
4.2	Methodology	74
4.2.1	DATASET I: Intact-Limbed Subjects	75
4.2.1.1	Subjects and Data Acquisition	75
4.2.1.2	Experimental Protocol	75
4.2.2	DATASET II: Amputee Subjects	77
4.2.2.1	Subjects and Data Acquisition	77
4.2.2.2	Experimental Protocol	77
4.2.3	System Overview	78
4.2.3.1	Pre-processing, Segmentation, and Feature Extraction	78
4.2.3.2	Dynamic Time Warping (DTW)	79
4.2.4	Data Analysis	83
4.2.4.1	DATASET I: Intact Limbed Subjects	83
4.2.4.2	DATASET II: Amputee Subjects	83
4.2.5	Statistical Test	83
4.3	Results on the study of force level variations	84
4.3.1	Experiments on DATASET I	84
4.3.1.1	Experimental Scheme I : Training the DTW template on the part of the data pertaining to a single force level and testing on all possible force levels	84
4.3.1.2	Experimental Scheme II: Training the DTW template with all three levels of force and testing it with all unseen force levels	87
4.3.2	Experiments on DATASET II	88

4.3.2.1	Experimental Scheme I: Training the DTW template on the part of the data pertaining to a single force level and testing on two unseen force levels	88
4.4	Discussion on the study of force level variations	91
4.4.1	DATASET I: Intact-Limbed Subjects	91
4.4.1.1	Impact of training methods on the performance of PR based myoelectric control under force level variation	92
4.4.2	DATASET II: Amputee Subjects	93
4.5	Results on the study of wrist orientation changes	93
4.5.1	<i>Training Protocol I</i> : Training the DTW template with the data generated at single wrist orientation and testing with the remaining two wrist orientations	94
4.5.2	<i>Training Protocol II</i> : Training the DTW template with the data generated at all wrist orientations and testing with unseen data from all orientations	95
4.5.3	Processing time	96
4.5.4	Confusion Matrix	96
4.6	Discussion on the study of wrist orientation changes	98
4.6.1	Performance of proposed method under different wrist orientation for the two training protocols	98
4.7	Conclusion	99
5	Summary and Future scope	101
5.1	Summary	101
5.2	Future scope	103
A	Definition of variables	105
B	Description of Dimensionality Reduction and Classification Methods	107
B.1	Wrapper based Dimensionality Reduction	107
B.1.1	Greedy Step Wise	107
B.1.2	Best First Search	108
B.1.3	Linear Forward Selection (LFS)	109
B.1.4	Particle Swarm Optimization (PSO)	110

B.2	Classifiers	110
B.2.1	Naive Bayes	110
B.2.2	J-48	111
B.2.3	Linear Discriminant Analysis (LDA)	112
B.2.4	k-Nearest Neighbors (kNN)	113
	Bibliography	115
	Publications based on the thesis	131

List of Figures

1.1	Evolution of Prosthetics (Source: (Finch, 2011, Norton, 2007, Dellon and Matsuoka, 2007))	2
1.2	Different levels of upper limb amputation (Source: (National Academies of Sciences et al., 2017))	4
1.3	sEMG driven prosthetic arm	6
1.4	Body powered prosthetic hand (Source: (Geethanjali, 2016))	6
1.5	ON /OFF control with one electrode (Source: (Roche et al., 2014))	7
1.6	Proportional control with two electrodes (Source: (Roche et al., 2014))	8
1.7	Steps for the sEMG pattern recognition	9
1.8	Outline of the thesis	13
2.1	Myoelectric signal generation (Source: (Brody et al., 1974))	16
2.2	Raw sEMG signal (Source: (Konrad, 2005))	17
2.3	Raw sEMG converted into positive amplitude	19
2.4	Active part of the signal is taken	20
2.5	Windowing using disjoint scheme wherein, W1, W2, and W3 are the analysis window segments. D1, D2 and D3 represent the decision made for W1, W2, and W3 respectively, with a processing time of τ (Source: (Englehart and Hudgins, 2003))	21
2.6	Windowing using overlapped scheme wherein, R1, R2, and R3 are the analysis window segments. D1, D2 and D3 represent the decision made for R1, R2, and R3 respectively, with a processing time of τ (Source: (Englehart and Hudgins, 2003))	22
2.7	Dimensionality reduction techniques	26

3.1	Eight classes of hand movements considered in this research, a) wrist flexion b) wrist radial deviation c) hand close d) tripod e) wrist extension f)wrist ulnar deviation g) cylindrical and h) key grip	43
3.2	Overall process of classification based on proposed MEDA method . .	50
3.3	Column graph of average classification accuracy using four classifiers and three filters	55
3.4	Column graph of average classification accuracy using four classifiers and three filters after dimensionality reduction	56
3.5	Average confusion matrix across seven subjects using a) Weiner filter and J48 classifier b) SS filter and KNN classifier and c) Butterworth and KNN classifier	59
3.6	Noisy sEMG signal before applying MEDA (green colour) and de-noised sEMG signal after applying MEDA (red colour) for eight different movements (a) wrist flexion b) wrist radial deviation c) hand close d) tripod e) wrist extension f)wrist ulnar deviation g) cylindrical and h) key grip) for channel 1 (a) and channel 2 (b)	61
3.7	Bar plot of average classification accuracy across seven subjects for eight upper limb movements using J-48, k-nearest neighbours (KNN), Naives Bayes and Linear Discriminant Analysis (LDA) classifiers with and without MEDA using a window size of 200ms	62
3.8	Confusion matrix showing classwise accuracy for eight classes of hand movements (wrist flexion (FX), wrist radial deviation (WRD), hand close (HC), tripod (TD), wrist extension (EX), wrist ulnar deviation (WUD), cylindrical (CL) and key grip (KG)) for two subjects before and after MEDA using LDA as a classifier	63
3.9	Scatter plot of a pair of sEMG features for different hand movements before and after applying MEDA for Subject 1 and Subject 6	64
3.10	Average classification accuracy across seven subjects using LDA as a classifier after applying MEDA for eight classes of hand movements (wrist flexion (FX), wrist radial deviation (WRD), hand close (HC), tripod (TD), wrist extension (EX), wrist ulnar deviation (WUD), cylindrical (CL) and key grip (KG))	65

3.11	Average classification accuracy after feature reduction using with J-48, k-nearest neighbours (KNN), Naives Bayes and Linear Discriminant Analysis (LDA) classifiers with best first, greedy stepwise, PSO and Linear forward selection search method across seven subjects for eight upper limb movements, after applying MEDA	67
3.12	Average classification accuracy for eight upper limb movement with varying window size using MEDA	68
3.13	Bar plot of average classification accuracy across seven subjects for eight upper limb movements using J-48, k-nearest neighbors (KNN), Naive Bayes and Linear Discriminant Analysis (LDA) classifiers for Butterworth (red) and MEDA (orange) using a window size of 200 ms	69
4.1	Three force levels acquired from single channel sEMG signal for hand close movement	76
4.2	Data collection at three forearm orientations at three force levels at each movement	76
4.3	The overall framework of the suggested PR system	78
4.4	(a) In Euclidean distance, the two time series are not similar. (b) The allignment in time axis is not well; although they have same overall waveforms. (c) After DTW a refined distance measure is calculated. (d) Nonlinear alignment is provided by DTW for the two time series	80
4.5	An example of hand movement recognition. (a) After filtering, the sEMG signal for hand close movement (b) Feature extraction is done by taking the RMS which is represented in continious line (c) Comparison is done with all the templates (dotted line), the system recognizes the hand movement corresponding to the minimum distance. The x axis represnts the time in seconds which is of 5 s duration. The y axis represnts the (a) amplitude of sEMG signal in milli-Volts; which ranges between -0.8 mV and +0.8 mV (b)RMS value of the raw sEMG signal in (a) which ranges between 0 and 0.15.	82
4.6	Average classification accuracy with <i>Scheme I</i> obtained across ten subjects for six hand motions at orientation 1 (a), orientation 2 (b) and orientation 3 (c)	85

4.7	Average confusion matrix with <i>Scheme I</i> obtained across ten subjects for six hand movements (hand close (C1), hand open (C2), wrist extension (C3), wrist flexion (C4), ulnar deviation (C5), and radial deviation (C6)) at orientation 2	86
4.8	Average classification accuracy with <i>Scheme II</i> obtained across ten subjects for six hand motions from three different orientations	87
4.9	Average confusion matrix with <i>Scheme II</i> obtained across ten subjects for six hand movements (hand close (C1), hand open (C2), wrist extension (C3), wrist flexion (C4), ulnar deviation (C5), and radial deviation (C6)) at orientation 2	89
4.10	Average classification accuracy with <i>Training Protocol I</i> obtained across ten subjects for six hand motions	94
4.11	Average classification accuracy with <i>Training Protocol II</i> obtained across ten subjects for six hand motions	95
4.12	(a) Average confusion matrix with <i>Training Protocol II</i> obtained across ten subjects for six hand movements (C1–C6) in percentage and (b) in terms of classified instances.	97

List of Tables

3.1	Time and frequency domain features along with mathematical definition	51
3.2	Average classification accuracy after feature reduction with greedy stepwise search method after applying Butterworth filter	57
3.3	Average classification accuracy after feature reduction with greedy stepwise search method after applying SS filter	57
3.4	Average classification accuracy after feature reduction with greedy stepwise search method after applying Weiner filter	57
3.5	Classification accuracy and standard deviation of seven individual subjects using LDA as a classifier with and without MEDA	62
4.1	Comparison of average classification accuracy for the TD-PSD method and the DTW method for DATASET I	88
4.2	Average classification accuracy (and the standard deviation in %) for nine amputees when trained with single force level and tested with unseen force level for the TD-PSD method and the DTW method with average processing time	90
4.3	Average classification accuracy (%) for ten subjects with <i>Training Protocol II</i> , comparing TD-PSD method with the proposed method . . .	96
4.4	Average processing time (ms) for ten intact subjects for TD-PSD method and DTW method for generating decision	96

Acronyms and Abbreviations

ADC	Analog to Digital Converter
ANN	Artificial Neural Network
ANOVA	Analysis of Variance
AR	Autoregressive
ARIMA	Autoregressive Integrated Moving Average
ARMA	Autoregressive Moving Average
BSS	Blind Source Separation
CWT	Continuous Wavelet Transform
DBI	Davies-Bouldin Index
DOF	Degree-of-Freedom
DR	Dimensionality Reduction
DT	Decision Tree
DTW	Dynamic Time Warping
DWT	Discrete Wavelet Transforms
ECG	Electrocardiography
EEG	Electroencephalography
EMD	Empirical Mode Decomposition
EMG	Electromyography
FAM	Fourier Transform Accumulation
FD	Frequency Domain
FFT	Fast Fourier Transform
FIR	Finite Impulse Response
FLDI	Fishers Linear Discriminant Index
GA	Genetic Algorithm
HMI	Human-Machine Interfacing
HOS	Higher Order Statistics
ICA	Independent Component Analysis
IIR	Infinite Impulse Response
IMF	Intrinsic Mode Function
kNN	k-Nearest-Neighbor
LDA	Linear Discriminant Analysis
MEC	Myoelectric Control

MED	Minimum Entropy Deconvolution
MEDA	Minimum Entropy Deconvolution Adjusted
MLP	Multilayer Perceptron
MU	Motor Unit
OFNDA	Orthogonal Fuzzy Neighborhood Discriminant Analysis
PCA	Principal Components Analysis
PR	Pattern Recognition
PSD	Power Spectral Density
PSO	Particle Swarm Optimization
RMS	Root Mean Square
SCD	Spectral Correlation Density
sEMG	Surface Electromyography
SNR	Signal to Noise Ratio
SOFM	Self-Organizing Feature Map
SS	Spectral Subtraction
SSCA	Strip Spectral Correlation Algorithm
STFT	Short Time Fourier Transform
SVM	Support Vector Machine
TD	Time Domain
TD-PSD	Time-Dependent Power Spectrum Descriptors
TFD	Time-Frequency Domain
WPT	Wavelet Packet Transform
WT	Wavelet Transform

Chapter 1

Introduction

1.1 Background

The artificial device which replaces the missing part of our body is known as prostheses. Such amputation may be due to trauma, diseases, or accidents. Amputation of the limb, in particular, affects the person's ability to interact with the outer world. It is now known for a fact that the development of the thumb of a human gave us the capability of complex maneuvers, giving us an evolutionary advantage over other animals. Statistics show that forty percent of our day-to-day activities can be associated with our hands directly or indirectly (Edeer and Martin, 2011). Losing a hand can create a massive void from a physical viewpoint, and it can have much more devastating consequences psychologically (Bhuvanewar et al., 2007). Due to these reasons, there has been growing interest in the field of artificial limbs for the upper-limb amputees with many companies giving the patient with advanced features. Even though the research in this field is happening for centuries, the solutions still lack their reachability to the needy giving ample scope of improvements in this area of research.

Considering developing economies like India, the cost becomes the prime factor in deciding the use of such products. It is evident that the people whose daily work involves dealing with dangerous machinery are more likely to suffer such ill fate of losing a hand or a limb. Typically such population belongs to the middle class or the lower-middle class who unfortunately cannot afford such high-cost products as a replacement for their hand. Despite this fact, there is very little ongoing research for developing a cost-effective solution to cater to the basic needs of such people.

This chapter provides a necessary background in history and present-day prosthetics. Further, the amputation statistics and the cause for prostheses rejection by the amputees is highlighted. This chapter gives the reader an overview of surface Electromyography (sEMG) driven prosthetic arm. The various methods of control for the prosthetic arm are discussed with emphasis on problems associated with the current prostheses control. The main aim of this chapter is to provide the motivation behind the work and to list the major issues that need to be resolved to enhance the performance of Myoelectric Controller (MEC). The chapter also describes the main objectives of the thesis and gives an overview of how the thesis is structured for better readability.

1.2 History and present day prostheses

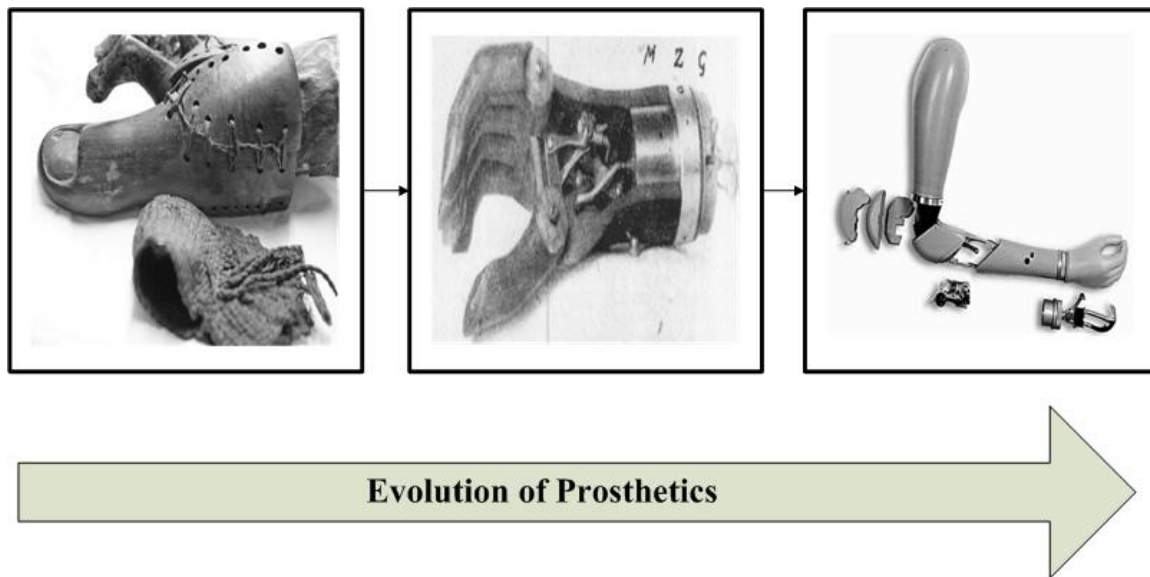


Figure 1.1: Evolution of Prosthetics (Source: (Finch, 2011, Norton, 2007, Dellon and Matsuoka, 2007))

It is mentioned in the Rig Veda that, an iron leg was made for the warrior queen Vishpala. She lost her leg in Khela’s battle; so they gave her a “leg of iron” (Muneer and Pearce, 2016). The early pioneers of prosthetic technology are Egyptians. An ancient Egyptian false toe was found on the female mummy buried near Luxor (Finch, 2011) and is shown in Figure 1.1. The prosthetic limb was made of fiber. In the second Punic war, Roman general who was a right arm amputee had an iron hand to hold his

shield. By the medical discoveries of the Greeks and Romans concerning prosthetics, prostheses during the Renaissance period were generally made of iron, steel, copper and wood (Norton, 2007).

The first myoelectric prosthetic hand was used around 1943, and the system was not portable. The commonly used modern-day prosthetics range from hook to ON/OFF control which uses sEMG signal for control (Dellon and Matsuoka, 2007) as shown in Figure 1.1. To provide amputees with many functions, today's prosthetics are much lighter and user-friendly, made of plastics, aluminum, and composite materials.

1.3 Amputation Statistics and Prostheses Rejection

To get a better understanding, the Ministry of Statistics and Programme Implementation has provided the statistics on disabled people in India based on the census from 2011 (Division, 2016). It showed that around 2.21% of the total population constituted of disabled people. The persons with disability in the movement are about 20% of the disabled community. Lower limb amputation cases are more than the upper limb (Division, 2016). In India, it has been assessed that for thousand populations there are 0.62 amputees (Sahu et al., 2016). The primary cause of amputation in a developing country like India is diabetes. Around 35 million people are affected by diabetes. Approximately forty to seventy percent of limb amputation occurs due to diabetes. The majority is from Southern parts of the country. The primary lower limb amputation is due to a foot ulcer, which is caused by infection and improper foot care. Males are most commonly affected when compared to women (Viswanathan and Kumpatla, 2011). Losing an arm is particularly difficult because it performs most of the complex activities and interaction with the outside environment is done by it (Division, 2016).

The below-elbow amputation occurs mainly through the long bones of the radius and ulna (National Academies of Sciences et al., 2017). There are four major categories of upper limb amputation, as shown in Fig 1.2. They are, 1) wrist disarticulation, 2) transradial amputation, 3) transhumeral amputation, and 4) shoulder disarticulation. The focus of this work is on below elbow amputation, i.e. (transra-

dial and wrist disarticulation) and develop efficient myoelectric control strategies for prosthesis devices for such amputees, thereby improving the quality of life of such individuals.

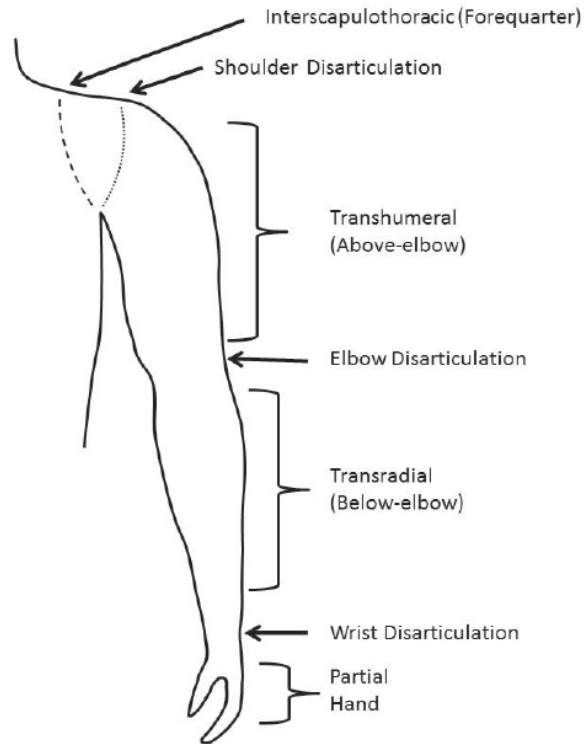


Figure 1.2: Different levels of upper limb amputation (Source: (National Academies of Sciences et al., 2017))

A survey was conducted on 71 traumatic upper-limb amputees, to measure the success of prosthetics, which was based on patient satisfaction, prosthetic usage, and activity level. The study was conducted at Kasturba Medical College, India. Among the 71 traumatic upper-limb amputees, significant causes of amputation were occupation and traffic accidents. The age group was around 40 (plus or minus 11.7) years. All the amputees were using a body-powered prosthesis (subsection 1.5.1), which is the most commonly used prosthesis in India. The primary causes for rejection were found to be a mechanical failure, stump pain, discomfort, weight and cost of replacement and repair of prosthetics (Bhaskaranand et al., 2003).

Another survey of 60 patients was carried out in NGO limb-fitting center (Mobility India, Bangalore) to examine the satisfaction level and functionality of upper limb prostheses for Indian users (Nagaraja et al., 2016). The age group was around 15-

54 years. The most common causes of amputation were either occupational or road traffic accidents, which accounted for about 85%. The remaining was congenital amputation. The amputees used cosmetic, body-powered, and myoelectric prostheses. The minimum duration of usage of prosthetics was around three months. Among the prostheses users, 93% used cosmetic and body-powered, and 90% of them used the prosthesis for less than six hours per day due to the heavyweight prosthetic arm design. In the findings of the survey, it was noted that prosthetic users preferred function, comfort, and durability over their appearance and usability (Nagaraja et al., 2016). From the survey, it has been concluded that the currently available prostheses are not providing the amputees with the required functionality, which is the vital requirement for daily prosthetic use. Secondly, the study recommends to bring down the weight of the device with fewer components.

1.4 sEMG driven Prosthetic arm

Electromyography is the process of recording and analyzing the electrical activity produced by the contraction of the muscles, and the signal is known as Electromyogram (EMG)(Ahmad Nasrul and Mohd Hanafi, 2009). They are useful electrophysiological signals which are non-stationary, non-linear, and highly complex with large variations that carry the distinct signature of voluntary intent of central nervous system (Khushaba et al., 2009b). EMG signals are measured by electrodes that are placed on the target muscles using needle electrode (invasive method) or surface electrode (non-invasive method), and since the use of needle electrode involves medical skill and can cause pain and discomfort to the subject (Phinyomark et al., 2012b), surface electrodes have been used in this work. Surface EMG (sEMG) finds its application in the field of electric wheelchair control, determination of muscle fatigue and muscle contraction, cursor control, biomechanics, ergonomics, diagnosis of neuromuscular disorder and prosthetics control (Phinyomark et al., 2012c, Farina et al., 2017). In this thesis, the sEMG is used in the identification of hand motion commands for the control of upper limb prostheses.

sEMG signals, when used as the control signal for prosthetic devices it is referred to as myoelectric control (MEC). MEC convey the commands given by the sEMG signals to the prosthesis in an appropriate manner. Amputees can generate varying sEMG signal patterns during different levels of static muscle contraction or dynamic

limb motion. They are comparable to that of healthy subjects (Herberts et al., 1973, Su et al., 2007). The pattern generated can be used in controlling the prosthetic hand with a machine learning framework. The block diagram of sEMG driven prosthetic arm is shown in Figure 1.3.

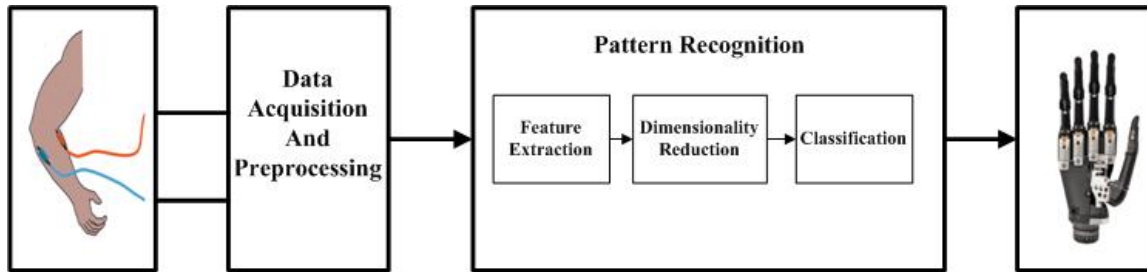


Figure 1.3: sEMG driven prosthetic arm

The work involves the analysis of sEMG signals for the classification of patterns generated for different movements to control prostheses. The main aim of the work is to assist upper limb amputees in efficiently controlling the prosthetic arm. The arm acts as an aid and helps the amputees in interacting with the outer world with limited efforts. The main problem is to control the prostheses with high accuracy, less delay, and in an intuitive manner for different patterns of sEMG signals.

1.5 Methods of Prostheses Control

1.5.1 Body powered control



Figure 1.4: Body powered prosthetic hand (Source: (Geethanjali, 2016))

The body-powered prostheses use muscle energy to operate a cable link. These

are the most widely used prosthetic devices owing to easier maintenance and lower cost. The main disadvantage is the significant effort involved in getting only a single degree of freedom. These generally consist of a hook, which has less weight, better gripping, less maintenance, and excellent durability and is made up of materials like stainless steel and aluminum. Nowadays, the hooks are replaced by a cosmetic hand (Geethanjali, 2016).

1.5.2 ON/ OFF Control

This control scheme was developed at the end of world war II by Reinhold (Weihe, 1999); wherein sEMG signals were used from one or two muscle groups to control the prosthesis. This is a simple control mode with immense popularity. In this control mode, a function of prostheses (e.g., movement with constant speed in two directions) is turned ON or OFF (Fougner et al., 2012). The most straightforward ON-OFF control is based on a threshold of sEMG.

If the sEMG is sensed using a single electrode, an upper and lower threshold will be used to monitor hand open (ON), or hand close (OFF) commands respectively. The same technique is deployed, even when two electrodes are used to measure sEMG signal from two muscle groups, namely flexors and extensors (Battye et al., 1955, Popov, 1965). The main disadvantage of this control is that it is sequential, and the classes of movements generated are limited (Roche et al., 2014).

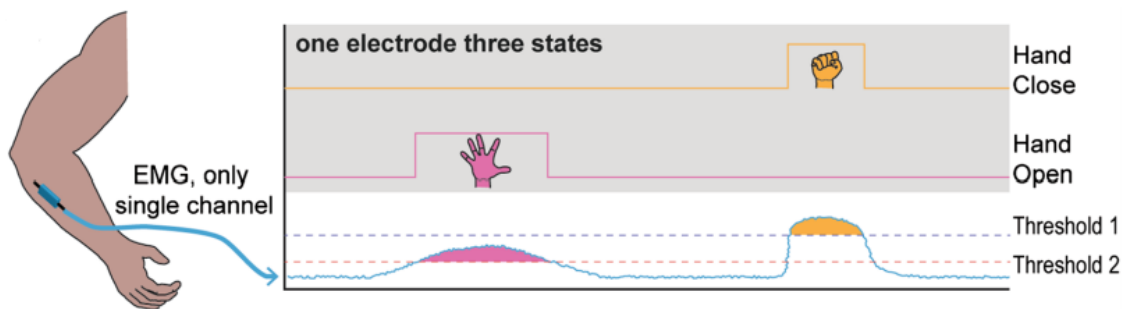


Figure 1.5: ON /OFF control with one electrode (Source: (Roche et al., 2014))

1.5.3 Proportional control

In this type of control, the user can control at least one mechanical parameter, such as force, position, etc., within a finite, useful, and substantially continuous interval by varying his/her control input within a corresponding continuous interval. Here a single channel of sEMG is assigned with only one class of motion (Fougner et al., 2012).

To achieve hand open/ close; if the velocity or force of the prosthetic hand is varied continuously and proportionally to the recorded sEMG signal, then it is proportional control. In this scheme, the voltage applied to the motor of prostheses is proportional to the intensity of sEMG signal (Fougner et al., 2012). The main disadvantage here is the lack of a multifunctional control, with less degree of freedom (Roche et al., 2014).

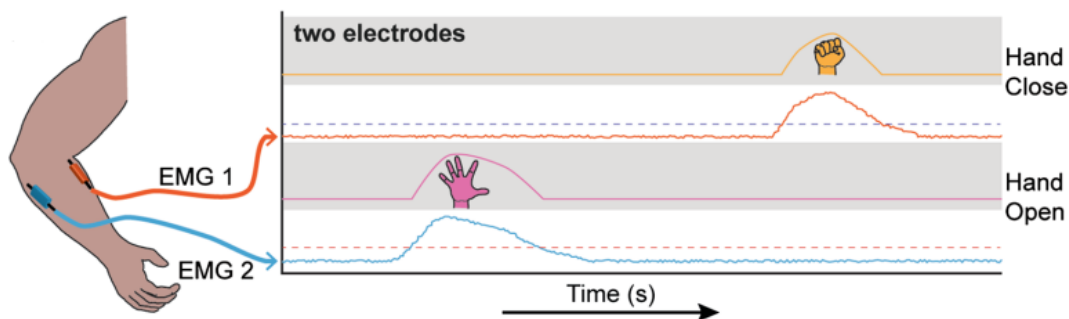


Figure 1.6: Proportional control with two electrodes (Source: (Roche et al., 2014))

1.5.4 Pattern Recognition Based MEC Control

This method was introduced around 1970 for multifunctional control, where the previously discussed methods have limited scope. In 1993, Hudgins et al. (1993) showed that a more refined interpretation of the content of the sEMG signal could be achieved, setting the basis for pattern recognition control (Fougner et al., 2012). For a given electrode location, features which help distinguish different movements are extracted from sEMG signals for a specified duration. Based on the values of these extracted features, a pattern recognition algorithm helps classify various movement commands for the prostheses. These control algorithms have the potential for achieving higher degrees of Freedom (DOF) when compared to the traditional control

schemes (Hargrove et al., 2010). The steps involved in sEMG pattern recognition system is shown in Figure 1.7. The three main stages of classification of sEMG signals are feature extraction, dimensionality reduction, and classification.

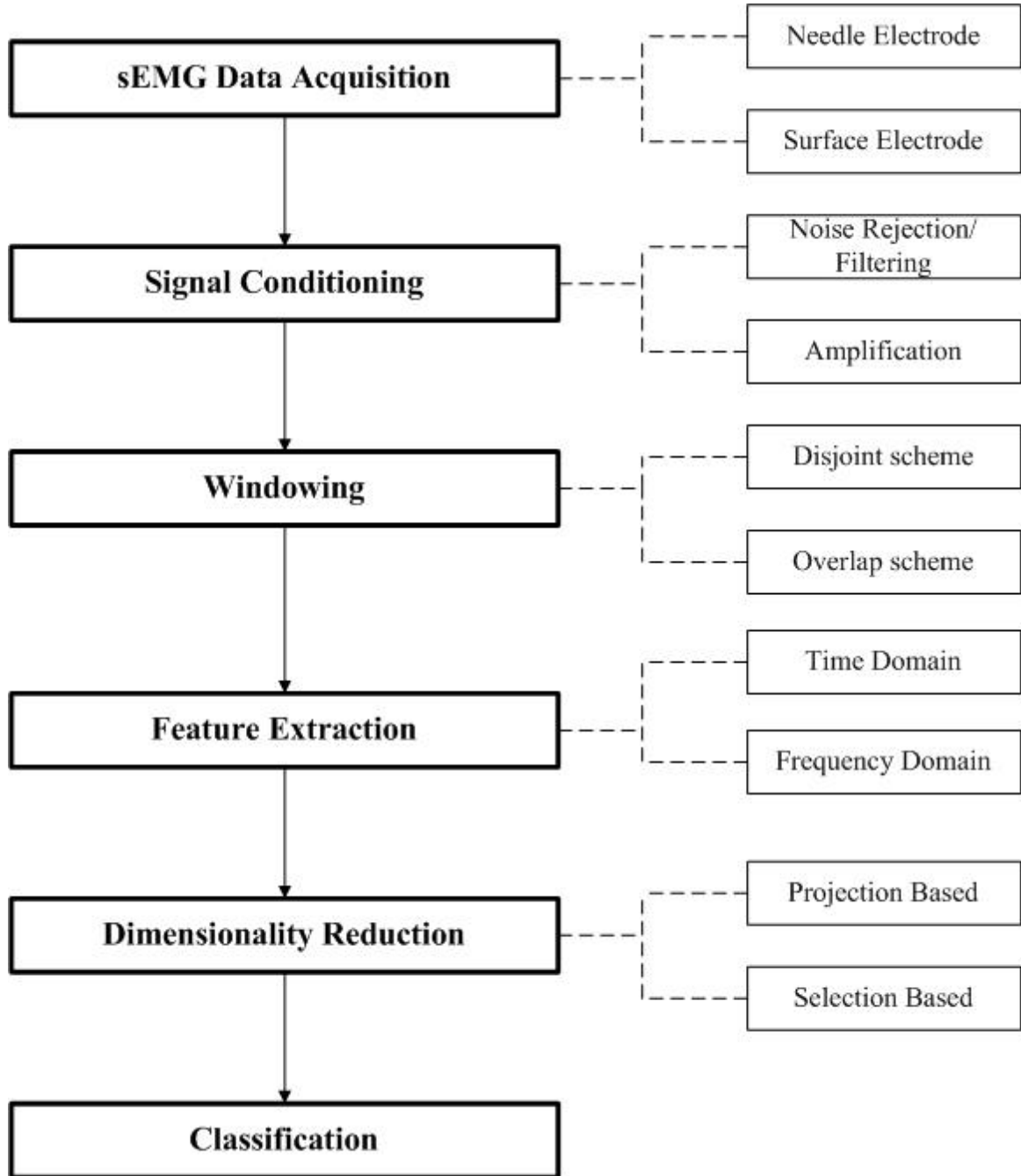


Figure 1.7: Steps for the sEMG pattern recognition

Feature extraction highlights the relevant structures which are hidden in the data

stream and removes the interferences and irrelevant sEMG signals (Phinyomark et al., 2012a). The features extracted may be in the time domain, frequency domain, or time-frequency domain. The obtained features should have maximum class separability, robustness, and low computational complexity (Phinyomark et al., 2009d). Dimensionality reduction aims to select a subset of features to reduce feature set dimensionality, which is achieved by removing irrelevant and redundant features. This reduces the computational complexity and results in better generalization for the classifier (Khushaba et al., 2008). The classifier generates the control command by mapping the extracted features to the target class. Finally, the control algorithm takes the command from the classifier to control the actuators.

1.6 Challenges with MEC

In MEC of upper limb prostheses, the two significant challenges lie in (i) pre-processing the sEMG signal for better pattern recognition, and (ii) improving the robustness of the pattern recognition algorithm in the presence of various factors such as varying force levels of the muscles, the change in orientation of the wrist, etc. These two factors are elaborated in the following paragraphs.

In the case of sEMG signals, the extracted signal will not have the same waveform as the source due to contamination with various noise sources. If the conventional filters are used, they attenuate the noise by removing some of the important information present in the signal. This affects the accuracy with which the sEMG signal is classified. In practice, pre-processing is a challenging issue that should be more carefully investigated. To achieve good performance of the MEC system, selection of filters becomes essential. The main challenges in pre-processing sEMG signal are the limited tools that can be used to minimize the noise such as power line interface, electrode noise, broadband noise from the instruments, motion artifacts, white Gaussian noise, etc., and to enhance the feature with the recovery of the signal without much loss of information.

PR of sEMG signals have been used to control prosthetic devices with the aid of advanced signal processing methods. Though high classification accuracy of around 98% has been reported in the literature, the practical deployment of the prostheses has not taken place. This is due to the gap between research and clinical study. PR has shown great promise in predefined settings in laboratory conditions. For PR to

be commercially available, real-time factors that affect the performance have to be taken into consideration. Many of the real-life aspects, such as wrist orientation, force variation, electrode shift, limb position, etc., degrade the performance of PR. Since the studies conducted in a laboratory environment have a lesser possibility of occurrence of such issues, the classification accuracy thus reported may not be conceived in practice. Hence the PR scheme has to be designed by considering these factors.

This research work aims to overcome such challenges and build an efficient and practical MEC for the upper limb prosthesis. In addition to these, it was observed during the research that most of the previous work analyzed sEMG signals from healthy subjects rather than the amputees. This research has also worked towards bridging this gap by adopting methods that can be used for amputees as well.

In summary, the sEMG driven prostheses require accuracy, speed, and robustness of PR. This can only be addressed with the help of novel pre-processing methods, efficient machine learning schemes which are computationally cheap, thereby developing a MEC which can be used in practice.

1.7 Research Objectives

After an extensive literature review and having a deeper understanding of the challenges involved in MEC, the following research objectives are formed towards developing a sEMG driven PR system which is accurate and efficient with respect to the state-of-the-art techniques. The main objectives identified are listed below.

1. The main aim is to improve the classification accuracy of the sEMG based pattern recognition system. This is approached by a) developing novel pre-processing method since the main challenge lies in pre-processing of sEMG signal is the limited tools that can be used to minimize the noise, and b) investigating on dimensionality reduction methods, since the success of pattern recognition depends on the quality of features selected, there is a need to produce a subset of features that bring about a better separability between movement classes. Feature projection or reduction techniques help in improving the real-time performance of the classifier by selecting a fewer set of features, making it convenient for the prostheses user.

2. To improve the practical robustness of sEMG pattern recognition system. The performance of sEMG pattern recognition system decreases due to various factors such as electrode shift, force variation, limb position variation, and changes in the wrist orientation. There is very little research on tackling the robustness of pattern recognition under such conditions. Out of such effects, force level variation and wrist orientation changes are reported to be the most common and the most influential factors affecting the performance of the PR system. This research proposes an appropriate scheme to handle such effects, and the suitability of the scheme is demonstrated by comparing it with the state-of-the-art schemes on sEMG data extracted from amputee subjects.

The research outcome will be supported by:

1. Demonstrating the performance of the proposed methods on available sEMG database
2. Comparing them with the previously used MEC schemes in the literature on the same database
3. Building own sEMG dataset using the in-house laboratory equipment from different subjects and validating the performance of the developed algorithm on this database

1.8 Thesis Structure

The thesis document consists of five chapters, an outline of which is highlighted in Figure 1.8.

Chapter 2 : introduces the background information on sEMG, which includes the sEMG signal generation, its properties, and how it is measured using electrodes. An overview of a different aspect of MEC such as sEMG signal windowing, feature extraction, dimensionality reduction, classification, real-time implementation challenges such as controller delay, etc. is given in this chapter. In addition to this, a detailed literature survey is presented here with a focus on the challenges to the performance of MEC.

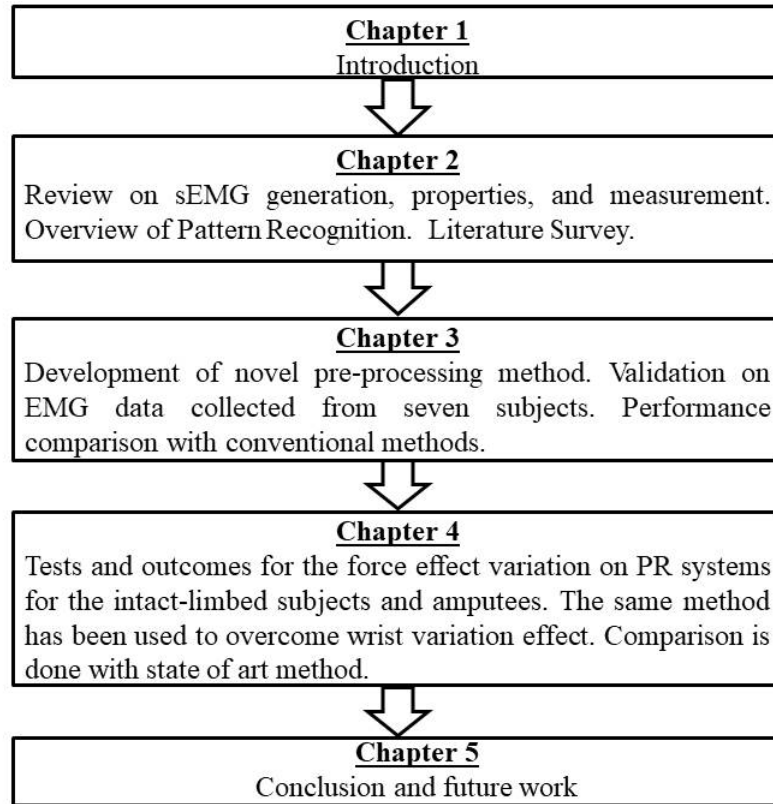


Figure 1.8: Outline of the thesis

Chapter 3 and **Chapter 4** forms the major contributing chapters of this thesis by proposing different algorithms for improving the MEC performance.

Chapter 3 : Here, a novel pre-processing method called Minimum Entropy Deconvolution Adjusted (MEDA) is used for sEMG signal enhancement and better characterization. The technique is validated on sEMG data collected from seven subjects in the institute laboratory. A detailed comparison of the proposed scheme is performed with the other popular pre-processing schemes from the literature.

Chapter 4 : presents the tests and outcomes for the force effect variation on PR systems for the intact-limbed subjects and amputees. The technique used here for overcoming force level variation is also tested to overcome wrist orientation variation on PR. The method is compared with the results achieved by the state-of-the-art.

Chapter 5 : summarizes the conclusion of the work and suggests possible future research.

1.9 Summary

The basic overview of the problem of sEMG driven prostheses is provided in this chapter. The history and present-day prosthesis, the amputation statistics, and the reason for prosthesis rejection are presented. Different approaches for controlling the prosthetic arm is discussed with special emphasis on MEC. The challenges associated with MEC are also elaborated here. The chapter also highlights the factors which motivated this research. Finally, the thesis structure is provided.

Chapter 2

Background and Literature Survey

2.1 Introduction

This chapter covers the relevant introduction to sEMG signal generation, characteristics, and measurement. The general overview of Myoelectric Control (MEC) is provided. The steps for Pattern Recognition (PR) for sEMG classification is reviewed from the literature. A thorough literature survey on the research problems is carried out with the state-of-the-art literature on PR based MEC. Finally, the summary of the chapter is provided.

2.2 sEMG Signal Generation, Characteristics, Measurements and Signal conditioning

2.2.1 sEMG Signal Generation

The motor unit is made up of a group of fibers, axon, and the nerve-cell body. It undergoes contraction and is the smallest subdivision of the muscle. Depending on the type of muscle, the number of motor units varies from 2 to 2000. The muscle is made of a large number of motor units. Whenever there is a need for the contraction of the muscle, a train of nerve impulses is generated in the motor cortex of the brain. Depending on the level of contraction, the required number of motor units are simulated. Motor units, after receiving the impulse train successfully, generate motor-unit trains and summate to form the myoelectric signal. The generation of the

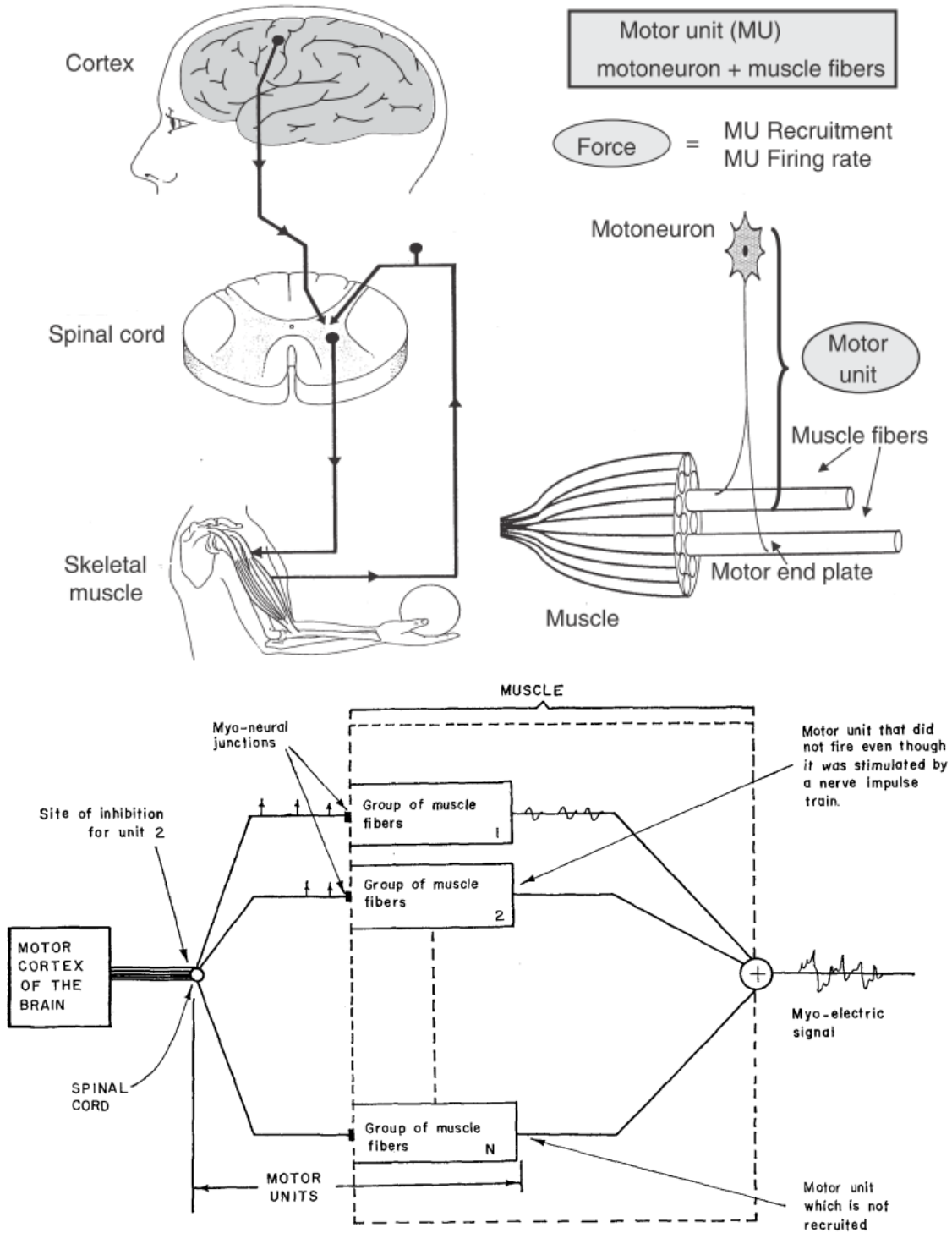


Figure 2.1: Myoelectric signal generation (Source: (Brody et al., 1974))

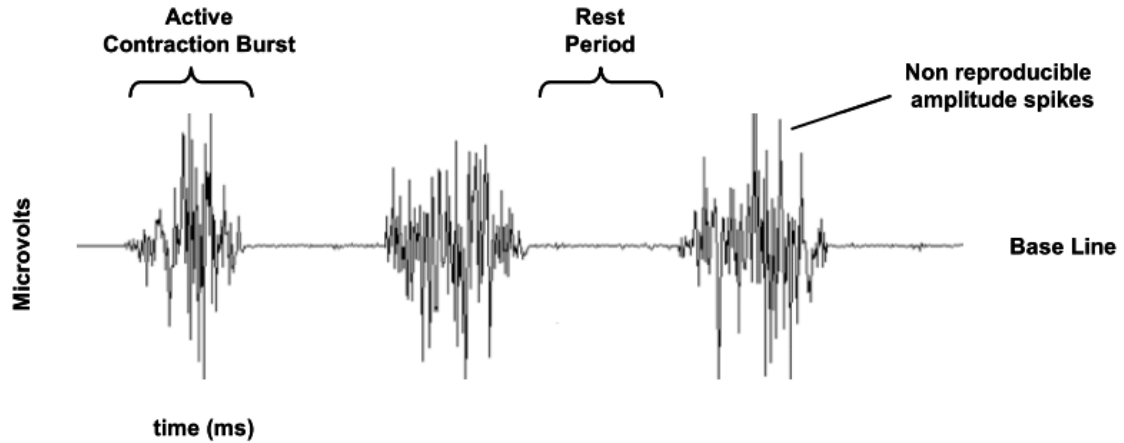


Figure 2.2: Raw sEMG signal (Source: (Konrad, 2005))

myoelectric signal is shown in Figure 2.1.

2.2.2 sEMG Characteristics

The amplitude of sEMG signal is random and can range from 0 to 10 mV (peak-to-peak). The usable energy lies in the range of 0 – 500 Hz frequency range. The raw sEMG is shown in Figure 2.2 (Konrad, 2005). Whenever there is no movement of the muscle, a noise-free line can be seen. The quality of the sEMG amplifier can be decided using the baseline; usually, the amplitude should not be more than 3 – 5 mV for a good recording. The baseline is affected by the quality of the sEMG amplifier, the noise, and the detection condition. Whenever there is a muscle activity, a spike or a burst is produced. These bursts differ for different hand movements since the set of recruited motor units constantly change for different movements. The raw sEMG is in the range of $+/- 5000 \mu V$.

2.2.3 sEMG Measurements

sEMG signals are measured by electrodes that are placed on the target muscles using a needle electrode (invasive method) or surface electrode (non-invasive method). Since the use of a needle electrode involves medical skill and can cause pain and discomfort to the subject (Phinyomark et al., 2012b), surface electrodes have been used in this research. Differential amplifiers are used to measure the potential difference generated between two electrodes and to eliminate the artifacts. The sEMG

signal which is not amplified lies in the range of 2 – 5 mV. This signal is generally amplified with a gain in the range of 500 to 1000. Analog to digital conversion is performed before the signal is displayed on the screen with a minimum resolution of 12 bit (Khushaba et al., 2012). Since most of the signal power components lie in the range of 20 – 500 Hz; the minimum sampling frequency must be twice the maximum frequency, i.e., 1000 Hz for efficiently reproducing the signal. In most of the literature, sampling rate is chosen to be 2000 Hz (Khushaba et al., 2012, Oskoei and Hu, 2006).

2.2.4 sEMG Signal Conditioning

Signal processing is used to increase the reliability and validity of the findings. Here, the signal is acquired from the electrodes and is filtered to reduce the noise produced due to motion artifacts, equipment, and other noise. Process of rectification takes the absolute value of the signal, as shown in Figure 2.3. Most of the literature associated with MEC uses rectification or RMS value calculation before extracting information for the signal.

Filtering of sEMG signals: apart from the essential anti-alias filter, the pre-processing of sEMG signal almost always involve digital filters. In fact, a considerable amount of research goes into preprocessing of sEMG signal, and Chapter 3 of this thesis discusses that aspect in detail. Additionally, as a part of the filtering, the active part of the signal is extracted for further processing, as shown in Figure 2.4.

2.3 Windowing

The sEMG signal is a non-stationary signal, i.e., every time a movement is made, the shape of the signal varies; even if the hand movements are identical. This is because when identical movements are made, the set of recruited motor units are different. To capture this, time domain windowing is utilized. The time slot (W) required for acquiring myoelectric data during feature extraction is called a window. The time taken by the controller to extract signal features and perform pattern recognition is called processing time (τ). The class decisions cannot be generated instantaneously because of the processing time.

In general, there are two methods of windowing (Englehart and Hudgins, 2003):

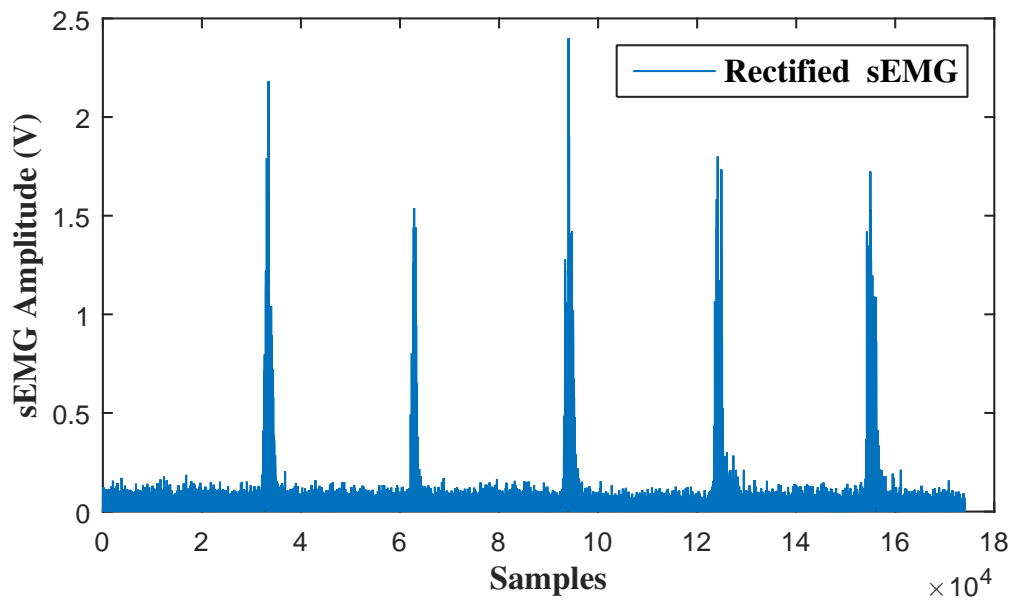
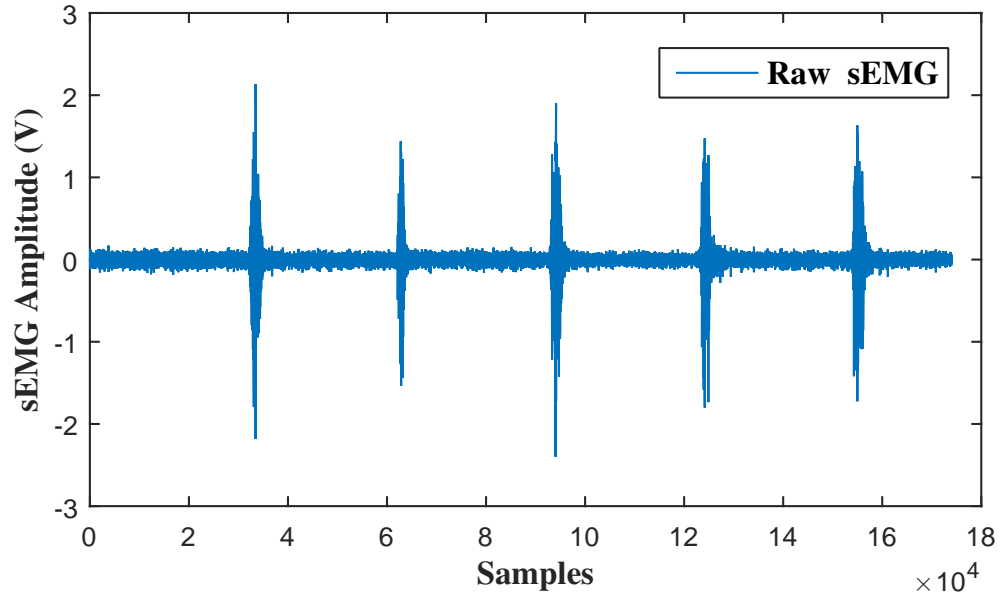


Figure 2.3: Raw sEMG converted into positive amplitude

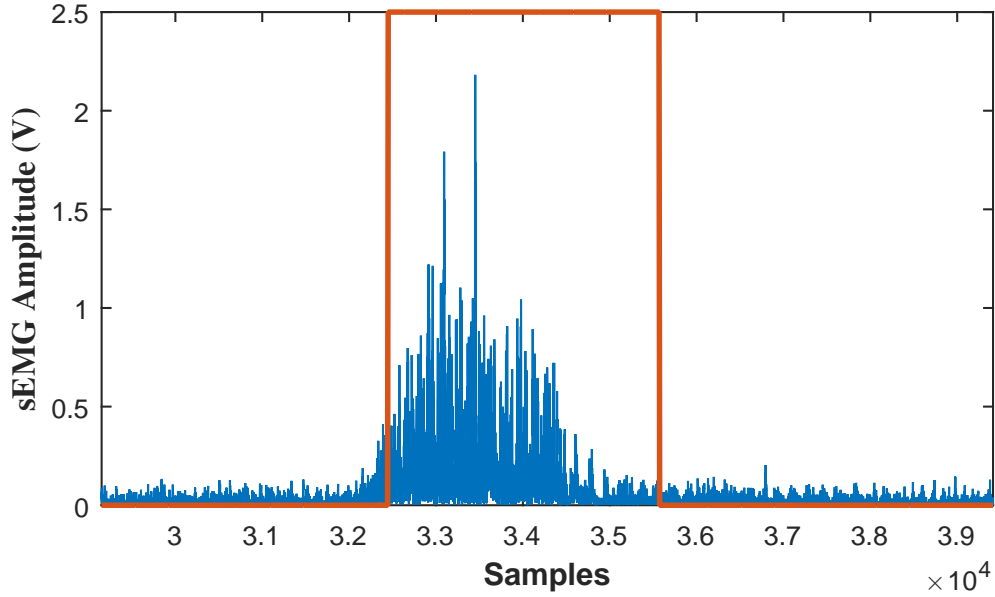


Figure 2.4: Active part of the signal is taken

2.3.1 Disjoint Windowing Scheme

For feature extraction, segments with predefined lengths (W) are used. After an inevitable processing delay, the classification of motion occurs, and it is associated with only the segment length. The processor remains idle during the time ($W - \tau$) as shown in Figure 2.5. Processing system is not entirely utilized since processing (feature extraction and classification) occurs in only a portion of the time spent acquiring data. Even though it does not utilize the processor optimally, due to the simplicity in implementation, it is commonly used in the literature (Khushaba et al., 2012).

2.3.2 Overlapped Windowing Scheme

As the name indicates, in the case of overlapped windowing scheme, the new segment slides over the current section, with an increment time less than the segment length as shown in Figure 2.6. It is associated with both segment length and increment. Here the computing power of the system is better utilized. Englehart and Hudgins (2003) proved that overlapped windowing scheme produces better accuracy than disjoint window scheme. The class decisions are also provided at a higher rate while using

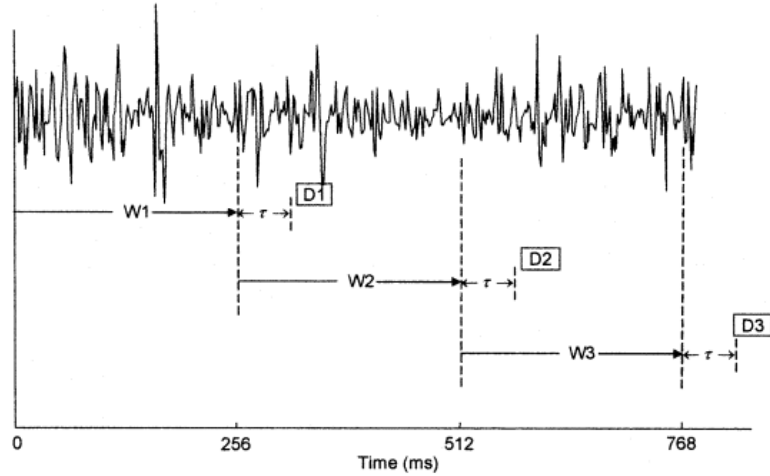


Figure 2.5: Windowing using disjoint scheme wherein, W1, W2, and W3 are the analysis window segments. D1, D2 and D3 represent the decision made for W1, W2, and W3 respectively, with a processing time of τ (Source: (Englehart and Hudgins, 2003))

this scheme since the data acquisition and classification runs in parallel.

These two parameters, i.e., the window length, and its configuration (disjoint or overlapped) is decided based on the controller delay in a practical implementation, which is explained below in Section 2.3.3.

2.3.3 Controller Delay

The maximum delay of the prostheses to respond to users' command (response time) depends on data segment length (W) and processing time (τ). The controller delay is the sum of segment length (W) and processing time (τ) while using a disjoint window scheme. Researchers have reported on different controller delays for the control of multifunctional upper-limb prostheses, and some of the interesting ones are described below:

- **Hudgins et al.** (Hudgins et al., 1993) stated that the delay should be less than 300 ms, to reduce the computational complexity and real-time delay. They also specified that to do feature extraction and classification, time left is less than 100 ms.
- **Graupe et al.** (Graupe et al., 1982) reported that a delay of 200 ms is acceptable for a prosthesis user.

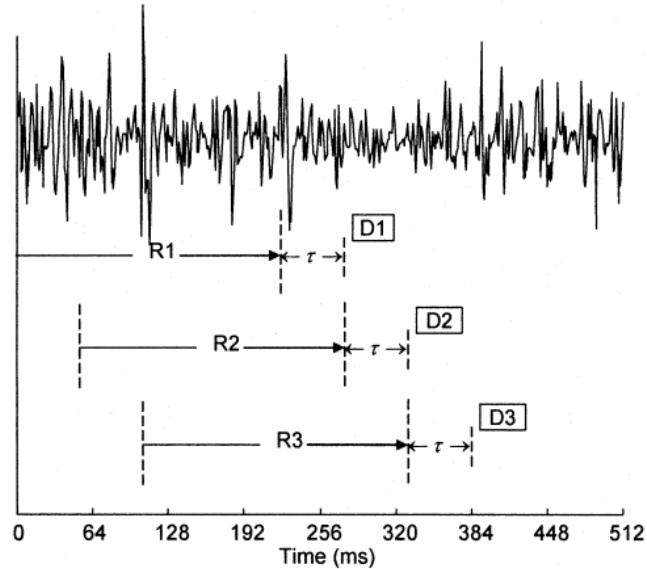


Figure 2.6: Windowing using overlapped scheme wherein, R1, R2, and R3 are the analysis window segments. D1, D2 and D3 represent the decision made for R1, R2, and R3 respectively, with a processing time of τ (Source: (Englehart and Hudgins, 2003))

- **Shenoy et al.** (Shenoy et al., 2008) stated that 128 ms window length is sufficient for developing a responsive sEMG-based controller. They mentioned that the update rate was sufficient for developing a responsive sEMG-based controller.
- **Chu et al.** (Chu et al., 2006) showed that, with an operation delay of less than 300 ms, the algorithm will be able to control multifunction myoelectric hand in real-time. They used an overlapping window of 250 ms with 125 ms window increment. The scheme generated two decisions within 300 ms which guarantees that a user can control a directed myoelectric hand function within 250 ms from the instant when the user's intention is given.
- **Farrell and Weir** (Farrell and Weir, 2007) tested on twenty-abled body subjects, with seven different levels of controller delay ranging from 0 – 300 ms and stated that optimal controller delay lies between 100 ms and 175 ms for the average user.
- **Smith et al.** (Smith et al., 2011) suggested the optimal window length to be between 150 ms and 250 ms for best performance. They tested a variety of analysis window lengths ranging from 50 ms to 550 ms using 12 different

classifiers. The study was performed on 13 healthy subjects who were trained and operated virtual prostheses using pattern recognition. A linear mixed effects model was created to determine the relationship between window length and classification error.

From the above literature, it can be observed that window length ranging from 100 to 300 ms is commonly employed for pattern recognition and classification. Considering this into account, a window length of 200 ms was chosen here.

2.4 Feature Extraction

Feature extraction highlights the relevant structures which are hidden in the data stream and removes the interference and irrelevant sEMG signals (Farina et al., 2017). It is the process of converting a pattern into features. This is the first step after the pre-processing step in pattern recognition and is the most crucial one. The success of sEMG classification depends on the selection of appropriate sEMG features. Features are computed from sEMG signal using windowing techniques to extract the temporal characteristics and to minimize the spectral leakage. The obtained features should have maximum class separability, robustness, and low computational complexity (Phinyomark et al., 2012a).

The features extracted may be in the time domain, frequency domain, or time-frequency domain. A detailed discussion regarding several sEMG features is given in the following subsections.

2.4.1 Time domain features

Time domain features are prevalent because they do not require any transformation and are quick to calculate (Phinyomark et al., 2013, Westerink et al., 2008, Zhang and Zhou, 2012).

- **Hudgins et al.** (Hudgins et al., 1993) was the first to extract features in the time domain where features such as Mean Absolute Value (MAV), Mean Absolute Value Slope (MAVS), Zero Crossings (ZC), Slope Sign Changes (SSC) and Waveform Length (WL) were used. The classification accuracy obtained was around 91.2% with normal limbed subjects and 85.5% with amputees for four different limb functions using a single bipolar surface electrode pair.

- **Shenoy et al.** (Shenoy et al., 2008) collected data from three subjects for eight movements using RMS as a feature. High accuracy of about 92 – 98% was obtained for eight classes of hand movements using eight bipolar electrodes.
- **Amsuss et al.** (Amsuss et al., 2013) used four time domain features namely RMS, Zero Crossings (ZC), Slope Sign Changes (SSC) and Waveform Length (WL) for eight class movements. The average classification accuracy of 97.9% was reported using eight dry bipolar electrodes.
- **Li et al.** (Li et al., 2010) used Mean Absolute Value (MAV), Zero Crossings (ZC), Waveform Length (WL), and Slope Sign Changes (SSC) as features and classification accuracy of 93.1% was reported for six movements using twelve self-adhesive Ag/AgCl snap bipolar electrodes.

2.4.2 Frequency domain features

Frequency domain features are calculated from the estimated power spectrum density (PSD) of a signal. Usually, frequency domain features have higher computation complexity in comparison to time domain features (Phinyomark et al., 2013).

Fourier analysis helps to find the frequency content of the signal by decomposing the original signal into sinusoids of specific magnitudes and phases.

- **Nishikawa and Kuribayashi** (Nishikawa and Kuribayashi, 1991) used the neural network to learn the relation between the power spectrum of sEMG signal analyzed by Fast Fourier transform and the performance needed by the amputees.
- **Matsumura et al.** (Matsumura et al., 2006) classified the sEMG signal into seven categories by using a neural network. The neural network learned FFT spectra to classify the sEMG signal into seven categories. They also mentioned that frequencies below 600 Hz are important for analyzing sEMG signals.

2.4.3 Time-Frequency domain features

To overcome the loss of temporal information associated with Fourier transform and to tackle the non-stationary behavior of sEMG signals, Short Time Fourier Transform (STFT) was introduced in the feature extraction process. Here, the longer time

signal is divided into shorter segments of equal length, and then Fourier transform is computed on each shorter segment.

- **Hannford and Lehman** (Hannaford and Lehman, 1986) applied STFT for sEMG signals. They used STFT to locate time dependencies in the sEMG signals that are normally averaged in the Fourier analysis.
- **Karlsson et al.** (Karlsson et al., 2000) compared STFT, the Wigner–Ville distribution, the Choi–Williams distribution, and the continuous wavelet transform for accuracy and precision. They found that the continuous wavelet transforms provided better accuracy and precision than other methods.

STFT extracts the temporal as well as the spectral information from the signal. However, it works on a fixed time and frequency resolution. Multi-resolution analysis tools such as Continuous Wavelet Transform (CWT), the Discrete Wavelet Transform (DWT), and the Wavelet Packet Transform (WPT) helps in achieving this. It is a time-frequency representation of the signal.

- **Englehart et al.** (Englehart et al., 1999) used feature sets based upon the STFT, the wavelet transform, and the wavelet packet transform. For dimensionality reduction, Principal Component Analysis (PCA) was employed with Linear Discriminant Analysis (LDA) as a classifier. The best performance was exhibited using WPT with an average classification error of 6.25%.
- **Boostani and Moradi** (Boostani and Moradi, 2003) used features from the wavelet transform. The energy of wavelet coefficients of sEMG signals in nine scales and the cepstrum coefficients were found to produce the best features.
- **Li et al.** (Li et al., 2005) developed an efficient fuzzy wavelet packet (WP) based feature extraction method for the classification. They found that the combination of fuzzy theory and wavelet can achieve improved sEMG signal classification performance.

2.5 Dimensionality Reduction

The second step, which is dimensionality reduction of features aims at reducing the data complexity while preserving essential information. This step helps to reduce

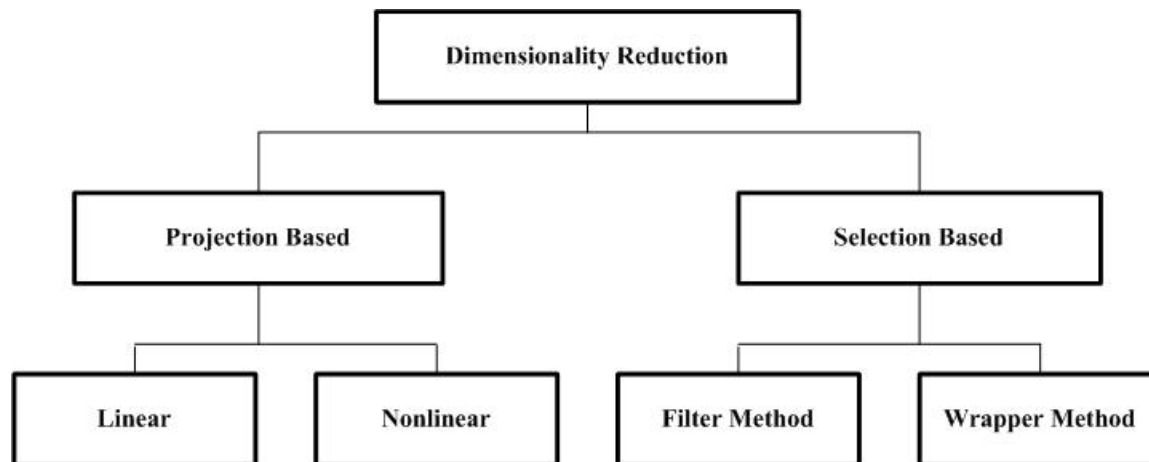


Figure 2.7: Dimensionality reduction techniques

the amount of processed data. The main problem that occurs in pattern recognition is the curse of dimensionality due to a very high order feature vector. Also, as the number of channels increases, the size of the feature set is further increased, i.e., the total number of features = number of features/channel \times number of channels. Dimensionality reduction also helps in improving the real-time performance of the classifier with a fewer feature set, making it convenient for the prosthesis user since shorter training sessions are required (Hargrove et al., 2010). This also helps in removing redundant and irrelevant features.

Dimensionality reduction techniques can be classified into two major categories as shown in Figure 2.7.

2.5.1 Feature projection

Feature projection maps the original data set into another space with reduced dimension using linear or non-linear mapping. Principal Component Analysis (PCA) and Linear Discriminant Analysis (LDA) are the two widely used linear mapping methods. PCA finds the subset of variables, based on which original variables have the highest correlation with the principal component. The first principal component carries much of the variability in the signal, and the following components take the remaining variability. PCA finds the component axes that maximize the variance of data, while the LDA finds the axes that maximize the separation between multiple classes. Traceability of the features is not possible here (Hargrove et al., 2010).

2.5.2 Feature Selection

The main aim of feature selection is to reduce the dimensionality of the feature set by selecting a subset of features which performs best under some classification condition. Thus the usage of irrelevant and redundant features is avoided, which reduces the computational cost and results in better representation of patterns. The two most important aspects that need to be considered in feature subset selection are the evaluation measure and the search procedure. According to the dependence on the classification algorithm, evaluation measures are divided into two types, namely filters and wrappers. Filter based methods use a measure such as mutual information to estimate the relative significance of individual elements or subset of features. In the wrapper-based approach, the feature subset is selected with the help of a classifier. Hence the filter method is faster than the wrapper method, even though wrapper based methods are more accurate. To explore the feature space, a search strategy is needed. To search the solution space, various search algorithms have been employed (Khushaba et al., 2008).

Some of the literature associated with the dimensionality reduction technique for sEMG pattern recognition are reviewed here.

- **Chu et al.** (Chan et al., 2007) used a linear-nonlinear feature projection composed of PCA and a self-organizing feature map (SOFM) for dimensionality reduction with multilayer perceptron (MLP) as a classifier. The proposed projection method improved the class separability and recognition accuracy.
- **Hargrove et al.** (Hargrove et al., 2007) used the first forty principal components of a feature set. In the study, six different feature sets with six different classifiers were analyzed. They observed that there was some loss of useful data during the PCA when the number of channels was increased from 10 to 15 and also suggested to use other data reduction techniques.
- **Oskoei** (Oskoei and Hu, 2006) adopted genetic algorithm (GA) as a search strategy, Davies-Bouldin Index (DBI) and Fishers Linear Discriminant Index (FLDI) were employed as the filter objective functions, and linear discriminant analysis (LDA) has been used as the wrapper objective functions. Artificial neural network (ANN) was used as the main classifier. The study stated that the DBI index provides more reliable information.

- **Khushaba et al.** (Khushaba et al., 2010) proposed a new dimensionality reduction method, referred to as orthogonal fuzzy neighborhood discriminant analysis (OFNDA). OFNDA was compared to other feature projection methods and demonstrated that it performed better with accuracies ranging from 97.66% to 87.84% for 5 to 10 classes of movements.

2.6 Classification Techniques

For predicting different movements, the extracted features are given to the classifiers in the final stage. This section provides a brief overview of the classifiers used in the literature concerning sEMG. Several classifiers namely Decision Tree (DT), k-Nearest-Neighbor (kNN), Support Vector Machine (SVM), Linear Discriminant Analysis (LDA) and Artificial Neural Networks (ANN) have been used to obtain high classification accuracy.

- **Phinyomark et al.** (Phinyomark et al., 2012a) used LDA as a classifier with thirty-seven-time domain and frequency domain features to classify six movements. The results of LDA were performed by 10-fold cross validation for each subject.
- **Khushaba et al.** (Khushaba et al., 2010) used SVM to classify ten classes of the forearm movement collected from ten subjects. The results of SVM were tested using three-way data split.
- **Hangroove et al.** (Hargrove et al., 2007) compared the classification accuracy of several classifiers and showed that the choice of feature set and dimensionality reduction is more important than the choice of classifiers.

It is evident from the above discussion that for a sEMG based MEC, many classifiers are reported in the literature. The aim of this thesis is not to study different classifiers but rather use many of them to validate the other steps of pattern recognition, namely preprocessing, feature selection, etc. The aim here is also towards improving the system robustness against different factors such as the effort or force level variations, wrist orientation changes, etc., making it usable in a real-life situation. A thorough literature review will be done on these aspects in the following sections.

2.7 Literature review on Pre-processing of sEMG signal

In literature related to sEMG signal processing, it was found that the major challenge is to separate the noise from actual data. Unlike other physiological signals like electrocardiogram (ECG), there is no studied or well-understood pattern for sEMG signals. Additionally, sEMG signals are contaminated with a wide variety of noise, and this causes issues in signal onset detection, feature extraction, and pattern recognition (Reaz et al., 2006). Noise sources such as power-line interference, motion artifact, ambient noise, characteristic instability of the signal, and noise due to electronic and recording equipment could be present in the sEMG signal. By using high-quality equipment and intelligent circuits, noises can be reduced but cannot be entirely removed. Filtering methods are commonly used to remove noise (Powar et al., 2018). In some cases, time-frequency domain schemes like Wavelet transform have also been used in the literature as a filtering tool for sEMG signals. However, due to the computational complexity of these methods, conventional frequency-selective filters are preferred. But, if the noise from the recording instrument lies in the usable frequency range, it becomes hard to eliminate noise using conventional filters (Phinyomark et al., 2012c). Different noise reducing methods have been discussed in previous studies. In practice, filtering is a challenging issue that should be more carefully investigated.

2.7.1 Noise in sEMG signal

sEMG signal is contaminated with various noises during the recording, making it nearly impossible to recover the generated sEMG signal without any noise. A poorly extracted sEMG signal implies a poor performance from the MEC algorithm due to inaccurate values of the extracted feature, making it one of the critical issues to be addressed. The various factors that affect the recovery of the sEMG signal depend on the tissue structure, subject skin formation, internal structure of the subject, skin temperature, and more.

This section gives a detailed overview of the various noise sources that the sEMG signal extraction process is subjected to in a real-life environment (Chowdhury et al., 2013).

2.7.1.1 Inherent Noise in the Electrode

If the size of the electrode is large, the impedance decreases, but a large-sized electrode makes the regular usage of prosthesis uncomfortable for amputees. On the other hand, if the size of the electrode is reduced, the impedance increases resulting in deterioration of the signal-to-noise ratio (SNR) of the signal. Thus a careful selection of the electrode must be carried out before the recording.

2.7.1.2 Movement Artifact

Movement artifacts are generated due to movement between the skin and the surface of the electrode. It can also be caused due to the movement of the connecting cables between the electrode and the data acquisition system. These noises are reported to be in the frequency range of 1 – 10 Hz with an amplitude close to that of sEMG. Conforto et al. (1999) compared four filtering procedures; Chebyshev high pass filters, the moving average filter, the moving median filter, and the wavelet filter to remove the motion artifact from sEMG signal. The wavelet filter was found to be more precise than other methods since it retains most of the information.

2.7.1.3 Electromagnetic Noise

The human body is exposed to electric and magnetic radiation, and these electromagnetic noises cancel or superimpose on the actual sEMG signal being measured. The dominant noise arises from the radiation of power sources, whose frequency lies in the range of 50 – 60 Hz with an amplitude that is one to three times that of the measured sEMG signal. An efficient filter can eliminate power-line interference from sEMG signal.

2.7.1.4 Cross Talk

This is due to the undesired sEMG signal from a muscle group that is not commonly monitored. By carefully choosing electrode size and inter-electrode distances (typically 1 – 2 cm) this can be minimized.

2.7.1.5 Internal Noise

The thickness of the skin (body fat) affects the amplitude of the sEMG signal. As the thickness increases, the sEMG activity decreases. The choice of filters can partially reduce these.

2.7.1.6 Electrocardiographic (ECG) Artifacts

The activity of the heart affects the sEMG signal during recording. The effective method to eliminate this is by using a high pass filter.

2.7.2 Methods for pre-processing

De-noising is a challenging task, and it is difficult to obtain quality sEMG signal for PR of MEC. If the raw sEMG is adequately used, it gives us valuable information. Various pre-processing methods are applied to achieve a high classification accuracy of PR. This section provides an extensive literature review on the filtering schemes for preprocessing of sEMG signals .

2.7.2.1 Autoregressive Modeling (AR) and Autoregressive Moving Average Modeling (ARMA)

Autoregressive Modeling (AR modeling) has been a developing trend in sEMG pre-processing. Hefftner et al. (1988) investigated the suitability of the method for processing sEMG signals. In their work, a fourth order AR model was used with a sequential least square algorithm to determine the parameters. Graupe et al. (1983), Doerschuk et al. (1983), and Triolo and Moskowitz (1985) have also used AR model approach for sEMG processing.

Graupe and Cline (1975) extracted complete linear information of the sEMG signal using the ARMA model. The outcome of the study was that a 5th order ARMA model was acceptable in describing the sEMG signal, and the signal can be considered stationary over short intervals of time. Barişçi (2008) used ARMA model in the calculation of the spectrum of sEMG signals. Doerschuk et al. (1983) have also used ARMA model in their work.

The main disadvantage of AR and ARMA model is the high computational cost, and determining the model order is complex (Reaz et al., 2006, Kiryu et al., 1992).

2.7.2.2 Empirical Mode Decomposition (EMD)

The EMD method decomposes the dataset into a finite and small number of components called as Intrinsic Mode Function (IMF). The technique has been shown to attenuate background noise from the signal successfully. Here, the shifting process is involved, which is data-driven and adaptive. First, the signal is decomposed into different IMF components, then the components below a pre-specified threshold value are removed, and finally, the signal is reconstructed. The main advantage of this method is that it does not require prior information about the data. Andrade et al. (2006) used EMD method for filtering and compared with the wavelet filter. The results showed that the EMD method could successfully attenuate noise by preserving the information in the signal. Yang et al. (2014) have also used the technique for muscle fatigue analysis from the sEMG signals. In addition to EMD, Zhang and Zhou (2013) utilized the ensemble EMD (EEMD), where the comparison was made with traditional filters. In their work, they have shown that the EEMD method outperforms traditional filters. The main drawback of the method is that the non-linearities are frequently introduced by noise and is quickly captured by EMD. The computation time is high for this method (Andrade et al., 2006).

2.7.2.3 Cyclostationary Analysis

It is a spectrum based method applied to sEMG pre-processing which takes advantage of the non-stationary and cyclostationary property of the signal. Only a handful of work related to cyclostationary analysis of sEMG signals exists in the literature. To study the cyclostationary property of sEMG signal, the Spectral Correlation Density (SCD) function is used. Strip Spectral Correlation Algorithm (SSCA) and Fourier Transform Accumulation method (FAM) are used to estimate the SCD. Compared to SSCA, FAM provides a better representation of cyclostationary components. Roussel et al. (2017) have determined the mean firing rates, which are based on Blind Source Separation (BSS) decomposition method for multi-channel intramuscular sEMG. Karthick et al. (2016) have used FAM based SCD function to study the cyclostationarity related to dynamic contractions of biceps brachii muscle. The computational cost and complexity of this method are high as reported in the literature.

2.7.2.4 Cepstrum Analysis

Cepstrum analysis is the inverse Fourier Transform of the logarithm of the power spectrum magnitude of the signal. The coefficients can be obtained from autoregressive modeling. Kang et al. (1995) used cepstral analysis and maximum likelihood method (MLM) for sEMG pattern recognition. Comparison between conventional autoregressive (AR) coefficients and cepstral coefficients was performed in their study, and it was found that cepstral coefficients demonstrated improved separability in the feature space. The study also highlighted that the spectral difference is higher in the low-frequency band giving better discriminative information. Shokrollahi et al. (2009) and Phinyomark et al. (2012a) have also used the cepstral coefficients method for sEMG signature discrimination.

2.7.2.5 Independent Component Analysis (ICA)

By maximizing the statistical independence amid the estimated source signal, ICA extracts the source signal from the observed signal. It decomposes the signal into individual muscle activity. There are different ICA algorithms used to decompose sEMG signals. Ren et al. (2006) applied combined ICA and wavelet filtering to remove power line noise. The method was fast and robust when compared with conventional digital filtering methods. McKeown and Radtke (2001) used ICA and reported the decomposition of the signal for the PR of hand movements. Jung et al. (2000) applied ICA and obtained an improvement in classification accuracy of 40% when compared with raw sEMG. Naik and Kumar (2012) used the various estimation methods of the unmixing matrix to decompose the signal and reported an increase in accuracy of 34% during sEMG classification of hand motions. Willigenburg et al. (2012) applied ICA for removing ECG from sEMG and compared with other procedures and showed that ICA outperformed the other methods in terms of preserving the spectral information of the sEMG signal. Naik et al. (2007) compared the performance of four ICA algorithms for four different hand gestures using ANN. Subasi and Kiyimik (2010) studied ICA to detect fatigue of biceps brachia muscle. The results showed that ICA, when combined with ANN, separates sEMG signals from fresh and fatigued muscles. The major drawback of ICA is that it is an iterative process and has random initialization. The quality of separation has randomness, and the performance is not always optimum.

2.7.2.6 Higher Order Statistics (HOS)

HOS is applicable for efficient processing of sEMG signals because of the unique properties. The method can quickly identify deviations from linearity and Gaussianity in the signal. There has been growing interest in using this method. By using this method, precise phase reconstruction is possible. In HOS, cumulants and moments are used, which are the measures of asymmetry and peaks of the probability distribution. Kaplanis et al. (2000) used HOS to obtain new parameter (power spectrum median frequency) that could increase the analytic character of sEMG. Yana et al. (1989) applied this method to simulated sEMG signals to recover motor unit action potential from the sEMG signals. The technique is mainly used for diagnosis of the neuromuscular disorder. Shahid (2004) used HOS on the sEMG signal and proposed bispectrum of the linear system. The method had been improved by separating the skewness parameter. The developed technique showed better performance than the traditionally used methods.

2.7.2.7 Wavelet Transform

A wavelet transform performs a multiresolution analysis of a time domain signal. Unlike STFT where the time-frequency resolution is a constant, the wavelet transform has a varying resolution in the time-frequency plane, thereby better resolving both the time and frequency axes. When the wavelet transform is used in filtering, care must be taken to choose a particular wavelet function and decomposition levels that are suitable for the target application. Filtering using wavelet transform is performed in three steps: First, the signal is decomposed into discrete wavelet transform (DWT) to get detail and approximation coefficients. The high-frequency components and low-frequency components are obtained from detail and approximation coefficients respectively. The noise usually contributes to the detail coefficients. In the second step, based on the noise variance, a threshold value is calculated and applied to detail coefficients by the linear or non-linear transform. In the final step, using the remaining terms after the thresholding, the sEMG signal is reconstructed (Phinyomark et al., 2011). For estimation of denoised sEMG, Khezri and Jahed (2008) proposed Stein unbiased risk method and demonstrated an improvement in PR scheme with this pre-processing step. For upper limb motions, Hussain et al. (2009) suggested universal thresholding technique and was able to improve

the sEMG PR accuracy. Phinyomark et al. (2009b) proposed a novel pre-processing method based on wavelet-based denoising algorithm where the optimal weighted parameter is assigned for universal thresholding method. The results were evaluated for seven hand gestures. Ortolan et al. (2003) evaluated three noise reduction methods, namely adaptive filter using least mean square, finite-impulse-response nonadaptive filter, and wavelet transform. Wavelet filter outperformed other filtering methods in their study. Phinyomark et al. (2009a) compared four denoising algorithms, namely, universal thresholding, SURE thresholding, hybrid thresholding, and minimax thresholding for wavelet denoising. The best of wavelet denoising algorithm was found to be universal thresholding method.

Despite its popularity, wavelet transforms are computationally intensive techniques. Selection of wavelet function is also critical for effective noise removal.

Traditional finite impulse response (FIR) and infinite impulse response (IIR) filters are also widely used in the literature for sEMG signal processing. Since they are well known, they are not discussed in this thesis.

It is clear from the literature review that a significant amount of research is done in the area of denoising of sEMG signals. However, many of the advanced schemes are found to be computationally intensive. Literature also suggests that while removing noise, some of the critical information in the signal might also be removed. Overcoming these aspects will be a significant challenge in the area of MEC.

2.8 Literature review on factors affecting the robustness of myoelectric pattern recognition

A significant number of studies have been made on various stages of sEMG PR such as pre-processing, feature extraction, novel feature identification, dimensionality reduction, and classification (Powar et al., 2018, Powar and Chemmangat, 2017). Even though the previous studies report high classification accuracy of more than 90%, there have been problems during the clinical translation of the system. There are various other factors that affect the performance of PR system such as: variation in limb position, variation in forearm orientation, variation in electrode position, variation in force level and change in the characteristic of sEMG signal (Khushaba et al., 2016b, Staudenmann et al., 2010). Because of the gap between the ideal laboratory

condition and practical application of the myoelectric prostheses, it becomes crucial to test the PR with these various factors (Geng et al., 2012).

There exists a gap between research findings and clinical implementation of MEC. For example, when an experiment is conducted in the laboratory for data collection, the subject is made to sit in a fixed position with arm resting on the chair. This arrangement is made so that it is comfortable for the subject to produce repeatable contractions across trials resulting in higher accuracies. But in a clinical environment, data is collected more practically in a scenario with a wide variety of force levels for different limb positions, etc. For example, if a prosthetic user wants to hold an object, the control algorithm should be trained in a variety of limb position and various force levels (Scheme et al., 2010). The following subsection gives an overview of some of the crucial factors that can affect the performance of the MEC.

2.8.1 Force Level Variation

One of the challenging aspects is the force level changes that can arise due to activities such as the lifting of heavy objects, handling mechanical tools, etc., which can occasionally happen (Shin et al., 2016). Biologically, this is due to variation in the length of the forearm muscles (Hoozemans and Van Dieen, 2005). If the PR system is not trained for such scenarios, it misclassifies the pattern and produces the wrong control decision. Therefore, this study investigates the effect of force level changes on the classification accuracy of PR at three wrist positions.

Recently there has been significant research dedicated towards the problem of force level variations, as they significantly influence the performance of myoelectric control (Yang et al., 2016). Maclsaac et al. (2001) analyzed muscle fatigue, considering both force level variation and joint angle. They used conduction velocity, and EMG mean frequency in their work. The study states that both factors affect the performance of sEMG PR. Tkach et al. (2010) considered two force level variations (i.e., low and high) in their experiments. Apart from the force level variation, they have examined the impact of electrode shift and muscle fatigue on PR accuracy. Force level variation had significantly reduced the classification accuracy. They showed that selecting suitable sEMG feature combinations was not adequate. Developing effective training strategies for the classifier is suggested for improving the robustness, and they were able to achieve an accuracy of 86%. Scheme and Englehart (2011) demonstrated the

impact of force changes on PR based EMG control. The sEMG data were recorded from eleven subjects with nine classes of hand movements. The subjects varied the force level from 20% to 80% of maximum voluntary contraction. LDA classifier with time domain features was used. The classifier was trained at the individual force level and examined at all force level. The classification inaccuracy ranged between 8% and 19%. He et al. (2015) recommended a feature extraction technique based on muscle coordination and discrete Fourier transform. By the usage of the approach, the classification accuracy was improved by 11% for the sEMG data gathered from nine instructions of motions with three different force levels. Yang et al. (2017) inspected four distinctive data-collection procedures and calculated their efficiency for getting robust classification, despite dissimilarities presented by unlike muscle variations, dynamic arm movements, and outside interfering forces. They used mean absolute value as a feature for evaluation. Al-Timemy et al. (2015) investigated the problem of force level on the sEMG pattern recognition system. The sEMG information was recorded from nine amputee subjects executing six instructions of motions with different force ranges (i.e., low, medium and high). Maximum classification accuracy of 93% was achieved when trained with all three force levels. Additionally, a novel set of features was proposed to enhance the execution. Khushaba et al. (2016b) made a thorough study on the impact of force level variation and used time-dependent spectral feature extraction method to diminish the effect of muscular contraction levels. The sEMG records from six classes of hand actions at three force levels were considered. Classification accuracy of up to 91% was attained.

2.8.2 Wrist Level orientation

Amputees with functional wrist preserve the ability to move the wrist and are essential for their routine activity. Usually, the prosthesis is trained at a specific wrist orientation, and if the prosthesis is operated in another orientation the performance of PR scheme is degraded. This leads to misclassification of movements. The PR must be robust against such conditions allowing the amputees to use their wrist at different orientations (Adewuyi et al., 2016, 2017). Therefore, this study investigates the effect of changing wrist orientation on the classification accuracy of PR.

Recently, some relevant studies have been reported in the literature which checks the PR performance in the presence of wrist variation. Peng et al. (2013) conducted a

pilot study on how the forearm orientation degrades the classification accuracy. The solution for this was proposed by using an additional accelerometer by estimating the rotation angles. The classification error achieved was less than 3.3%. Adewuyi et al. (2013) examined the result of statically and dynamically changing wrist position on PR to classify hand movements in able-bodied persons. It was observed that varying the wrist degraded the system performance. The system's accuracy was improved when trained in all wrist positions. Roman-Liu and Bartuzi (2013) inspected how different wrist positions affects the association among the time and frequency measures of the sEMG signal among thirteen participants. It was observed that the spectral measures of the sEMG signal change at different wrist positions and should be considered. Tkach et al. (2010) validated that wrist variation affected PR accuracy. The study was conducted at seven different wrist positions for three different hand movements. As in the case of Roman-Liu and Bartuzi (2013) and Adewuyi et al. (2013), it was shown that including the training data from different wrist position decreased the classification error. Scheme and Englehart (2011) conducted a study on seventeen non-amputee subjects and two partial hand amputees to determine the PR classification accuracy at various static and dynamic wrist positions. The sEMG PR accuracy reduced by 35% for six hand grasps. A dual-window classifier was proposed in the study to increase the classification accuracy. Adewuyi et al. (2016) investigated the performance of non-linear and linear pattern recognition algorithms and also optimal sEMG feature subsets on sixteen non-amputees and four amputee subject for four-hand movements at different wrist positions. The results suggested some widely used time domain features for classification of data with multiple wrist positions. It was shown that LDA and non-linear artificial neural networks performed significantly better than the quadratic discriminant analysis. Khushaba et al. (2016b) conducted an exhaustive study on the influence of wrist variation for six classes of hand motions. The accuracy of about 91% was achieved using the time-dependent spectral feature extraction method. Adewuyi et al. (2017) assessed approaches for partial hand amputees to control hand in multiple wrist positions without affecting classification accuracy. An experiment was conducted for four hand motions at thirteen different wrist positions. For developing a wrist independent scheme, the relation between sEMG features and wrist position was modeled using the neural network from the recorded wrist position data.

2.8.3 Electrode Shift

Shifting of the electrode from its intended position can occur during multiple usage cycles or even due to loading of the limb. Electrode displacement affects the classification accuracy. To overcome such a scenario robust features must be derived, training has to be done, and some calibration must be carried out.

- **Hargrove et al.** (Hargrove et al., 2008) worked on the effect of electrode displacements on pattern classification accuracy and stated that electrode displacements adversely affect classification accuracy. They came up with the solution that trains the system to recognize possible displacement locations, thereby mitigating the effect.
- **Young et al.** (Young et al., 2012) investigated the optimal inter-electrode distance, channel configuration, and electromyography feature sets for myoelectric pattern recognition in the presence of electrode shift. For reducing the system sensitivity to electrode shift, they suggested larger inter-electrode distances and a combination of longitudinal and transverse channels. The work proposes that Time Domain Auto-Regressive (TDAR) feature set can be utilized to reduce the effect of electrode shift.

2.8.4 Variation in Position of Limb

For daily activities, there will be variation in limb position. The sEMG patterns obtained are different for different positions. The degradation of performance of pattern recognition is observed when the limb is fixed in one position and classifier is trained, but tested with other limb position. The effects can be minimized by training the pattern recognition system with different position, multiple classifiers; each trained for a single position, and use of accelerometers.

- **Scheme et al.** (Scheme et al., 2010) demonstrated that variations in limb position will have a substantial impact on the robustness of myoelectric pattern recognition.
- **Fougner et al.** (Fougner et al., 2011) proposed a solution to overcome the effects. They solved the problem by collecting sEMG data and training the classifier in multiple limb positions and by measuring the limb position with accelerometers.

Most of the previous work focused on experiments with healthy subjects rather than amputees. In this work, the method is tested on both healthy and amputee subjects. Also previously, complicated process with more time delay was used. Taking this into consideration, the work is directed towards minimization of force and wrist position variation on PR.

2.9 Summary

In this chapter, background on basic concepts associated with sEMG signal generation, characteristics, noise, and measurements was explained. The different parts of the pattern recognition system have been described with the literature review. The detailed literature on various methods of pre-processing was presented along with their limitations. Also, the factors affecting the clinical application of PR have been discussed with the previous work. Based on the thorough literature review detailed in this chapter, the objectives were defined and justified. The major concern during the recording of the sEMG data is the noise contamination in the signal. This causes major problems in the analysis since the noise bandwidth overlaps the frequency band of the signal. In such scenarios, it is challenging to remove noise by using conventional filters alone. The second problem is the limited attention to the factors that influence the clinical translation of this myoelectric control. Multiple dynamic factors can significantly degrade the accuracy of sEMG pattern recognition. The effect of force variation and wrist orientation has been studied in isolation on the classification accuracy of pattern recognition. This thesis attempts to address these issues by implementing a novel pre-processing stage in the analysis of sEMG signal and designing a more robust and viable sEMG pattern recognition system for upper limb prostheses to mitigate the effect of force variation and wrist orientation with reduced computational time. The next two chapters will address the major objectives presented in this chapter. It will be supported by detailed analysis and experimental results.

Chapter 3

A Novel Pre-processing Procedure for Enhanced Feature Extraction and Characterization of sEMG Signals

3.1 Introduction

The main challenges in pre-processing of sEMG signal are the limited tools that can be used to minimize the noise such as power line interference, electrode noise, broadband noise from the instrument, motion artifacts and white Gaussian noise (Phinyomark et al., 2009c) and to enhance the feature. This chapter proposes a novel pre-processing procedure for the sEMG signal, namely the Minimum Entropy Deconvolution Adjusted (MEDA) before feature extraction. Wiggins first introduced Minimum Entropy Deconvolution (MED) in 1978 for seismic recordings. Geoff L. McDonald proposed the convolution fix for MED for vibration fault detection (McDonald and Zhao, 2017). MEDA differentiates the original sEMG signals from noise using higher-order statistics such as kurtosis, which is the fourth moment of distribution. MEDA is designed to find the filter coefficients that recover the output signal with a maximum value of kurtosis while minimizing the low kurtosis noise components. This motivated the use of MEDA for sEMG signals in this research work to enhance features and identify patterns for efficient classification. Practical results demonstrate the feasibility of the

approach with the mean percentage increase in classification accuracy of 20.5% across seven subjects demonstrating the significance of MEDA in classification.

The work mainly focuses on the following aspects: 1) To study the classification accuracy of sEMG feature extraction without and with the pre-processing step using MEDA, 2) After pre-processing stage with MEDA, removing redundant features in the classifier and finding the most stable feature combination with different classifiers, 3) Comparison of performance of MEDA with the conventional methods from the literature.

The chapter begins with the data collection procedure. Next, conventional filtering approaches for sEMG signal pre-processing from the literature are explained. Later, a detailed description of the proposed method is given. Other stages involved in the overall process of MEC, such as feature extraction and dimensionality reduction, are then explained. The overall process of the proposed MEC is then validated on the data collected in the laboratory. The results presented here are divided into two parts: In the first part, conventional pre-processing methods are used on the data set, and the one which performs the best amongst them in terms of the classification accuracy is selected, and in the second part, the selected scheme is compared with the proposed pre-processing method, and the effectiveness of the later is demonstrated.

3.2 Material and Data collection

Seven subjects, three males and four females, aged between 25 and 35 years participated in the study. The subjects were normally limbed with no neurological or muscular disorder. Before participating, all the subjects gave their written consent to participate in this study and were briefed about the experiment. The required ethical approval was obtained from the National Institute of Technology Karnataka, Surathkal. To display and store signals a Virtual Instrument was developed in LABVIEW (NI). To avoid the effect of different limb position on the generated sEMG signals subjects were seated on an armchair, with their arm supported and fixed at one position (the shoulder adducted and neutrally rotated, elbow flexed at 90° , forearm and wrist in the neutral position).

The sEMG data was recorded from flexor carpi radialis (channel 1) and extensor carpi radialis (channel 2) of a subject by using two pairs of surface electrodes (3M red dot Ag/AgCl) on the right forearm (Phinyomark et al., 2010). These muscle groups

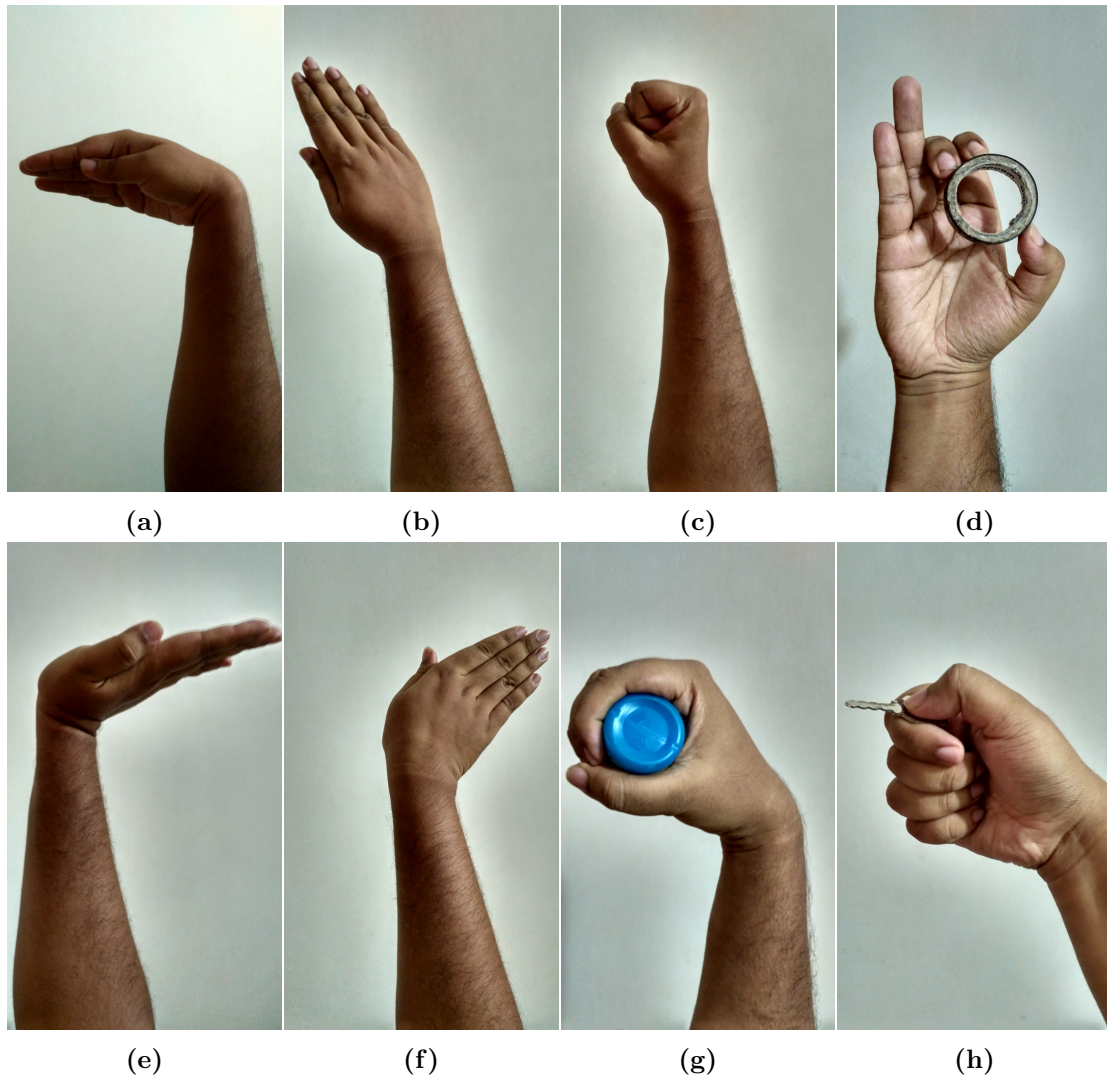


Figure 3.1: Eight classes of hand movements considered in this research, a) wrist flexion b) wrist radial deviation c) hand close d) tripod e) wrist extension f)wrist ulnar deviation g) cylindrical and h) key grip

represent the most important location on the human forearm, and they largely contribute to wrist movements (Mayor et al., 2017). Reducing the number of electrodes simplifies the requirements for controlling prostheses without compromising on the classification accuracy. To avoid crosstalk between the two muscles, an inter-electrode distance of 20 mm was maintained for a 5 mm diameter electrode. The sEMG signals collected from the electrodes were amplified with a gain of 1000. A 16 bit analog to digital converter (National Instruments, PXIe-4300) was used to sample the signal at 2000 Hz. A bandpass filter with a frequency band of 20 Hz to 500 Hz was used to extract the sEMG signal with an additional notch filter at 50 Hz to remove the power line interference.

For the experiment, subjects were asked to perform eight different hand movements: wrist flexion (FX), wrist radial deviation (WRD), hand close (HC), tripod (TD), wrist extension (EX), wrist ulnar deviation (WUD), cylindrical (CL) and key grip (KG) as shown in Figure 3.1. The subject performed each movement for a duration of 3 s and a rest period of 5 to 8 s between each movement. Each action was repeated five times. The movements were performed sequentially.

3.3 Methodology

3.3.1 Conventional filtering methods from the literature

3.3.1.1 Wiener filter

In Wiener filtering, according to the ratio between desired and actual signal spectrum, the re-scaling of the Fourier coefficients is done. Since Wiener filter is a non-causal filter, a *priori* Signal to Noise Ratio (SNR) is required to be estimated. Here, a decision direct (DD) method is used for the estimation of *priori* SNR. *Priori* SNR requires an estimation of *posteriori* SNR of previous and the current frame (Liu et al., 2014, Ephraim and Malah, 1984).

Let the noisy sEMG signal be $x(t)$, which is the sum of clean sEMG signal $s(t)$ that is not corrupted by noise and the noise $n(t)$.

$$x(t) = s(t) + n(t) \tag{3.1}$$

Let $S(p, k)$, $N(p, k)$, and $X(p, k)$ denote the k^{th} spectral component in a time

frame p of the clean sEMG signal $s(t)$, the noise $n(t)$ and the noisy sEMG signal $x(t)$ respectively.

The important goal here is to find the estimate $\hat{S}(p, k)$. By the application of spectral gain function $G(p, k)$ to the noisy spectral component $X(p, k)$, an estimate of $S(p, k)$ is obtained.

$$\hat{S}(p, k) = G(p, k)X(p, k) \quad (3.2)$$

The gain function $G(p, k)$ minimizes the mean square error between the estimated and desired spectral component. $G(p, k)$ is a function of *priori* SNR and can be expressed in terms of *priori* SNR ($S\hat{N}R_{prio}(p, k)$) as,

$$G(p, k) = S\hat{N}R_{prio}(p, k) + 1 \quad (3.3)$$

The *priori* SNR is calculated using decision direct (DD) method as,

$$S\hat{N}R_{prio}(p, k) = \beta \frac{|\hat{S}(p-1, k)|^2}{\hat{\gamma}_n(p, k)} + (1 - \beta)P[S\hat{N}R_{post}(p, k) - 1] \quad (3.4)$$

Where,

$$S\hat{N}R_{post} = \frac{|X(p, k)|^2}{\hat{\gamma}_n(p, k)} \quad (3.5)$$

$P[\]$ denotes the half wave rectification, $\hat{S}(p-1, k)$ is the estimated sEMG spectrum at previous frame. The behavior of SNR estimator is controlled by the parameter β which is typically set to 0.98.

$\hat{\gamma}_n(p, k)$ is estimated during the rest period when no movement is made, it is the noise Power Spectral density and is equal to $E[|N(p, k)|^2]$; where $E[\]$ is the expectation operator.

3.3.1.2 Spectral Subtraction (SS) Approach

The spectral estimator $\hat{S}(p, k)$ of the clean sEMG signal is obtained by subtracting an estimate of the noise spectrum $E[|\hat{N}(p, k)|]$ from the noisy sEMG spectrum $X(p, k)$. During the rest period, (i.e. when no movement is made), the spectral information of noise spectrum $|\hat{N}(p, k)|$ is obtained. Then the spectral error is estimated. The magnitude averaging and residual noise reduction have been used to minimize the error (Boll, 1979, Paliwal et al., 2010).

$$|\hat{S}(p, k)| = |X(p, k)| - |\hat{N}(p, k)| \quad (3.6)$$

Or

$$|\hat{S}(p, k)| = |X(p, k)|G(p, k) \quad (3.7)$$

Where,

$$G(p, k) = 1 - \frac{\hat{N}(p, k)}{X(p, k)} \quad (3.8)$$

Now the spectral error (ϵ) is reduced using,

$$\epsilon = |\hat{S}(p, k)| - |S(p, k)| \quad (3.9)$$

3.3.1.3 Butterworth Filter

The filter is designed to have a frequency response as flat as possible in the passband and rolls off towards zero in the stopband. Similar to all filters, the typical prototype is the low-pass filter. The low-pass filter can be modified into a high-pass filter, band-pass and band-stop filters.

The gain $G(\omega)$ of an N-order Butterworth low-pass filter is given in terms of the transfer function as:

$$|H(\omega)|^2 = \frac{1}{1 + (\omega/\omega_c)^{2N}} \quad (3.10)$$

where $|H(\omega)|^2$ is the square magnitude of the frequency response of the filter, ω the angular frequency and ω_c is the filter's cutoff frequency.

The Butterworth frequency response $|H(\omega)|^2$ is obtained from $H(s)$ by assuming $s = j\omega$.

$$H(s)H(-s)|_{s=j\omega} = |H(j\omega)|^2 \quad (3.11)$$

Consequently:

$$H(s)H(-s)|_{s=j\omega} = \frac{1}{1 + (s/j\omega_c)^{2N}} \quad (3.12)$$

The filter poles are located in the following points in s plane:

$$s = j\omega_c(-1)^{1/2N} = \omega_c e^{j\pi(2k+N-1)/2N}, \quad k = 0, 1, \dots, 2N - 1 \quad (3.13)$$

These poles form a symmetrical pattern of a circle with radius ω_C . For stability, the transfer function, $H(s)$, is therefore chosen such that it contains only the poles in the negative real half-plane of s . This low-pass filter is used as prototype for construction of others filter's class by mathematical methods of frequency transformation.

3.3.2 Novel method used for pre-processing

MED was originally proposed by Ralph Wiggins in 1978 to aid extraction of reflectivity information in subterranean layers in seismic data (Wiggins, 1978). MED was initially applied in the field of multisensor data fusion, pitch period estimation, restoration of star field images, seismic signal processing, an ultrasonic inspection of composite materials and pipes and machine fault diagnosis (McCormick and Nandi, 1998, Jiang et al., 2013). It was used by Endo and Randall in machine condition monitoring field to detect gear tooth fault (Endo and Randall, 2007). MED operator suppresses frequencies over which the signal to noise ratio is low and emphasizes dominant signals. MED iteratively selects an FIR filter to minimize the entropy of filtered signal, thereby enhancing the kurtosis information in the signal. A higher value of entropy associated with the signal indicates a lower SNR (McCormick and Nandi, 1998).

3.3.2.1 Minimum Entropy Deconvolution (MED)

Here, a kurtosis norm is defined and then a FIR filter is designed such that the filtered output sEMG signal reaches a maximum according to the norm. The signal is assumed to be corrupted with noise and is expressed as:

$$\vec{x} = \vec{d} + \vec{e} \quad (3.14)$$

In equation (3.14), $\vec{x} \in R^N$ is the final measured sEMG signal with noise, and $\vec{d} \in R^N$ is Original sEMG, and $\vec{e} \in R^N$ is White Gaussian noise.

Generally, for sEMG signal, Kurtosis is large for \vec{d} when compared to noise \vec{e} . Selection of FIR filter with coefficients \vec{f} to maximize kurtosis leads to a filter design that extracts high kurtosis sEMG, which minimizes the noise component.

An approximation $\vec{y} \in R^N$ of the signal \vec{d} is reconstructed by convolving the FIR

filter $\vec{f} \in R^L$ with the measured sEMG signal \vec{x} .

$$\vec{y} = \vec{f} * \vec{x} \quad (3.15)$$

where ‘*’ denotes convolution.

$$y_k = \sum_{l=1}^L f_l x_{k-l+1}, \quad k = 1, 2, \dots, N$$

where ‘L’ and ‘N’ denote the filter length and input sample length respectively.

In matrix form:

$$\vec{y} = \bar{X}_0^T \vec{f}, \quad (3.16)$$

$$\bar{X}_0 = \begin{bmatrix} x_1 & x_2 & x_3 & \dots & \dots & x_N \\ 0 & x_1 & x_2 & \dots & \dots & x_{N-1} \\ 0 & 0 & x_1 & \dots & \dots & x_{N-2} \\ \vdots & \vdots & \vdots & \ddots & \dots & \vdots \\ 0 & 0 & 0 & \dots & \dots & x_{N-L+1} \end{bmatrix}_{L \times N}$$

The filtered signal \vec{y} should approach the original sEMG \vec{d} and this is found by selecting filter \vec{f} to minimize the noise effect $\vec{f} * \vec{e} \rightarrow 0$ and extracting original sEMG signal $\vec{f} * \vec{x} \simeq \vec{d}$. For MED to work satisfactorily, the signal \vec{d} is expected to have very high kurtosis while \vec{e} is of very low kurtosis.

To achieve this, an optimization problem is formulated with objective function under assumed zero mean output \vec{y} ,

$$\max_{\vec{f}} kurtosis = \max_{\vec{f}} \frac{\sum_{n=1}^N y_n^4}{\left(\sum_{n=1}^N y_n^2\right)^2} \quad (3.17)$$

Taking derivative of above equation and equating it to zero,

$$\vec{f} = \frac{\sum_{n=1}^N y_n^2}{\sum_{n=1}^N y_n^4} (\bar{X}_0 \bar{X}_0^T)^{-1} \bar{X}_0 [y_1^3 y_2^3 \dots y_N^3]^T \quad (3.18)$$

Equation (3.18) requires an initial estimate of \vec{y} and that is obtained by assuming initial filter as centered initial difference filter $\vec{f} = [0, 0, \dots, 1, -1, 0, \dots, 0]$, (3.18) is applied repeatedly to calculate \vec{f} . The updated value of \vec{f} is used to calculate \vec{y} before each iteration. Termination is done when there is minimum change in filter coefficients between iterations.

3.3.2.2 Minimum Entropy Deconvolution with convolution adjustment (MEDA)

In order to avoid deconvolving a single impulse, causing disturbance at the start of the output signal \vec{y} , Geoff L. McDonald suggested a convolution fix (McDonald and Zhao, 2017) to tackle this issue which is described below.

$$\vec{y} = \vec{f} * \vec{x} \quad (3.19)$$

$$\vec{y}_k = \sum_{l=1}^L f_l x_{k+l-1}, \quad k = 1, 2, \dots, N - L + 1$$

In matrix form:

$$\vec{y} = X_0^T \vec{f}, \quad (3.20)$$

$$\bar{X}_0 = \begin{bmatrix} x_L & x_{L+1} & x_{L+2} & \dots & \dots & x_N \\ x_{L-1} & x_L & x_{L+1} & \dots & \dots & x_{N-1} \\ x_{L-2} & x_{L-1} & x_L & \dots & \dots & x_{N-2} \\ \vdots & \vdots & \vdots & \ddots & \dots & \vdots \\ x_1 & x_2 & x_3 & \dots & \dots & x_{N-L+1} \end{bmatrix}_{L \text{ by } N-L+1}$$

Resulting in the MEDA iterative selection:

$$\vec{f} = \frac{\sum_{n=1}^{N-L} y_n^2}{\sum_{n=1}^{N-L} y_n^4} (X_0 X_0^T)^{-1} X_0 [y_1^3 y_2^3 \dots y_{N-L}^3]^T \quad (3.21)$$

The above is solved iteratively similar to MED.

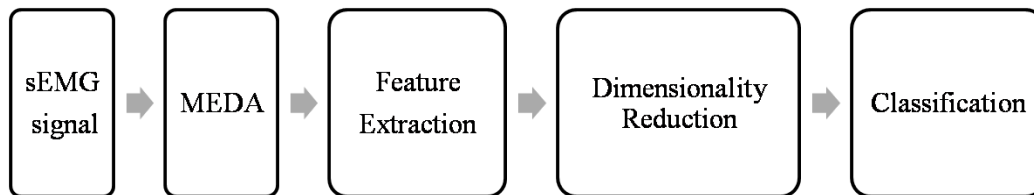


Figure 3.2: Overall process of classification based on proposed MEDA method

3.3.3 Feature extraction

The proposed pre-processing step with MEDA was applied after sEMG data acquisition, and the resultant signal was used in the feature extraction process. The stages involved in the overall process of classification is shown in Figure 3.2.

The technique of obtaining useful information from raw input data into a reduced representative set of features is called feature extraction. The success of sEMG classification depends on the selection of appropriate sEMG features. Features are computed from sEMG signal using windowing techniques to extract the temporal characteristics and to minimize the spectral leakage. Windowing can be disjoint or overlapping, and due to the lower computational cost and simplicity, disjoint window scheme is employed in this work with a duration of 200 ms (Khushaba et al., 2016a). Features in the analysis of sEMG signals can be divided into three groups namely the time domain, the frequency domain and the time-frequency domain of which the first two feature groups have been considered. Time domain features are directly extracted from raw sEMG time series. Frequency domain features are obtained from the Power Spectral density (PSD) of sEMG signal. Eighteen features used in this study with their mathematical definition are presented in Table 3.1. In Table 3.1, the first thirteen features are the time domain features and the remaining five are the frequency domain features. The detailed definition for each feature is reported in Appendix A.

3.3.4 Dimensionality reduction and Classification

The dimension of the feature set obtained after feature extraction is very large, which increases the complexity of the classifier and also reduces the convergence of learning error (Khushaba et al., 2009a). To reduce the computational complexity and enhance generalization on unseen data, reducing the number of features to a minimum is very important. Feature set dimensionality can be reduced using feature projection or

Table 3.1: Time and frequency domain features along with mathematical definition

Feature extracted	Abbr.	Mathematical definition
Average Amplitude Change	AAC	$AAC = \frac{1}{N} \sum_{n=1}^{N-1} x_{n+1} - x_n $
Approximate entropy	ApEn	$ApEn(m, r, N) = [\Phi^m(r) - \Phi^{m+1}(r)]$ $\Phi^m(r) = (N - m + 1)^{-1} \sum_{n=1}^{N-m+1} \log C_n^m(r)$
Difference absolute standard deviation value	DASDV	$DASDV = \sqrt{\frac{1}{N-1} \sum_{n=1}^{N-1} (x_{n+1} - x_n)^2}$
Integrated EMG	IEMG	$IEMG = \sum_{n=1}^N x_n $
Kurtosis	Kurt	$Kurt = \left(\frac{1}{N} \sum_{n=1}^N \left[\frac{x_n - \bar{x}}{\sigma} \right]^4 \right) - 3$
Log detector	LOG	$LOG = e^{\left(\frac{1}{N} \sum_{n=1}^N \log x_n \right)}$
Mean absolute value	MAV	$MAV = \frac{1}{N} \sum_{n=1}^N x_n $
Root mean square	RMS	$RMS = \sqrt{\frac{1}{N} \sum_{n=1}^N x_n ^2}$
Sample entropy	SampEn	$SampEn(x, m, r) = -\ln \left(\frac{A^m(r)}{B^m(r)} \right)$
Simple square integral	SSI	$SSI = \sum_{n=1}^N x_n ^2$
Variance	VAR	$VAR = \frac{1}{N-1} \sum_{n=1}^N x_n ^2$
Waveform length	WL	$WL = \sum_{n=1}^{N-1} x_{n+1} - x_n $
Skewness	Skew	$Skew = \left(\frac{1}{N} \sum_{n=1}^N \left[\frac{x_n - \bar{x}}{\sigma} \right]^3 \right)$
Mean frequency	MNF	$MNF = \frac{\sum_{j=1}^M f_j P_j}{\sum_{j=1}^M P_j}$
Median frequency	MDF	$MDF = \frac{1}{2} \sum_{j=1}^M P_j$
Mean power	MNP	$MNP = \frac{\sum_{j=1}^M P_j}{M}$
Spectral moment of order= 2	SM	$SM = \sum_{j=1}^M P_j f_j^2$
Total power	TTP	$TTP = \sum_{j=1}^M P_j$

Let x_n represent the n th sample of the sEMG signal with the length N . P_j is the EMG power spectrum at frequency bin j . f_j is the frequency of the sEMG power spectrum at frequency bin j . M is the length of the frequency bin, $m =$ maximum epoch length, $r =$ tolerance, $C_n^m(r) =$ correlation sum, $A^m(r)$ and $B^m(r)$ are defined for dimensions $m + 1$ and m .

feature selection. This chapter focuses on feature selection method which removes the redundant features. Feature selection aims at (i) reducing the dimension, (ii) eliminating irrelevant and redundant features, (iii) reducing the amount of data for classification, and (iv) improving the classification accuracy (Khushaba et al., 2011). The important aspects that need to be considered for the feature subset selection process are the evaluation method and the search strategy. The evaluation method includes filters and wrappers. On the other hand, a search strategy is needed to explore the feature space. In this study, we have used wrapper method based evaluation with four different search strategies namely, Particle Swarm Optimisation (PSO), Best First, Linear Forward Selection and Greedy Step Wise search. A brief description of each of these methods is given below:

In a wrapper based approach, the feature subset selection algorithm searches for a good subset of features using the classifier itself as a part of the evaluation function. This approach requires a state space, a search engine, an initial state and termination condition (refer Appendix B.1 for more details).

3.3.4.1 Greedy stepwise

It is a simple search strategy which considers local changes to the current feature subset. The local change may be the addition or deletion of a single feature from the subset. Feature subset is known as a forward selection if the algorithm considers only additions to the feature subset, and backward elimination if it considers the only deletion. Additionally, there is also bi-directional search which uses both addition and deletion. By including all these variations, the method expands on the current node and moves towards the child with the highest accuracy. The method terminates, when no child improves over the current node. The disadvantage of this search method is that it gets stuck in local maxima and plateau (Hall, 1999). The algorithm used here is from Kohavi and John (1997) (refer Appendix B.1.1 for more details).

3.3.4.2 Best First

The method allows backtracking along the search path. By making local changes to the current feature subset, best first moves through the search space. It can backtrack to a more promising previous subset and continue the search from there if the path being explored looks less promising. The entire search space is explored, and

hence a stopping criterion is to be defined. The search is terminated when there is no improvement in the expansion of the node. This method is more robust than the greedy stepwise. The disadvantage of this method is that a thorough search will increase variance and thus reduce accuracy. The method is computationally costly to explore the entire search space (Hall, 1999). The algorithm used here is from Kohavi and John (1997) (refer Appendix B.1.2 for more details).

3.3.4.3 Linear Forward Selection

Here, the number of attributes expansions is reduced in each forward selection step. The standard forward selection is modified to obtain efficient attribute selection and to reduce the number of attribute extension in each forward step. The search method ranks all the attributes and selects the top-ranked attributes which are employed in the subsequent forward selection. The main objective of this approach is to take away the irrelevant attributes so that it can focus on the relevant attributes. The disadvantage of this method is that weakly relevant attributes that perform poorly on their own are lost. The algorithm used in this chapter is from Gutlein et al. (2009) (refer Appendix B.1.3 for more details).

3.3.4.4 Particle Swarm Optimization

PSO is an evolutionary computation technique which is based on the principle that each solution is encoded as a particle with a position in search space. The algorithm begins by creating the initial particles and assigning them initial velocities. The particles move in the search space. Based on the experience of its own and neighboring particles, each particle updates its velocity and position. The best position obtained by the population thus far is called *gbest*, and the best previous position of the particle is recorded as the personal best *pbest*. The algorithm searches optimal solutions by updating the velocity and the position of each particle according to the equations given in Moraglio et al. (2007). When the predefined criterion is met, the search is stopped. The algorithm suffers from stagnation once particles have prematurely converged to any particular region of the search space (Xue et al., 2013) (refer Appendix B.1.4 for more details).

In the classification stage, the signal corresponding to each movement is recognized and classified into different classes. The classification accuracy obtained from J-48,

k-nearest neighbors (KNN), Naive Bayes and Linear Discriminant Analysis (LDA) were used to assess the suitability of different sEMG features for classification of hand movements. The classifiers were tested using ten-fold cross-validation (refer Appendix B.2 for more details).

3.4 Results and Discussion on the previously used filters from literature

The three filters described in Section 3.3.1 have been used to pre-process the two-channel sEMG signals collected from the subjects. Then, the active segment of the signal representing a movement is detected using the threshold, and the rest past is removed. A rectangular window is applied to the active portions of the data of 200 ms length during feature extraction. Eighteen features in time and frequency domain have been extracted from each channel to represent the sEMG activity. Thus, the total number of extracted features is 36 features (18 feature/channel $\times \times 2 = 36$ features). Two schemes of experiments are employed. In the first scheme, the comparison of filters is carried out without dimensionality reduction and for the second set of experiment dimensionality reduction is applied to obtain the same classification accuracy with the reduced number of features. The filter performance is compared by using four classifiers with ten-fold cross validation. The justification behind employing the ten-fold cross-validation is to make sure that there is no over-fitting in the results.

The involuntary background activities present in the signal can impose challenges while implementing a myoelectric system. The Weiner filter can be used as a successful tool in minimizing the involuntary background spikes and help in building more accurate myoelectric controller.

3.4.1 Comparison of filters without dimensionality reduction

The achieved average classification accuracy for eight movements for seven subjects is shown in the bar graph in Figure 3.3. The classification accuracy shown in the figure is obtained using all 36 features. From the classification accuracy, some important inferences can be observed. A lower value of classification accuracy can be attributed to the fact that a large set of movements were considered while extracting signals from only two muscle groups. The accuracy could be enhanced in the future

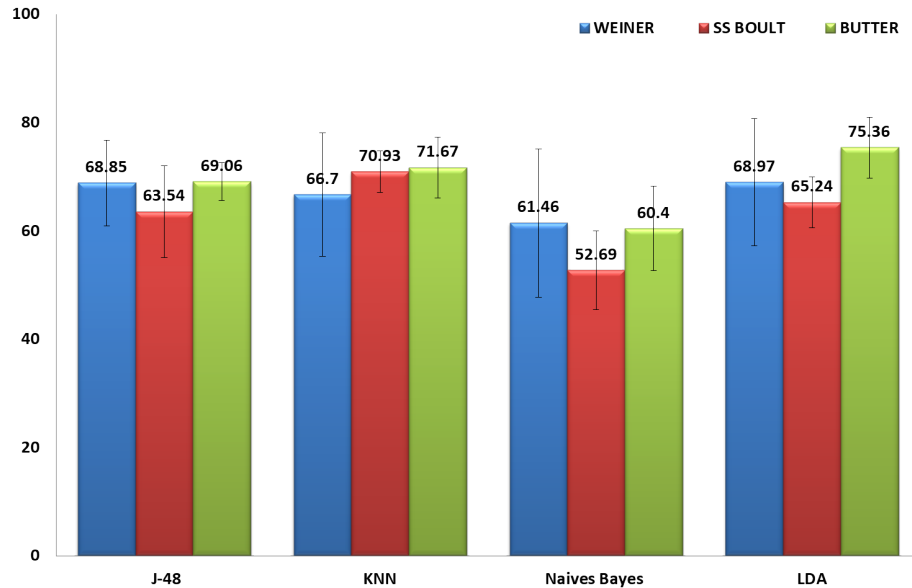


Figure 3.3: Column graph of average classification accuracy using four classifiers and three filters

by selecting the optimum number of movements. From the bar graph, the maximum classification accuracy of 75.36% was achieved using a Butterworth filter with LDA as a classifier. SS filter obtained maximum classification accuracy using KNN classifier, reaching 70.93%. Weiner filter achieved maximum accuracy of 68.97% with LDA as the classifier. It can also be seen that for this experiment, LDA produced better accuracy than other classifiers. The change in accuracy is due to various reasons. While applying Weiner and SS filter, there must have been the removal of some important components from the sEMG signal considering them as noise. It can be observed from the bar graph that there were no noteworthy changes among the performances of the filters.

3.4.2 Comparison of filters with dimensionality reduction

Figure 3.4 shows the classification accuracy for eight movements for seven subjects after applying dimensionality reduction. The main aim here is to attain a similar classification accuracy with the reduced features. It can be observed from the bar graph in Figure 3.4 that the maximum classification accuracy was obtained using a

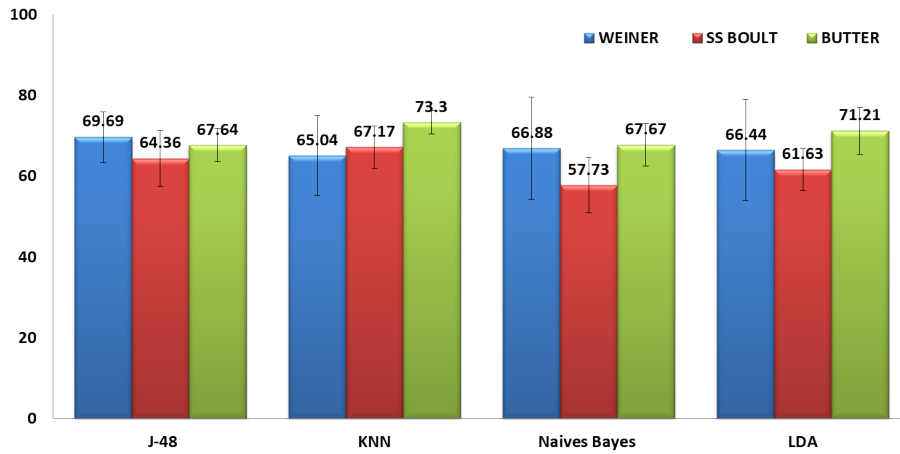


Figure 3.4: Column graph of average classification accuracy using four classifiers and three filters after dimensionality reduction

Butterworth filter achieved a classification accuracy of 73.3% with KNN as a classifier. Wiener filter achieved maximum accuracy of 69.7% using J-48 classifier. SS filter attained an accuracy of 67.17 % with KNN classifier. The classifiers attained almost comparable performance with different classifiers due to the robustness of the reduced feature set.

Here, a greedy search method is used to search the minimum number of features with the wrapper-based evaluator. The minimized set of features obtained from the evaluator were then used for classification. The results are presented in Tables 3.2, 3.3 and 3.4.

In Tables 3.2, 3.3 and 3.4, it can be observed that the Butterworth filter used only 8 features to obtain the same classification accuracy with KNN classifier. SS used 9 features, and Wiener used 7 features. This shows how dimensionality reduction can help bring down the computational complexity without compromising on the classification accuracy. The reduced computational complexity helps bring down the delay in decision making for real-time control.

3.4.3 Confusion matrix

The confusion matrices for the three filters are shown in Figure 3.5. The classifier that performs the best in terms of the accuracy is selected for each filter. From the confusion matrix, the difference in accuracy for each movement can be observed.

Classifier	No of features per channel	Classification Accuracy% (Std dev)
J-48	8	67.64 (4.1)
KNN	8	73.3 (2.9)
Naives Bayes	6	67.67 (5.3)
LDA	12	71.21 (5.8)

Table 3.2: Average classification accuracy after feature reduction with greedy stepwise search method after applying Butterworth filter

Classifier	No of features per channel	Classification Accuracy% (Std dev)
J-48	7	64.36 (6.9)
KNN	9	67.17 (5.3)
Naives Bayes	8	57.73 (6.8)
LDA	13	61.63 (5.2)

Table 3.3: Average classification accuracy after feature reduction with greedy stepwise search method after applying SS filter

Classifier	No of features per channel	Classification Accuracy% (Std dev)
J-48	7	69.69 (6.3)
KNN	8	65.04 (9.9)
Naives Bayes	6	66.88 (12.7)
LDA	10	66.44 (12.4)

Table 3.4: Average classification accuracy after feature reduction with greedy stepwise search method after applying Weiner filter

The difference in classification accuracy is due to the signals generated by muscles of dissimilar limbs and the force-length relationship of the muscle. This causes changes in signal shape, amplitude, frequency spectrum, and time scaling. The second factor is the significant degrees of nonlinear overlapping among each class and also the availability of only two channels.

3.4.4 Performance comparison in terms of processing time

The time taken for filtering is evaluated on a personal computer with 1.7 GHz Intel Core *i5* CPU (RAM 4GB) with Matlab. The time taken by Butterworth filter, Weiner filter, and SS filter is 38 ms, 48 ms, and 0.33 ms respectively. Rendering to the computational time of distinctive filters, SS delivers a substantial savings in computational cost of $(38 - 0.33)/38 * 100 = 99.13\%$ when compared with Butterworth filter and $(48 - 0.33)/48 * 100 = 99.31\%$ when compared with Weiner filter. The processing time consumed by the SS filter was least when compared to other filters. So whenever the system requires less delay or processing time, it is advisable to use the SS filter. Weiner filter is costly concerning the computational cost.

3.4.5 Discussion

This section gives a detailed discussion of the classification performance comparison of the three filters. Butterworth filter obtained marginally high classification accuracy when compared with the Weiner filter and SS filter. When it is required to detect the onset of the movement corrupted by background noise, the Weiner filter could be a better choice. But in terms of computational cost, SS filter is less expensive. The work also studies the effect of feature selection on the accuracy, and a reduced set of features are selected without compromising on the classification performance. The confusion matrix is also observed for three filters for different class movements.

3.5 Results and Discussion on novel MEDA filter

Experimental evaluation is conducted on seven subjects, the sEMG data is divided into 200 ms window, and features have been extracted from each window. The delay is chosen to be 200 ms since the total delay in the sEMG system needs to be kept

Target Class	CL	79.15	2.4	1.43	2.89	3.83	3.37	6.29	0.65
	FX	2.94	76.27	8.04	3.62	3.52	1.34	3.43	0.84
	EX	4.17	9.73	69.84	2.74	1.99	4.16	3.03	4.35
	HC	4.49	4.14	0	77	3.63	1.5	8.41	0.82
	KG	1.99	2.03	1.85	4.09	75.31	7.54	3.87	3.31
	WUD	3.15	1.7	5.76	0	6.16	52.05	18.93	12.24
	TD	4.61	0.78	2.19	6.4	4.51	3.46	71.42	6.63
	WRD	1.92	1.34	6.85	3.51	5.71	21.49	10.21	48.98
		CL	FX	EX	HC	KG	WUD	TD	WRD
Predicted Class									

(a)

Target Class	CL	67.79	1.61	2.24	7.25	5.83	1.67	9.69	3.92
	FX	4.13	64.64	5.69	7.99	2.34	2.68	5.55	6.98
	EX	4.53	3.57	69.81	3.26	2.91	5.9	2.22	7.8
	HC	7.49	3.72	1.89	63.99	4.45	4.37	8.67	5.42
	KG	2.41	2.44	3.26	3.3	71.43	4.68	8.24	4.24
	WUD	4.94	1.4	4.5	7.02	6.4	59.27	5.87	10.59
	TD	3.57	0.72	0.71	5.14	9.64	2.69	74.05	3.48
	WRD	3.11	0.92	8.13	5.61	6.75	7.14	5.65	62.69
		CL	FX	EX	HC	KG	WUD	TD	WRD
Predicted Class									

(b)

Target Class	CL	71.08	0	1.54	10.3	7.45	0.79	7.26	1.59
	FX	1.26	88.16	0	1.39	1.66	2.66	1.76	3.11
	EX	2.36	0.36	74.45	4.55	4.01	8.32	1.79	4.17
	HC	11.16	0.3	1.72	62.17	5.24	4.03	11.24	4.14
	KG	3.22	0.49	2.93	2.4	71.86	5.12	7.55	6.44
	WUD	2.99	2.11	6.42	2.16	6.47	65.07	4.16	10.62
	TD	3.58	0.26	0.75	6.65	6.76	2.3	76.95	2.75
	WRD	1.48	0.86	5.27	2.05	5.14	11.96	4.38	68.85
		CL	FX	EX	HC	KG	WUD	TD	WRD
Predicted Class									

(c)

Figure 3.5: Average confusion matrix across seven subjects using a) Weiner filter and J48 classifier b) SS filter and KNN classifier and c) Butterworth and KNN classifier

below 300 ms for real-time control (Khushaba et al., 2014). Total of 18 features per channel is extracted in both time and frequency domain.

For MEDA parameters, the value of N is chosen to be equal to the window length. For obtaining the filter length L , N is kept constant and filter length L is varied. The value of L is chosen based on keeping the processing time to be less than 50 ms (so that the total delay is less than 300ms). The processing time is calculated with Matlab on a PC with 1.7 GHz Intel Core i5 CPU and 4GB RAM.

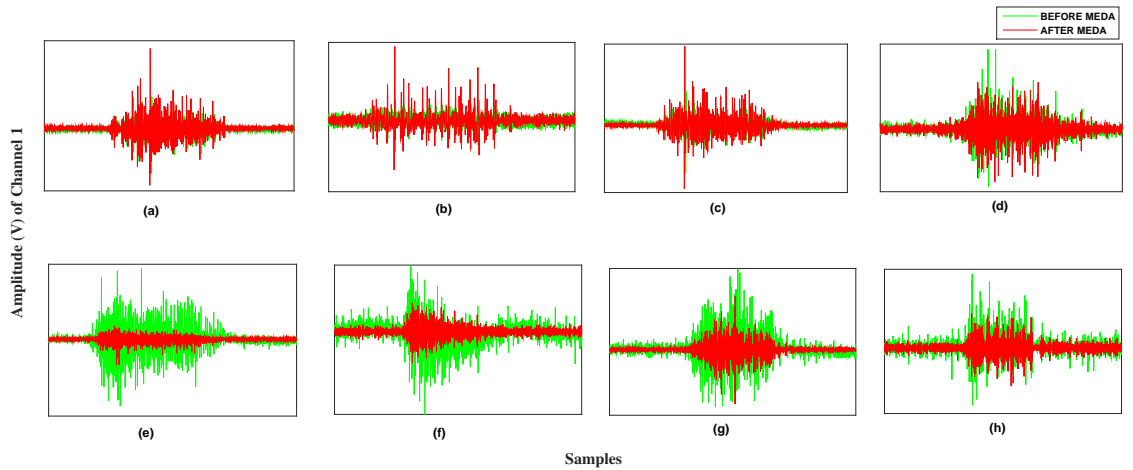
MATLAB software is used for signal processing and feature extraction step; then the extracted data have been fed into Weka tool for dimensionality reduction and classification.

The study is divided into three parts: (i) Demonstrating the advantage of the pre-processing step using MEDA on improving the classification accuracy, (ii) Removing redundant sEMG features and search the best subset of features and (iii) Comparing the proposed scheme with the best results obtained in Section 3.4 from Butterworth filter.

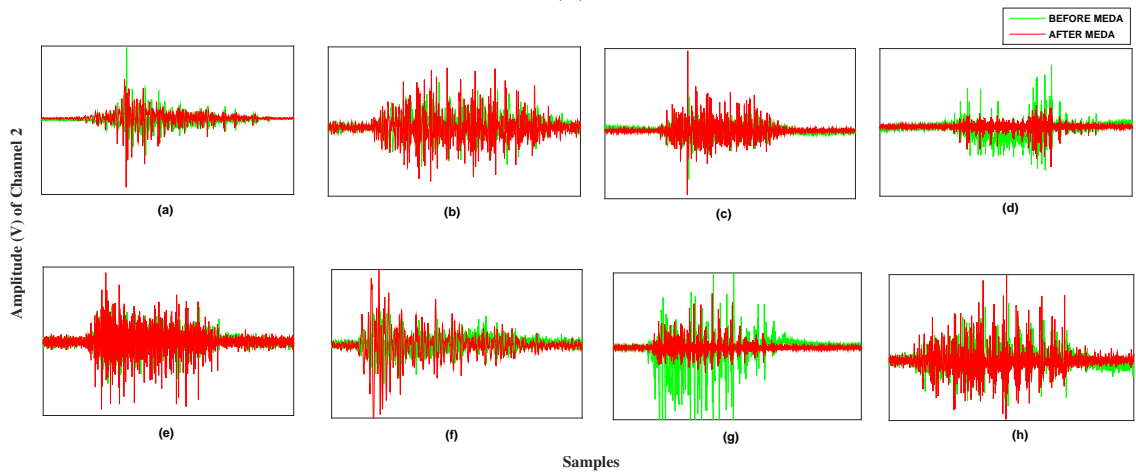
3.5.1 Impact of MEDA on classification accuracy

Experimental results are compared for eight different upper limb movements across seven subjects with and without applying MEDA before feature extraction. Example of the sEMG signals acquired from two channels with eight upper-limb movements before and after applying MEDA is illustrated in Figure 3.6. The results of the classifier were evaluated using ten-fold cross-validation for each subject. The original sEMG data was divided into 10 equal sub-data sets, single sub-data set will be re-trained as testing data and remaining 9 sub-data sets were used to train the classifier model in each fold and using each sub-data set once for training the whole procedure is repeated 10 times. Here, classification accuracy is used as the main index to indicate the impact of MEDA. Figure 3.7 shows the bar graph of average classification accuracy across seven subjects for different classifiers with and without employing the pre-processing step of MEDA.

From Figure 3.7 it is clear that MEDA generates greater discriminating information. The high classification accuracy achieved using MEDA suggests that more challenging problem can be addressed. From the figure, it is observed that the mean percentage increase in classification accuracy was 14.80%, 7.72%, 7.25%, and 20.48%



(a)



(b)

Figure 3.6: Noisy sEMG signal before applying MEDA (green colour) and de-noised sEMG signal after applying MEDA (red colour) for eight different movements (a) wrist flexion b) wrist radial deviation c) hand close d) tripod e) wrist extension f)wrist ulnar deviation g) cylindrical and h) key grip) for channel 1 (a) and channel 2 (b)

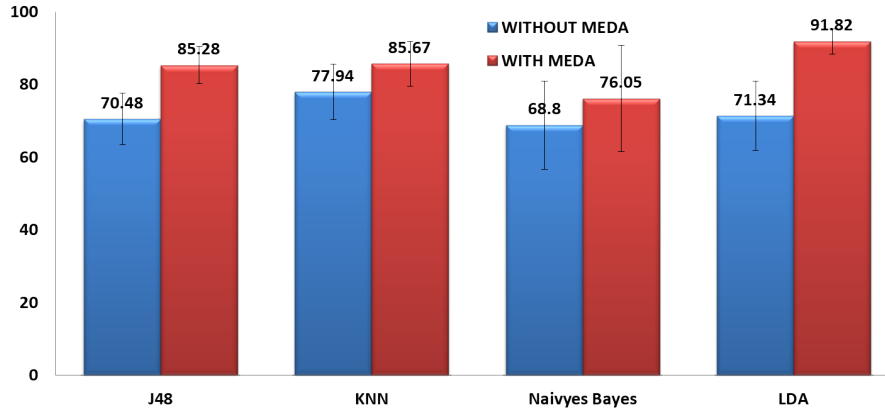


Figure 3.7: Bar plot of average classification accuracy across seven subjects for eight upper limb movements using J-48, k-nearest neighbours (KNN), Naives Bayes and Linear Discriminant Analysis (LDA) classifiers with and without MEDA using a window size of 200ms

Table 3.5: Classification accuracy and standard deviation of seven individual subjects using LDA as a classifier with and without MEDA

SUBJECTS	WITHOUT MEDA Accuracy%(Std dev)	WITH MEDA Accuracy%(Std dev)
Subject 1	75.94(6.48)	97.05(3.01)
Subject 2	82.66(6.81)	94.50(4.31)
Subject 3	82.66(6.81)	91.97(4.20)
Subject 4	59.66(6.90)	86.59(5.67)
Subject 5	60.65(5.86)	89.13(4.50)
Subject 6	68.90(8.01)	92.29(4.17)
Subject 7	68.92(6.46)	91.19(5.01)

respectively for J-48, KNN, Naive Bayes, and LDA classifiers. The result indicates that LDA performed better than the rest of the classifier on this data. However, to get such an improvement in accuracy, there was an additional increase in the computational burden of 35 ms due to the pre-processing. Table 3.5 shows the classification accuracy using LDA as a classifier with and without MEDA for an individual subject. The variation in classification accuracy among subjects is due to the difference in muscle anatomy. Changes in the performance may also be due to dissimilarity in muscle contraction effort and muscle fatigue among the subjects.

Confusion matrix for two subjects using LDA is shown in Figure 3.8 since LDA

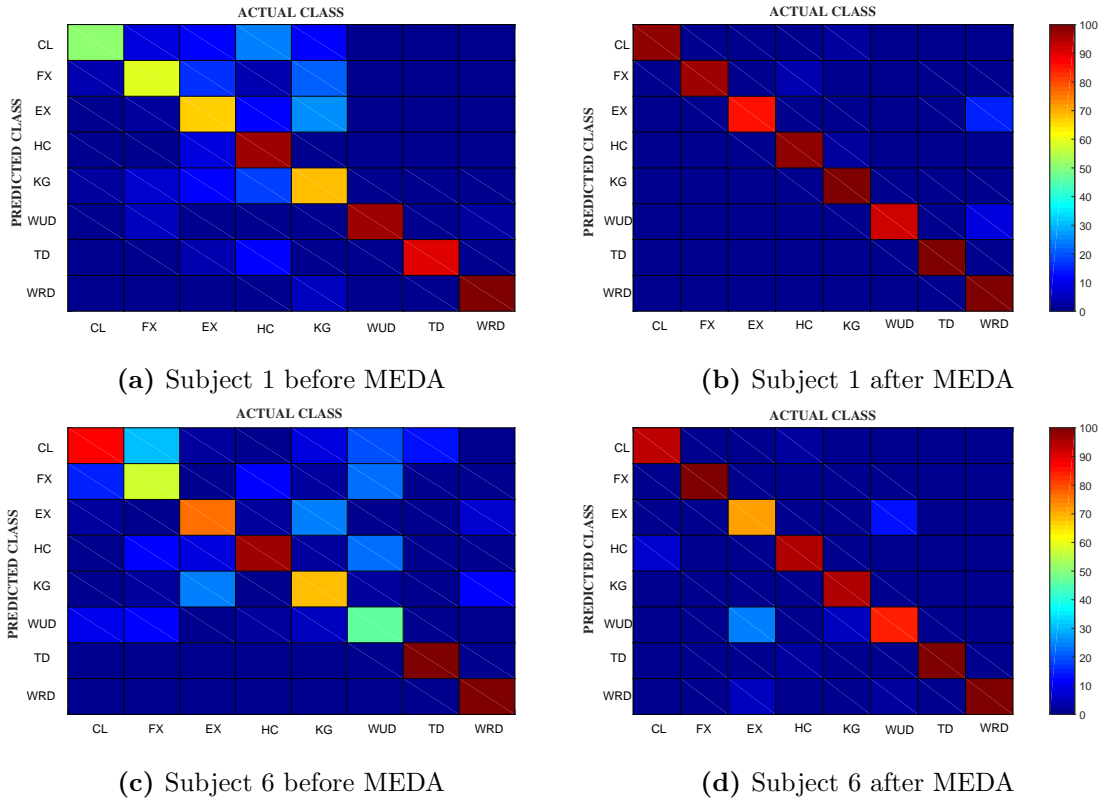


Figure 3.8: Confusion matrix showing classwise accuracy for eight classes of hand movements (wrist flexion (FX), wrist radial deviation (WRD), hand close (HC), tripod (TD), wrist extension (EX), wrist ulnar deviation (WUD), cylindrical (CL) and key grip (KG)) for two subjects before and after MEDA using LDA as a classifier

performed slightly better than other classifiers. From the figure, it can be observed that there were difficulties in separating hand movements before applying MEDA. The low accuracy without MEDA is due to difficulty in separating the patterns for different movements. Further, to observe the distribution of extracted features, scatter graph is plotted as shown in Figure 3.9. It is clear from the figure that without MEDA, the distribution of the features was overlapping, while with MEDA the data points were well separated. This leads to good classification accuracy.

3.5.1.1 Average confusion matrix for the classification of eight hand movements

For the investigation of different class separability of the proposed MEDA, the confusion matrix across seven subjects was averaged. The average confusion matrix is

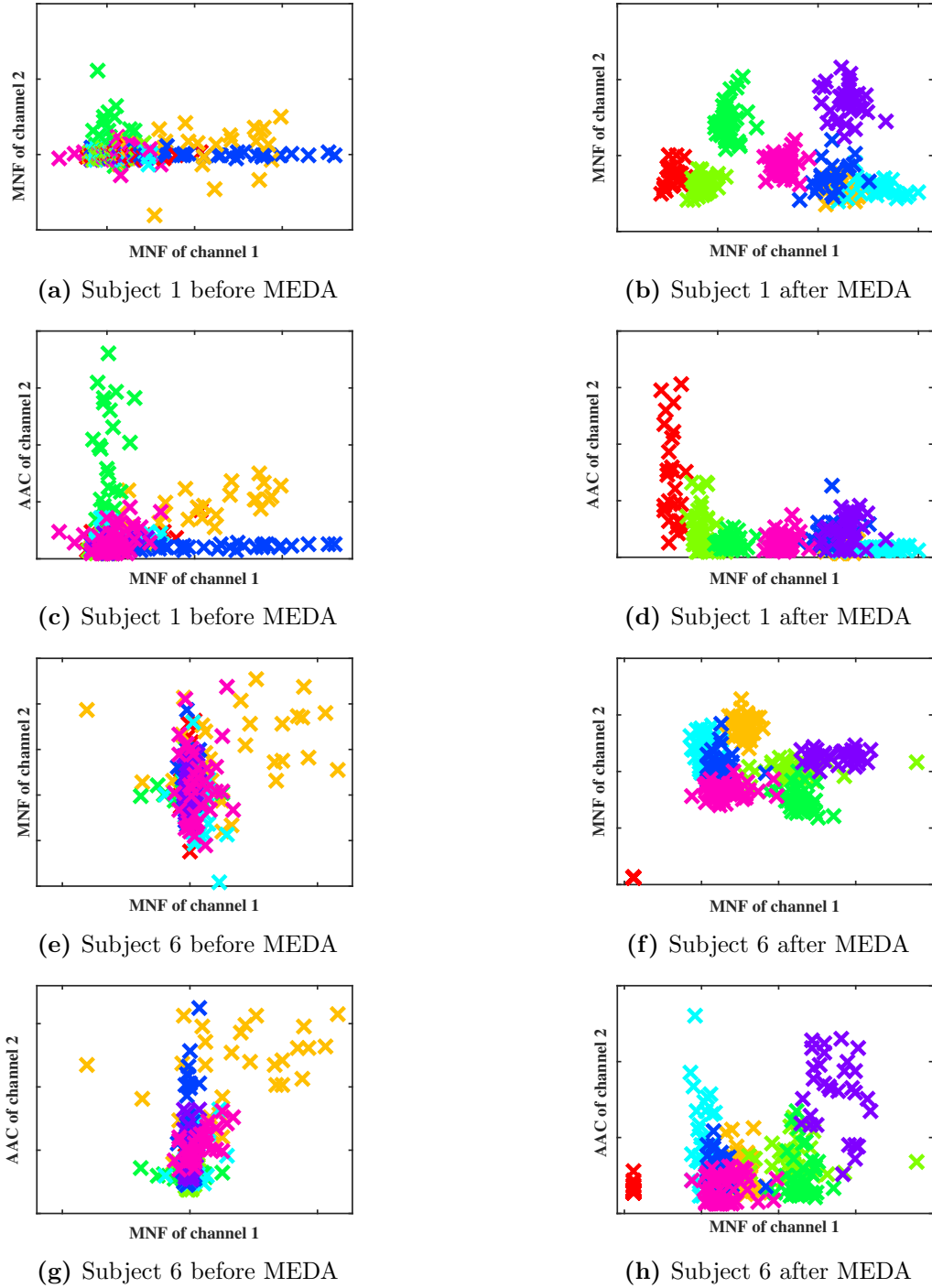


Figure 3.9: Scatter plot of a pair of sEMG features for different hand movements before and after applying MEDA for Subject 1 and Subject 6

Target Class	CL	94.1	0	0	3.05	0.76	0	1.6	0.48
	FX	0.92	92.71	0	3.29	0	0.46	2.16	0.46
	EX	0.32	0	85.85	0.22	2.04	5.73	0	5.84
	HC	3.27	2.33	0	84.27	2.25	0	7.42	0.46
	KG	0	0	0.35	0	96.36	3.29	0	0
	WUD	0	0	8.95	0.38	1.67	86.45	0	2.55
	TD	0.48	0.17	0	2.28	0	0.69	96.02	0.36
	WRD	0.4	1.9	0.6	0	0	0.73	0.6	95.77
		CL	FX	EX	HC	KG	WUD	TD	WRD
Predicted Class									

Figure 3.10: Average classification accuracy across seven subjects using LDA as a classifier after applying MEDA for eight classes of hand movements (wrist flexion (FX), wrist radial deviation (WRD), hand close (HC), tripod (TD), wrist extension (EX), wrist ulnar deviation (WUD), cylindrical (CL) and key grip (KG))

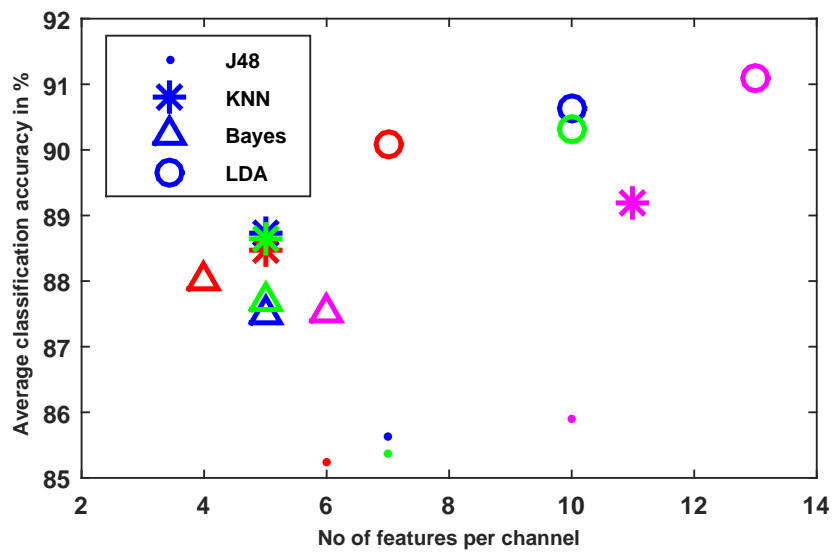
as shown in Figure 3.10 for LDA as a classifier. From the diagonal of the confusion matrix, it can be observed that the classifiers were successful in classifying different hand movements. However, there were difficulties in separating wrist extension (EX), hand close (HC) and wrist ulnar deviation (WUD) from the other movements. The misclassification could be due to the overlapping of patterns associated with the movements and also the availability of only two channels.

The maximum classification accuracy with MEDA was $\approx 91\%$ using LDA as a classifier which seems acceptable for two sEMG channels in comparison to other work from the literature. The results also suggest the success of classifying eight different movements using two channels sEMG system.

3.5.2 Performance of MEDA with reduced feature set

The main objective in the second part is to find the smallest subset of features that best interacts together and achieves high classification accuracies. Experimental results are compared using the wrapper method as an evaluator with the four classifiers. The four search methods namely Particle Swarm Optimisation (PSO), best first, linear forward selection and greedy stepwise for each classifier were employed to search the most important subset of features. The average classification accuracy of different classifiers for different search strategy is plotted with the corresponding average number of selected features per channel in Figure 3.11 across seven subjects. The maximum and minimum standard deviation obtained was $\pm 6\%$ and $\pm 3\%$ respectively.

The results from Figure 3.11 indicate that all classifiers achieved similar performance due to the removal of redundant and irrelevant features using search methods across classifiers. The desired number of selected features varied between four and thirteen. It was observed that for achieving the same classification accuracy, PSO used the highest number of features while the greedy stepwise used the least. The minimal feature set was obtained using greedy stepwise search method with Naive Bayes as a classifier, and the combination gave a classification accuracy of $88 \pm 6\%$. The selected features were MNF, AAC, ApEn, and DASDV. These features were selected because removal of these will result in huge performance deterioration of the classifier.



The colours blue, red, pink and green indicates best first, greedy stepwise, PSO and Linear forward selection search method respectively.

Figure 3.11: Average classification accuracy after feature reduction using with J-48, k-nearest neighbours (KNN), Naives Bayes and Linear Discriminant Analysis (LDA) classifiers with best first, greedy stepwise, PSO and Linear forward selection search method across seven subjects for eight upper limb movements, after applying MEDA

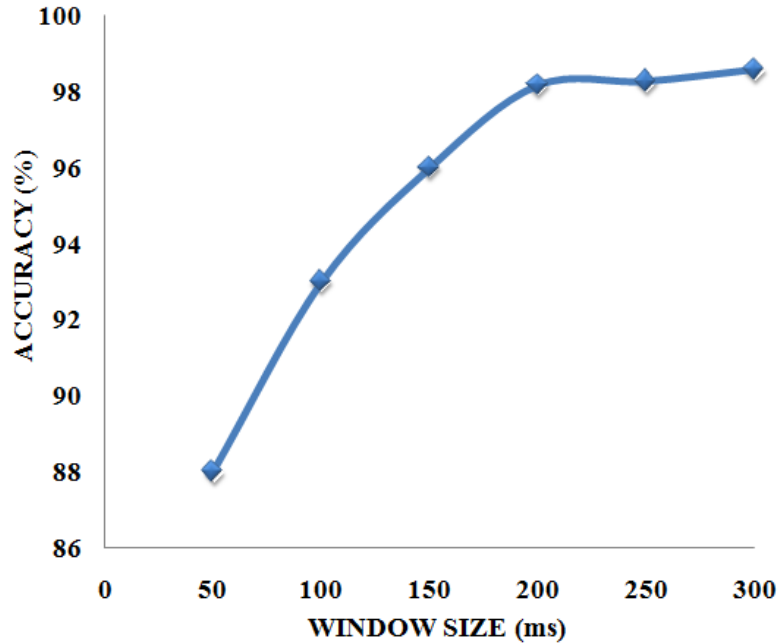


Figure 3.12: Average classification accuracy for eight upper limb movement with varying window size using MEDA

3.5.3 Effect of window size on accuracy

The classification accuracy of eight movements in response to sEMG window size variation was studied using Naive Bayes classifier on a single subject. Figure 3.12 shows the classification accuracy; all the window size used 36 features with MEDA as a pre-processing step. It can be observed from the figure 3.12 that the classification accuracy increased as the window size increased to an optimal value beyond which the curve saturates. The window length of 200 ms was chosen for faster system response.

3.5.4 Performance Comparison with other noise reducing method

The performance of the proposed MEDA method is compared against 4th order Butterworth bandpass filter (20 Hz to 500 Hz). Here the comparison is made with Butterworth because the Butterworth filter had a marginally better performance with respect to the Wiener and SS filter. Figure 3.13 shows the bar graph of average classification accuracy across seven subjects for different classifiers with Butterworth filter and MEDA. From the bar graph, it is observed that the performance of MEDA is better than that of Butterworth and mean percentage increase in classification ac-

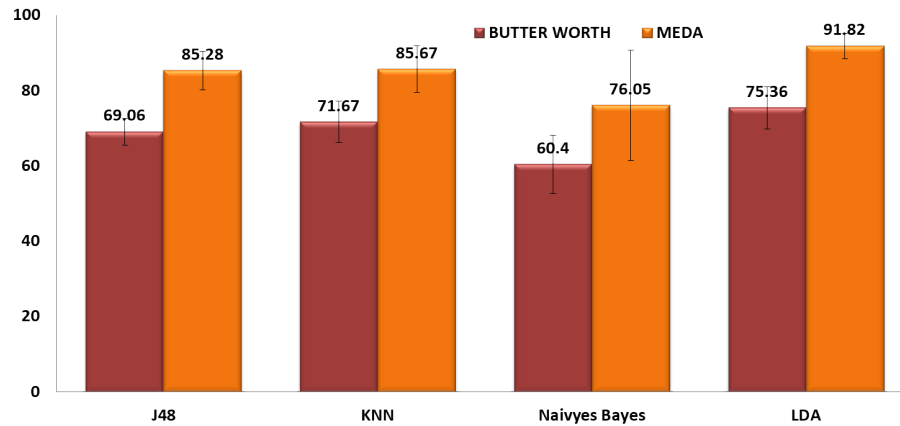


Figure 3.13: Bar plot of average classification accuracy across seven subjects for eight upper limb movements using J-48, k-nearest neighbors (KNN), Naive Bayes and Linear Discriminant Analysis (LDA) classifiers for Butterworth (red) and MEDA (orange) using a window size of 200 ms

accuracy was 16%, 14%, 16%, and 16% respectively for J-48, KNN, Naive Bayes and LDA classifiers.

The processing time taken for MEDA and Butterworth was calculated within Matlab on a PC with 1.7 GHz Intel Core i5 CPU and 4 GB RAM. For a fixed window length N , the time taken for Butterworth filter was 38 ms and for MEDA 35 ms. Thus, MEDA can be preferred over Butterworth filter as it provides around 8% savings in the computational cost, with an additional 16% increase in the classification accuracy.

3.6 Summary

In this chapter, a pre-processing method MEDA was proposed for sEMG application. The results indicate the significance of MEDA in achieving improved classification accuracy across subjects. The method recovers the output signal with a maximum value of kurtosis, which in turn enhances the classification accuracy. The redundant sEMG features were removed, and the best subset of features that characterize the different movements was obtained. The performance of three commonly used pre-processing method, namely Weiner, SS, and Butterworth filter was discussed. The performance of MEDA was compared with the Butterworth filter since it performed better than Weiner and SS filters. The results indicated the significance of the proposed MEDA

in the context of PR based MEC.

Chapter 4

Reducing the Effect of Force Variation and Wrist Orientation on Pattern Recognition of Myoelectric Hand Prostheses Control

4.1 Introduction

PR of sEMG signals has been used to control prosthetic devices with the aid of advanced signal processing methods (Adewuyi et al., 2017). Though high classification accuracy of around 98% has been reported in the literature, the practical deployment of the prostheses has not taken place. This is due to the gap between research and clinical study (Peng et al., 2013). EMG PR-based control has shown great promise in predefined settings in laboratory conditions. For EMG PR-based control to be commercially available, real-time factors which affect the performance have to be taken into consideration (Adewuyi et al., 2016). Many of the physical constraints such as wrist orientation, force variation, electrode shift, limb variation, etc., degrade the performance of PR. The studies conducted in the laboratory will have the upper limb typically in a single position, and classification accuracy thus reported may not be conceived in practice. Hence the PR scheme has to be designed by considering these factors (Earley and Hargrove, 2016). Two of the main factors that affects the clinical application are force level variation and wrist orientation. Force level changes that

can arise due to activities such as lifting of heavy objects, handling mechanical tools, etc., which can occasionally happen (Shin et al., 2016). Biologically, most changes in force are due to changes in the effort level. Amputees with functional wrist preserve the ability to move the wrist and are essential for their routine activity. If the PR system is not trained for such scenarios, it misclassifies the pattern and produces the wrong control decisions. Therefore, this chapter intends to investigate the effect of force level changes and wrist orientation on the classification accuracy of the PR.

Previous research to overcome the effect of force level variation used sophisticated feature selection methods, which often required a higher degree of computation. The classification methods are of three types: a) feature-based, b) sequence distance based, and c) model-based. The present work proposes the use of the sequence classification approach, which does not possess evident features and uses the complete data sequence for the classification. The method has been widely used in handwriting recognition, which inspired the present work (Huang et al., 2010). In a sequence distance-based classification, the similarity between sequences is measured by a distance function, which defines the quality of the classification (Xing et al., 2010). Dynamic time warping (DTW) calculates the similarity between two series using a distance measure and has been used previously for the classification of hand movements (AbdelMaseeh et al., 2015). The major advantage of using the DTW method is a better performance with low computational time.

DTW is used to overcome force level variation in the first part, then the same algorithm is used for developing a wrist independent scheme in the later section.

4.1.1 Study on Force Level Variation

In most of the previous works, the performance of the method was evaluated on intact subjects rather than on amputees, and it is not known whether these methods can be generalized to amputees since, after the amputation, the muscle structure may change. Several methods were used to this end to overcome force level variation in the EMG classification including time-dependent power spectrum descriptors (TD-PSD) (Khushaba et al., 2016b), discrete Fourier transforms (He et al., 2015), time domain feature set (Scheme and Englehart, 2011), reduced spectral moments (Vuskovic and Du, 2005), a combination of time-domain and autoregressive model parameters (Os-koei and Hu, 2007), and wavelet features (Al-Timemy et al., 2015). Previous work

involved training from all the force levels, that the subject exerted during testing. However, training at all force levels applies only to intact-limbed subjects. Training must be done at a lower or medium force level, for robust applications in amputees. This is to reduce the training time and more importantly, because research shows that amputees are comfortable training in low or medium force levels, rather than at a high force level (Nazarpour et al., 2013).

In recent literature, Khushaba et al. (2016b) made a thorough study on the impact of force level variation and used the TD-PSD method to diminish the effect of muscular contraction levels. The sEMG records from six classes of hand actions at three force levels were considered, and the accuracy of up to 91% was attained. The technique achieved better performance than previously used methods. The database only contains data from intact-limbed subjects. Hence, the database from Al-Timemy et al. (2015) is also used in the present study, which has data extracted from nine amputee subjects executing six instructions of motions with three different force levels. The method used by Al-Timemy et al. (2015) to overcome force level variation for amputees was the same as used by Khushaba et al. (2016b).

The present research examines the practical problem of force level variation for PR-based systems when used by intact-limbed subjects as well as amputees. In the first database, the effectiveness of the DTW method is tested on intact-limbed subjects in terms of classification accuracy. The following schemes are used to test the performance of the DTW method: *Scheme I* wherein the training is done with a part of the data pertaining to a single force level and tested on all possible force levels, and *Scheme II* where both the training and testing data include all three force levels. The work demonstrates the capability of DTW on accurate classification for varying force levels and wrist orientations by deploying these two strategies. The work does look upon efficient training strategies to reduce the errors in pattern recognition. The suitability of the algorithm to real-time applications is also demonstrated.

In contrast to the earlier methods, which relied on computationally expensive feature extraction and classification techniques, the proposed solution uses DTW, an efficient method to achieve better performance. DTW has been widely used in speech processing, gesture recognition, and even in pattern recognition of biomedical signals (Mazandarani and Mohebbi, 2018). Adopting this simpler approach also reduces the time required for making the decision, significantly bringing down the cost of the hardware. Training only at a specific force level is considered for amputee subjects,

as this is the closest to a practical situation. Also, the DTW method is compared with the TD-PSD method regarding classification accuracy and computational cost. The main contributions of the study are: 1) proposing DTW as an alternative to the existing method for improving the robustness of a PR based myoelectric system in the presence of force level variation; and 2) demonstrating an improvement in classification accuracy when trained at a low force level with amputees in comparison with the TD-PSD scheme (Khushaba et al., 2016b, Al-Timemy et al., 2015), and with a reduced computational time. The results of the present study could help in designing a more robust and viable sEMG pattern recognition system for upper limb prostheses.

4.1.2 Study on the changes in Wrist Orientation

This study focuses on the classification performance of myoelectric controller at three different orientations. This work also uses simple Dynamic Time Warping (DTW) method to achieve high performance in terms of classification accuracy and less delay. The database of the intact-limbed subjects is used here since the amputee database did not have the data for varying wrist orientation. The classification of hand movements is done by calculating the distance between two sequences and finding the similarities between them. The primary objective of the study was to evaluate PR system at three different wrist orientations using DTW technique. The above is tested with two protocols: *Protocol I*: Training using the data generated from a particular wrist orientation and testing it with the remaining data, and, *Protocol II*: Training using data generated from all the possible wrist orientations and testing for all wrist orientation. The study validates DTW for changeable wrist orientations by testing the above two training protocols .

4.2 Methodology

Two databases were used to demonstrate the effectiveness of the DTW method. The first database has sEMG signals from non-amputee subjects for six hand motions at three force levels each, carried out at three different wrist orientations. The second database is the amputee database for six hand motions, each at three force levels at a single wrist orientation.

4.2.1 DATASET I: Intact-Limbed Subjects

4.2.1.1 Subjects and Data Acquisition

In the present work, the database from Khushaba et al. (2016b) is utilized. The database enables the comparison of the present work to the state-of-the-art to overcome force level variations and changes in the wrist orientation. The database of Khushaba et al. (2016b) consists of sEMG signals recorded from ten able-bodied subjects, who had no previous familiarity with the myoelectric framework. The age group varied between 20 to 30 years with forearm diameter of 26.6 ± 2.4 cm.

The sEMG signals were acquired from six sensors (Delsys DE 2.x series EMG sensors). The electrodes (bipolar) used were non-invasive 2-slot adhesive skin interfaces mounted on each of the sEMG sensors attached to the skin. A reference electrode (Dermatode reference electrode) was positioned near the wrist of each subject. The six electrodes were placed at equal distances around the forearm of the subject. Then, the sEMG signal was amplified with the gain of 1000 and band pass filtered between 20-450 Hz. The data was sampled at 4 kHz using a 12-bit ADC from National Instruments (BNC-2090). The database also contained data from the accelerometers attached to the wrist. However, this has not been included in the present study.

4.2.1.2 Experimental Protocol

The data collection strategy adopted in the work of Khushaba et al. (2016b) is briefly described in this section for better clarity. The subjects have to undergo a preparatory session before beginning the test. Six classes of movements were performed: a) hand close (C1), b) hand open (C2), c) wrist extension (C3), d) wrist flexion (C4), e) ulnar deviation (C5), and f) radial deviation (C6). The subjects repeated each of these six hand motions at three different force levels, i.e., low, medium, and high. Figure 4.1 shows a time series plot of an individual trial for varying force levels when a hand close movement was performed. The database also contains the data described above for three different forearm orientations (Orientation 1, Orientation 2, and Orientation 3) as shown in Figure 4.2. Thus, the total number of trials performed on a subject equals to 162 (3 forearm orientations \times 6 movements \times 3 force levels \times 3 trials/movement). Each trial lasted for 5s with a 10s break in between. The raw sEMG signals were displayed on the screen to help the subject to generate the movement with the necessary force level.

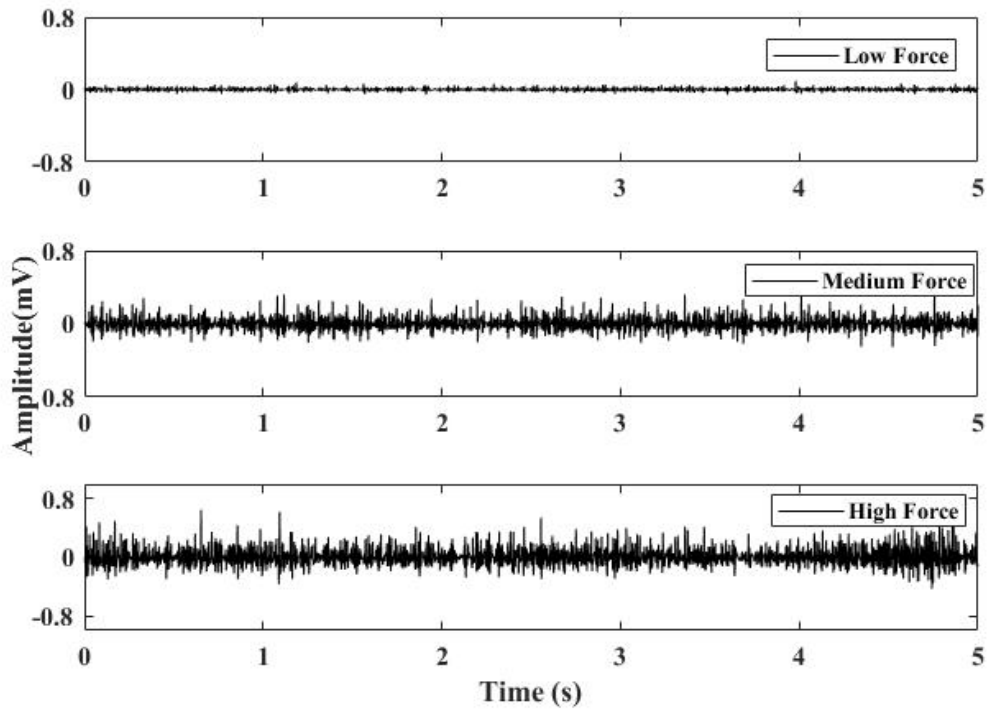


Figure 4.1: Three force levels acquired from single channel sEMG signal for hand close movement

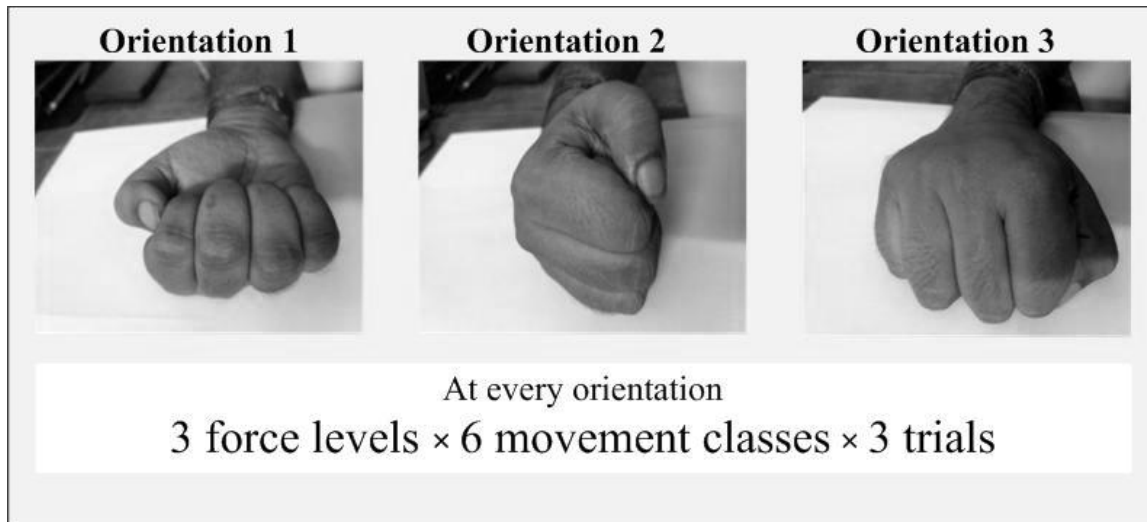


Figure 4.2: Data collection at three forearm orientations at three force levels at each movement

4.2.2 DATASET II: Amputee Subjects

4.2.2.1 Subjects and Data Acquisition

The second database is taken from Al-Timemy et al. (2015) and consists of sEMG signals recorded from nine amputees. The database was collected after getting approval from the local ethical committee. The age group varied between 20 and 57 years, in which the first seven subjects did not use prostheses, and the remaining two used one for a brief duration. A detailed description of the dataset can be found in Al-Timemy et al. (2015).

The Ag/AgCl electrodes (bipolar) (Tyco Healthcare, Germany) connected to a differential amplifier, placed around the left stump were used to acquire sEMG signals from eight channels. The electrode locations can be seen in Al-Timemy et al. (2015). The European recommendations (SENIAM) for the EMG were followed for the placement of the surface electrodes, and to mark the electrode locations, the elbow joint was used as a reference. The channels were connected to differential amplifiers with a gain factor of 1000 per channel and band pass filtered between 20-450 Hz. Finally, a custom-built multi-channel sEMG acquisition system acquired the signal at a sampling rate of 2 kHz using a 16-bit ADC from National Instruments (USB-6210).

4.2.2.2 Experimental Protocol

Six movements were performed: a) thumb flexion (P1), b) index flexion (P2), c) fine pinch (P3), d) tripod grip (P4), e) hook grip (P5), and f) spherical grip (P6). The amputees were asked to look at the signals on the screen to produce the required force level. They were given time to familiarize themselves with the different force levels. The forces at lower and higher levels were recorded than the normal force with which the prosthetic works. This was simulated since the force level changes during daily life usage. The sEMG data was recorded from the amputated hand. The amputees used their intact hand to generate the movement with the required force level. The signal was displayed in LABVIEW (National Instruments) to help the amputees produce the required force level. The amputees produced three force levels (i.e., low, medium, and high) for each of the six movements. Five to eight trials were recorded for each force level (Al-Timemy et al., 2015), for every amputee.

4.2.3 System Overview

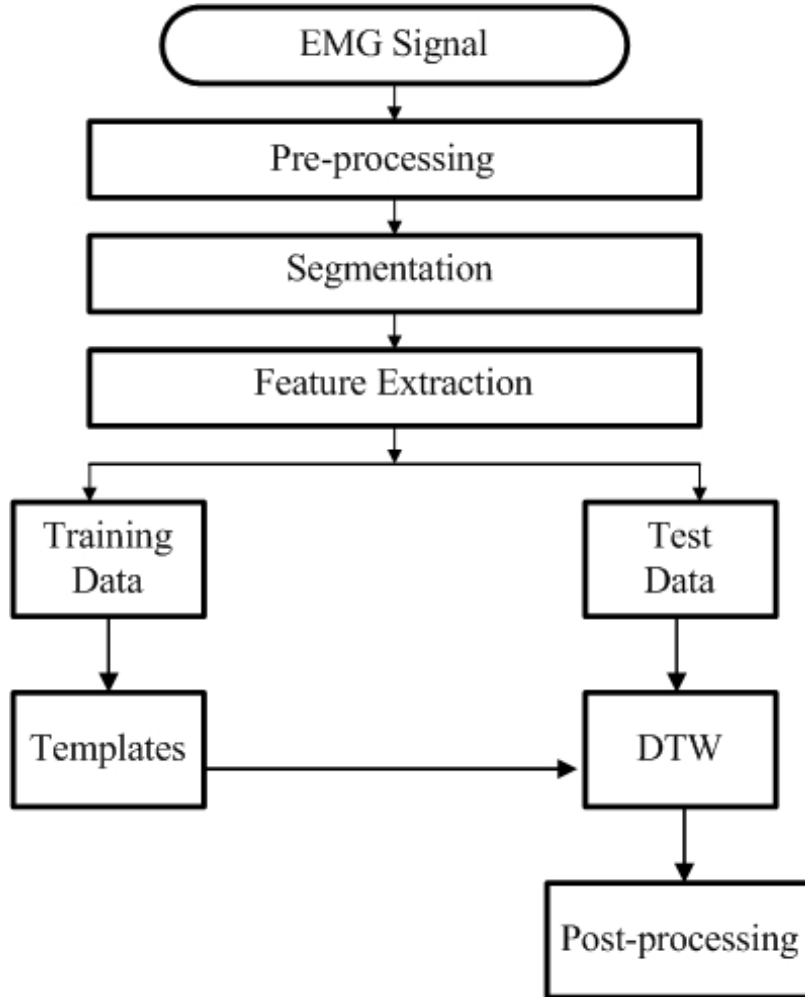


Figure 4.3: The overall framework of the suggested PR system

The information flow is shown in Figure 4.3. The blocks are explained individually in the following sections.

4.2.3.1 Pre-processing, Segmentation, and Feature Extraction

MATLAB software was used to perform the analysis. The recorded sEMG signal was sent to the pre-processing stage, where the noise was removed. The sEMG signals were filtered between 20-450 Hz using a fourth-order Butterworth filter to eliminate the effect of crosstalk and artifacts caused due to electrode movement. Also, a 50 Hz notch filter was used to remove the power line interference.

Two approaches were tested regarding the data segmentation, mainly to check their suitability for real-time decision-making, one that does not use a windowing scheme and takes the entire 5 s episode during a trial, and the other that uses a disjoint window of size 200 ms. The motivation behind the present study is to see the effect of the smaller window size on decision accuracy. The smaller window size also means that the time to make a decision is reduced significantly in real-time.

The well-known root mean square (RMS) value of the signal for a duration of 50 ms was used as the only feature in the present study. The RMS can measure the state of muscle activity, which represents the notable amplitude change of the sEMG signal widely used as a feature and also as a means to reduce the noise in the characterization of the sEMG signals.

4.2.3.2 Dynamic Time Warping (DTW)

The DTW provides a nonlinear alignment in the two-time series by calculating the distance more wisely. The best alignment between two-time sequence is considered. The two-time sequences are the sEMG data; one is the test data, and the other is the template, which is already stored. The users cannot keep their rhythm constant when they perform the same movement (e.g., hand close). The same movement can be performed at different force levels (low, medium, and high). Due to this, there will be a variation of patterns and some distortion, which is unavoidable. This results in pattern variations and distortions. DTW can be used to improve the performance of PR by permitting the transformation of the time series to identify similar profiles affected by distortion (Huang et al., 2010).

Consider computing the similarity between two arbitrary time series data as shown in Figure 4.4. In Figure 4.4(b), the Euclidean distance is used to measure the similarity. The Euclidean distance becomes misleading whenever there is a small distortion in the time axis. The distortion due to varying force levels is addressed in this work. It can be observed in Figure 4.4(b) that although the two sequences have the same waveform, they are not well aligned in the time axis. Figure 4.4(a) represents the two-time series that are dissimilar in the Euclidean distance. To align them in the time axis, the DTW algorithm provides a nonlinear mapping resulting in Figure 4.4(d). In the Euclidean distance, the two-time series have approximately the same overall waveforms but are not close to each other. The DTW warps the one-time series nonlinearity to calculate the distance with the other time series more wisely [Figure 4.4(c) and

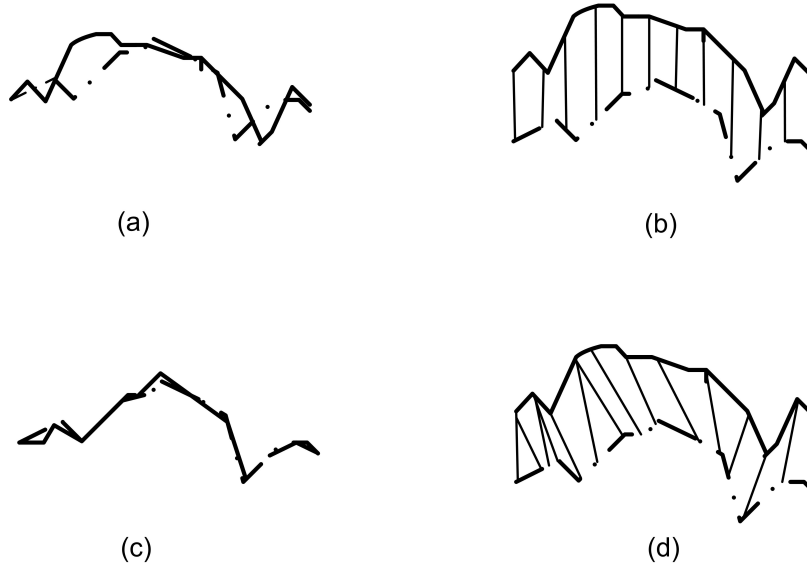


Figure 4.4: (a) In Euclidean distance, the two time series are not similar. (b) The alignment in time axis is not well; although they have same overall waveforms. (c) After DTW a refined distance measure is calculated. (d) Nonlinear alignment is provided by DTW for the two time series

Figure 4.4(d)].

Consider two sEMG signals (training template and test signal) to be compared, A and B of length n , $n \in N$. Let $A = \{a_1, a_2, a_3, \dots, a_n\}$ and $B = \{b_1, b_2, b_3, \dots, b_n\}$. The DTW aligns A and B by using the following two steps (Senin, 2008, Vial et al., 2009):

Step 1: Distance matrix C is constructed by pair-wise distance between A and B . Consider matrix C with dimension $n \times n$, where, the (i_{th}, j_{th}) element of matrix contains the distance d_{ij} .

$$C \in R^{n \times n} : d_{ij} = \|a_i - b_j\|, i \in [1 : n], j \in [1 : n] \quad (4.1)$$

This distance matrix C is called the local cost matrix for the sequence A and B .

Step 2: After the local cost matrix is constructed, a warping path that defines the mapping between A and B is found. Let W represents the warping path. The k_{th} element of W is defined as $w_k = (i, j)$. Therefore, we have:

$$W = w_1, w_2, w_3, \dots, w_k, \dots, w_K, \quad n \leq K \leq 2n - 1 \quad (4.2)$$

The warping path W must satisfy the following criteria: 1) Boundary condition: $w_1 = (1, 1)$ and $w_K = (n, n)$. The starting and ending point of the warping path must be diagonally opposite to the cost matrix; 2) Monotonicity condition: Given $w_k = (i, j)$, then $w_{k-1} = (i', j')$, where, $i - i' \geq 0$ and $j - j' \geq 0$. This makes the points in W to preserve the time-ordering; and 3) Continuity condition: Given $w_k = (i, j)$, then $w_{k-1} = (i', j')$, where, $i - i' \leq 1$ and $j - j' \leq 1$. This makes the allowable step in the warping path to be restricted to the adjacent cells.

Several warping paths fulfill the above conditions. But the path which minimizes the warping cost is of interest.

$$DTW(A, B) = \min \left(\sqrt{\sum_{k=1}^K w_k} \right) \quad (4.3)$$

Dynamic warping is used to find the path with minimum cost. The warp path $\lambda(i, j)$ is obtained by the sum of the distance $d(i, j)$ found in the current cell and the minimum of the cumulative distances of the adjacent elements.

$$\lambda(i, j) = d(a_i, b_j) + \min\{\lambda(i-1, j-1), \lambda(i-1, j), \lambda(i, j-1)\} \quad (4.4)$$

To sum up, first, the cost matrix is filled one column at a time from the left to the right from the bottom. When the cost matrix is built, a warped path must be found starting from $\lambda(n, n)$ to $\lambda(1, 1)$. The warping path is found by greedy search as described in (4.4). The smallest warping cost performs the matching of the two signals.

The template here is the training data from the first two trials, and the length of the template is the length of the trials which is the same for all cases. After creating the template, the DTW algorithm is applied to the test data to find the matching time points in the template. The distance between the sEMG signals for the performed hand movement template and the trained template is calculated. The hand movement is identified with the template of the smallest distance.

The example for hand close (C1) movement recognition is illustrated in Figure 4.5. The sEMG signals for hand close movement is plotted in the left Figure 4.5(a) with all six sEMG channels, which match the six forearm muscles. Then, the sEMG signal RMS feature is extracted, which is represented as a continuous line [Figure 4.5(b)]. A comparison is made with the six templates, which are the training templates of

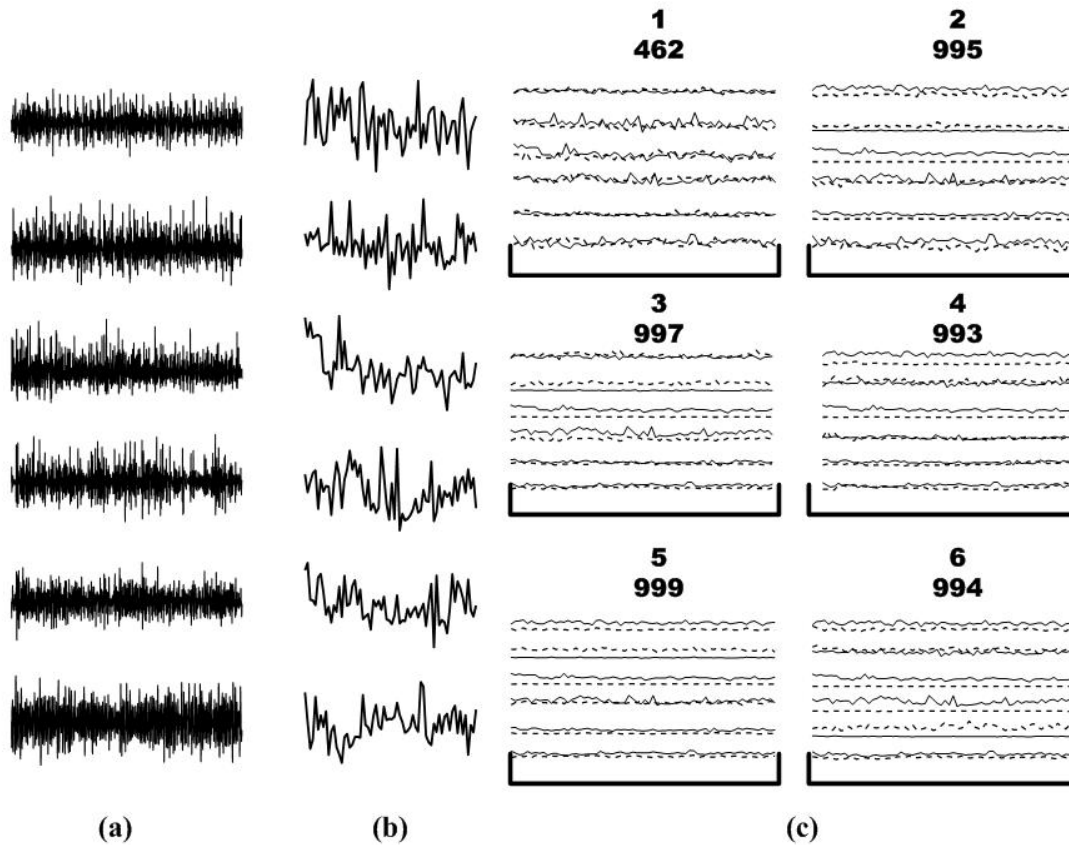


Figure 4.5: An example of hand movement recognition. (a) After filtering, the sEMG signal for hand close movement (b) Feature extraction is done by taking the RMS which is represented in continuous line (c) Comparison is done with all the templates (dotted line), the system recognizes the hand movement corresponding to the minimum distance. The x axis represents the time in seconds which is of 5 s duration. The y axis represents the (a) amplitude of sEMG signal in milli-Volts; which ranges between -0.8 mV and +0.8 mV (b)RMS value of the raw sEMG signal in (a) which ranges between 0 and 0.15.

the DTW [Figure 4.5(c)]. The intended movement is identified using the distance measure calculated by the DTW. The comparison is made on the right side as shown in Figure 4.5(c); the template for six hand movements is represented in the dotted line. The calculated distance between the training template and the test template is shown above the plots in Figure 4.5(c). The least distance corresponds to the performed hand movements, which is C1 in this example.

The post-processing is done to give this decision to an external prostheses hand from the decision generated using DTW. Classification accuracy is utilized to calculate the hand movement identification performance.

4.2.4 Data Analysis

4.2.4.1 DATASET I: Intact Limbed Subjects

The two schemes, as listed in Section 4.1, are employed for testing the execution of the framework proposed in Figure 4.3. The data from two out of the three trials of every subject is used to produce the training set, and the third trial is used for validation of the two schemes. As mentioned in Section 4.2 (i.e., 4.2.1), the effect of taking a shorter window on the classification performance is also studied here to check its feasibility for real-time implementation.

4.2.4.2 DATASET II: Amputee Subjects

In the case of an amputee practically using the prostheses, training should be done at a single force level. It is difficult for amputees to train data at a high force level due to fatigue, which may produce tremors on some occasions (Al-Timemy et al., 2015, Nazarpour et al., 2013). Hence for the amputee database, only training at a single force level is evaluated. In the present study, the first three trials were used for training, and the remainder (two to five trials) were used for testing.

4.2.5 Statistical Test

To test the statistical significance of the achieved results, one-way analysis of variance (ANOVA) was utilized. Also, the well-known two-way ANOVA was used, as multiple factors needed to be tested. An additional significance test known as the t-test was also used. The significance level was set to 0.05 for all the three tests.

4.3 Results on the study of force level variations

4.3.1 Experiments on DATASET I

In this section, the two training schemes briefly mentioned in Section 4.1 will be used and their performance with the DTW will be analyzed. The classification accuracy presented is averaged across ten subjects.

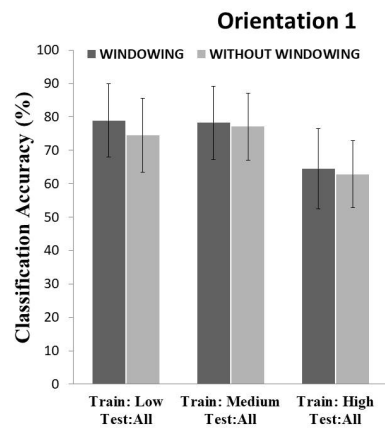
4.3.1.1 Experimental Scheme I : Training the DTW template on the part of the data pertaining to a single force level and testing on all possible force levels

The average classification accuracies for ten subjects are shown in Figure 4.6, where *Scheme I* is adopted. Figure 4.6 shows the results for all three orientations. The error bars represent the standard deviation across ten subjects. The following observations can be made from Figure 4.6 for all three possible forearm orientations: (i) there is a significant impact on the performance of the PR system when the subject executes unseen force levels. One-way ANOVA was applied to validate the statistical significance of the classification scores for the three force levels after DTW, which gave $p = 0.016$ at orientation 1, $p = 0.0024$ at orientation 2, and $p = 0.27$ at orientation 3. There was a significant effect of force level variation on the classification accuracy at orientation 1 and orientation 2 ($p < 0.05$), and no significant impact at orientation 3; (ii) the trend is similar across all the ten subjects since the error bar lies within $\pm 10\%$. The two-way ANOVA found no significant difference across the ten subjects ($p = 0.14$), and (iii) the effect of windowing (i.e., taking 200 ms data segments) is not significant on the performance of the PR system. To see the effect of windowing, the two-way ANOVA was applied. The values of p were 0.88, 0.74, and 0.82 at orientations 1, 2 and 3. There was no significant effect with and without windowing.

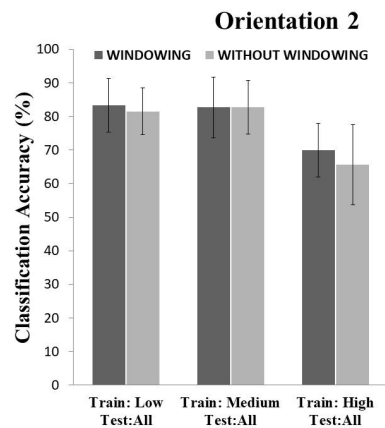
From Figure 4.6, the maximum classification accuracy was obtained at forearm orientation 2 when trained at a low force level (83.3%) and also at medium force level (82.7%). Relatively lower accuracy was obtained when trained at a high force level.

From this, it can be concluded that when the DTW template is trained with a single level of force, the classification accuracy is relatively poor and affects the performance of the PR system.

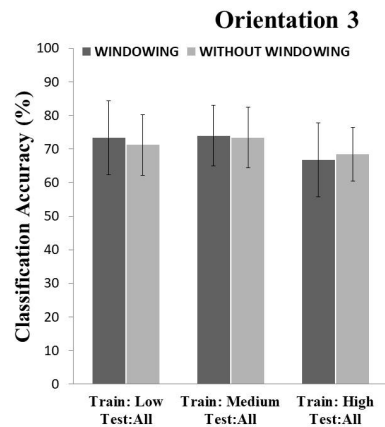
Figure 4.7 shows the average confusion matrix for the ten subjects with experimen-



(a)



(b)



(c)

Figure 4.6: Average classification accuracy with *Scheme I* obtained across ten subjects for six hand motions at orientation 1 (a), orientation 2 (b) and orientation 3 (c)

Target Class	C1	60	10	0	13.3	6.7	10
	C2	0	73.3	6.7	0	10	10
	C3	0	0	96.7	0	0	3.3
	C4	6.7	3.3	0	86.7	3.3	0
	C5	0	0	0	0	96.7	3.3
	C6	0	3.3	3.3	0	3.3	90
		C1	C2	C3	C4	C5	C6
		Predicted Class					

Figure 4.7: Average confusion matrix with *Scheme I* obtained across ten subjects for six hand movements (hand close (C1), hand open (C2), wrist extension (C3), wrist flexion (C4), ulnar deviation (C5), and radial deviation (C6)) at orientation 2

tal *Scheme I* at orientation 2 when training with low force. The average classification accuracy was 83.3%. Low classification accuracies were observed for hand close (C1), hand open (C2), and wrist extension (C4) movements ($< 90\%$). This will be further discussed further in the next section.

4.3.1.2 Experimental Scheme II: Training the DTW template with all three levels of force and testing it with all unseen force levels

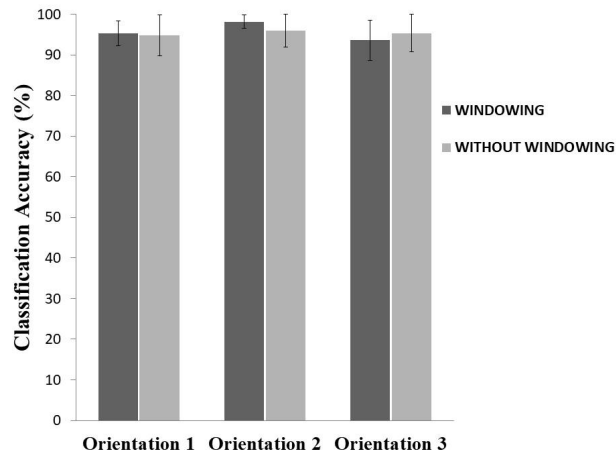


Figure 4.8: Average classification accuracy with *Scheme II* obtained across ten subjects for six hand motions from three different orientations

Figure 4.8 shows the average classification accuracy of the PR system when *Scheme II* is deployed. Similar to Figure 4.6, the following can be observed: (i) the accuracy is significantly not affected when a shorter window of 200 ms is used and the results are comparable with the case where the entire 5s data is used as the training and testing template. One-way ANOVA was applied to see the effect of windowing at each orientation. At orientations 1, 2, and 3, the values of p were 0.82, 0.22, and 0.46 respectively. There was no significant effect of windowing; and (ii) the results are consistent across the ten subjects. The one-way ANOVA showed that there is no significant difference across the ten subjects since the value of $p = 0.18$. However, it can be seen that in contrast to *Scheme I* (Figure 4.6), the accuracy has improved significantly owing to a wider training set and the results have become much more consistent with only a $\pm 5\%$ standard deviation. To validate this, one-way ANOVA was used. The values of p at each orientation (1, 2, and 3) was 0.0003, 0.0002,

and 0.0001 respectively. This indicated that there is a significant change in the classification accuracy in *Scheme II* when compared with *Scheme I*.

When deploying *Scheme II*, the average accuracy was always higher than 90%. Specifically, for orientation 2, it was as high as 98.3%, even when using a shorter 200 ms window. This is a significant improvement compared with the earlier reported works in this area.

This indicates the usability of the DTW for the PR system trained with all the force levels based on the analysis of the sEMG signals. From this, it can be concluded that training should be from all the force levels to increase the robustness of the sEMG PR system. This finding agrees with the work of Al-Timemy et al. (2015).

The DTW method was compared with the TD-PSD method by Khushaba et al. (2016b). The results of the evaluation are given in Table 4.1.

Table 4.1: Comparison of average classification accuracy for the TD-PSD method and the DTW method for DATASET I

Method	Classification accuracy %	Reference
Time-Dependent Power Spectrum Descriptors	93	(Khushaba et al., 2016b)
Dynamic Time Warping	98.3	Present study

The average confusion matrix for the ten subjects with the experimental *Scheme II* at orientation 2 is shown in Figure 4.9. From the confusion matrix, it can be observed that the DTW method was successful in classifying the hand motions of all classes with high accuracies ($> 90\%$). The movements hand close (C1), hand open (C2), wrist flexion (C4), and ulnar deviation (C5) were classified with a 100% accuracy.

4.3.2 Experiments on DATASET II

4.3.2.1 Experimental Scheme I: Training the DTW template on the part of the data pertaining to a single force level and testing on two unseen force levels

To test the generalization ability of the DTW method when implementing the same movement at different force levels, the data from an unseen force level was used for validation. Here, the windowing scheme with a 200 ms window is employed for the

Target Class	C1	100	0	0	0	0	0
	C2	0	100	0	0	0	0
	C3	0	0	96.7	0	0	3.3
	C4	0	0	0	100	0	0
	C5	0	0	0	0	100	0
	C6	3.3	0	0	0	3.3	93.3
		C1	C2	C3	C4	C5	C6
		Predicted Class					

Figure 4.9: Average confusion matrix with *Scheme II* obtained across ten subjects for six hand movements (hand close (C1), hand open (C2), wrist extension (C3), wrist flexion (C4), ulnar deviation (C5), and radial deviation (C6)) at orientation 2

validation of the DTW method for the amputee study. The main intention in choosing a 200 ms window is to keep the delay below 300 ms to achieve real-time control. For validating the method, the same scheme as Al-Timemy et al. (2015) was used in which the training data is acquired from a single force level and the testing data is taken from unseen force levels. Here, the comparison is made with the state-of-the-art TD-PSD method on the same database.

Table 4.2: Average classification accuracy (and the standard deviation in %) for nine amputees when trained with single force level and tested with unseen force level for the TD-PSD method and the DTW method with average processing time

Method	Low	Medium	High	Processing Time (ms)	Rectangular Window (ms)
TD-PSD	50 \pm 10	70 \pm 8	60 \pm 10	1.9	200
DTW	60 \pm 9	70 \pm 8	60 \pm 7	1.2	200

The average classification accuracy for nine amputees using *Scheme I* is shown in Table 4.2 along with the standard deviation. It can be seen that there is a difference in the accuracy obtained for individual amputees, which may be due to the difference in their amputation level and the time since amputation. As it is evident from the table, even though the accuracy is comparable with the TD-PSD while training the DTW with medium or high force levels, the proposed method achieved a 10% increase in classification accuracy when trained with a low force level. This was confirmed by the t-test with a p value of 0.03, which indicates that there is a significant difference. This is significant since amputees are comfortable training at lower or medium force levels (Al-Timemy et al., 2015, Nazarpour et al., 2013). Training at a higher force level is difficult for amputees.

The proposed method has been compared with the TD-PSD method on a personal computer with 1.7 GHz Intel Core i5 CPU (4GB RAM) using MATLAB. The processing time required for a 200 ms rectangular window is shown in Table 4.2. The DTW obtained a lower processing time and classification error when compared with the TD-PSD method.

The following can be inferred from the reported results: Firstly, there is a definite improvement in the classification results when using DTW trained at lower force levels in comparison with TD-PSD. A t-test was conducted for analyzing the statistical differences between the results achieved using DTW versus TD-PSD for nine amputees, each performing six movements at three force levels. There is a significant

improvement in classification accuracy when trained at a lower force level using DTW when compared to TD-PSD ($p = 0.03$). Secondly, the classification accuracy of both DTW and TD-PSD remained the same when trained at medium and higher force levels ($p = 1$). Thirdly, it is also evident that TD-PSD is more expensive in terms of computational cost than the DTW method.

4.4 Discussion on the study of force level variations

The main advantage of using the DTW method is that it can overcome the force level variability that affects the classification. Apart from the DTW method, many techniques have been used in the literature, most of them being complex for real-time implementation. In the present study, two datasets were used. In the first database, the performance of the DTW method was validated using two schemes and then compared with the previously used TD-PSD from the literature for non-amputee subjects. Since the database of Khushaba et al. (2016b) did not have amputee subject data, the database from Al-Timemy et al. (2015) was used to validate the DTW method for amputee subjects.

4.4.1 DATASET I: Intact-Limbed Subjects

The performance of the EMG PR should not vary for various force levels for practical usage. For this, the impact of force level variations on the myoelectric PR system has been studied. Recent literature reports multiple studies to tackle such issues with complex feature selection processes. In contrast, the aim in the present study is to use a simpler and computationally more efficient PR system, which can be deployed in real-time without compromising the accuracy. To check the utility of the proposed PR system, the classification accuracy was evaluated on ten individuals performing six hand movements at three different force levels, each at three different hand orientations. The effect of using shorter 200 ms windows on decision-making was also studied. The results indicate that the DTW method is less affected at different force levels and performs well as a PR scheme even when shorter data segments are available for decision-making. This significantly reduces the time to decision, making it a potential candidate for creating a robust, real-time PR system.

4.4.1.1 Impact of training methods on the performance of PR based myoelectric control under force level variation

In the experimental *Scheme I*, the performance of the DTW method was checked when using the data from one of the three force levels as the training template. The performance was low as seen in Figure 4.6. This finding agrees with the earlier work of Khushaba et al. (2016b). Low classification accuracy makes the training strategy adopted in *Scheme I* less suitable for the application. The low classification accuracy attained at individual force levels indicates that more information from other force levels should be included to improve the performance.

Additionally, it was observed that the performance was slightly better when low force or medium force was used instead of high force as the training template. This is due to the difficulty in producing a high force level when compared with generating low and medium force levels. Maintaining a high force is difficult for a substantial amount of time is difficult, and it causes fatigue.

An examination of the confusion matrix in Figure 4.7, when adopting *Scheme I*, reveals that the classification accuracy associated with the movements hand close (C1), hand open (C2), and wrist flexion (C4) were poor with respect to the other movements. The movements with lower error rates were wrist extension (C3), ulnar deviation (C5), and radial deviation (C6). The misclassification might be because of the variability of the force level and can be further improved by proper training.

Experimental *Scheme II* was employed to overcome the effect of force level variation, which uses all the three force levels to generate the training template. When adopting *Scheme II*, better performance was expected and is shown in Figure 4.8. The result shows a clear improvement in the DTW based PR system performance when deploying *Scheme II* obtaining an accuracy of 98.2%. This outcome of using the DTW method trained with all the force levels makes it suitable for real-time application.

The average confusion matrix across the ten subjects was calculated and is shown in Figure 4.9 to get a better understanding of the accuracy associated with each movement. It can be seen that four out of the six movements obtained 100% accuracy.

4.4.2 DATASET II: Amputee Subjects

The performance of the DTW method is studied under varying force level conditions and is found to be suitable for robust application. The DTW has been before for sEMG hand movement classification. The DTW method has never previously been investigated under force level variation on both intact and amputee subjects.

Force variation is one of the major obstacles for the practical implementation of the prostheses. The first database, which has data from ten intact-limbed subjects, was used to test the baseline performance of DTW under varying effort levels. The algorithm is further tested on amputee subjects. It performed better than the recently used TD-PSD method in terms of both accuracy and processing time. When considering training at a single force level for amputees, the results suggest that the DTW method provides a more dependable means of control than TD-PSD for six movements.

In the TD-PSD method, the error rates for lower force are much higher than the medium and high force levels. However, training an amputee at low and medium force level is relatively easy when compared with a high force level, since training at a higher force level requires a lot of effort and produces tremors in some cases (Al-Timemy et al., 2015, Nazarpour et al., 2013). This explains the importance of training at low and medium force levels rather than a high force level. With the suggested DTW method, as in Table 4.2, a 10% increase in classification accuracy was obtained when compared with the TD-PSD method with additional savings in computational cost making it an interesting alternative to the previously used PR schemes.

4.5 Results on the study of wrist orientation changes

The two training protocols are tested with the DTW algorithm to verify the suitability. The classification accuracy reported is averaged across ten subjects.

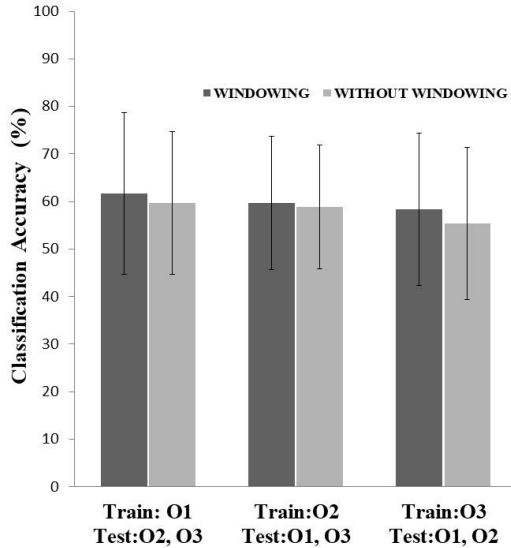


Figure 4.10: Average classification accuracy with *Training Protocol I* obtained across ten subjects for six hand motions

4.5.1 *Training Protocol I: Training the DTW template with the data generated at single wrist orientation and testing with the remaining two wrist orientations*

Figure 4.10 shows the average classification accuracy across ten subjects while implementing *Training Protocol I*. Error bars denote the standard deviation. From the figure, it can be observed that the classification accuracy while using the training data pertaining to any of the three orientation was almost the same which is quite poor. The error bar lies between $\pm 15\%$.

Further, it can be observed that the classification accuracy obtained is low. This is due to insufficient training data. The average accuracies obtained when trained at wrist orientations 1, 2 and 3 were 62%, 60% and 58% with windowing; and 60%, 59% and 55% without windowing respectively. To analyze the effect of windowing, a one-way ANOVA was applied to validate the statistical significance. From the statistical results, the values of $p = 0.79$ at orientation 1, $p = 0.9$ at orientation 2 and $p = 0.69$ at orientation 3 were obtained. Since the values of p were greater than 0.05 at all orientations, there was no significant effect with and without windowing.

The above results show that DTW accuracy is nearly the same across all wrist orientations. Further, the DTW must be trained with more data to obtain higher

accuracy.

4.5.2 *Training Protocol II*: Training the DTW template with the data generated at all wrist orientations and testing with unseen data from all orientations

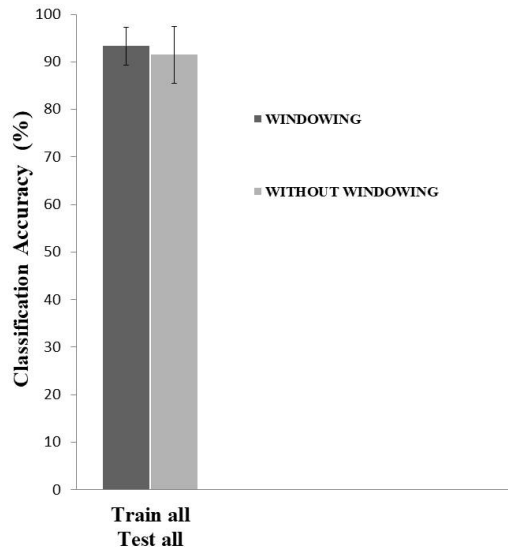


Figure 4.11: Average classification accuracy with *Training Protocol II* obtained across ten subjects for six hand motions

When *Training Protocol II* is implemented, the increase in accuracy is shown in Figure 4.11. From the column graph, it can be observed that the accuracy is comparable to with and without windowing. The error bar has reduced to $\pm 5\%$ which indicates that the results are consistent across trials and the classification accuracy has improved significantly by incorporating training data from the entire sampling space.

The maximum accuracy of 93.33% observed in this work is marginally higher than the earlier study on the same database as shown in Table 4.3. To see the effect of windowing, a one-way ANOVA was performed which resulted in a p value of 0.44 indicating that there is no significant effect of windowing and a shorter window duration of 200 ms is enough to do accurate classification.

The improved classification accuracy recommends the use of DTW trained at all wrist orientations for PR of EMG signals. The *Training Protocol II* agrees with the

Table 4.3: Average classification accuracy (%) for ten subjects with *Training Protocol II*, comparing TD-PSD method with the proposed method

Method	Classification accuracy %	Reference
Time-Dependent Power Spectrum Descriptors	92	Khushaba et al. (2016b)
Dynamic Time Warping	93.3	Present study

work of Khushaba et al. (2016b).

4.5.3 Processing time

The time taken by DTW for processing the data and generating the output was calculated on a PC (1.7 GHz Intel Core i5 CPU, 4 GB RAM) in Matlab when trained with all wrist orientations. The time taken for generating a decision for 200 ms data is shown in Table 4.4. Since the total time taken for decision is less than 300 ms; DTW algorithm becomes a likely candidate for real-time implementation.

Table 4.4: Average processing time (ms) for ten intact subjects for TD-PSD method and DTW method for generating decision

Method	Time (ms)	Rectangular Window (ms)
Time-Dependent Power Spectrum Descriptors	1.9	200
Dynamic Time Warping	1.2	200

4.5.4 Confusion Matrix

The average confusion matrix for ten subjects is shown in Figure 4.12 for *Training Protocol II*. Confusion matrix demonstrates the applicability of the DTW algorithm in effectively classifying hand motions (>85%). The hand motions C2, C3, C4, and C6 were classified with accuracy greater than 95%. A marginally low classification was observed in case of hand motions C1 and C5.

Figure 4.12 (b) shows the classification in instances for *Training Protocol II*. Here, the first and second trials of Orientation 1, 2 and 3 were used as training templates. For a windowing scheme, a total of 27,000 windowed sequences of 200 ms were used

Target Class	C1	86.7	7.8	0	3.3	2.2	0
	C2	0	95.6	0	1.1	2.2	1.1
	C3	0	3.3	93.4	0	2.2	1.1
	C4	0	1.1	1.1	97.8	0	0
	C5	0	6.6	2.2	0	90	1.1
	C6	0	1.1	1.1	0	1.1	96.7
		C1	C2	C3	C4	C5	C6

Predicted Class

(a)

							Total	
Target Class	C1	1951	176	0	74	49	0	2250
	C2	0	2153	0	24	49	24	2250
	C3	0	74	2103	0	49	24	2250
	C4	0	24	24	2202	0	0	2250
	C5	0	152	49	0	2025	24	2250
	C6	0	24	24	0	24	2178	2250
								13500
	C1	C2	C3	C4	C5	C6		

Predicted Class

(b)

Figure 4.12: (a) Average confusion matrix with *Training Protocol II* obtained across ten subjects for six hand movements (C1–C6) in percentage and (b) in terms of classified instances.

as training templates. The rest that is the third trial from Orientation 1, 2 and 3 were used as test templates. This gives a total of 13,500 windowed sequences of 200 ms as test templates. For each movement, 2,250 (13,500/6) windowed sequences were used as test templates.

4.6 Discussion on the study of wrist orientation changes

During the real-time application of prostheses, the PR accuracy should not degrade when operated in multiple wrist orientations. The main aim of this work was to diminish the effect of wrist orientation on PR of the myoelectric controller to facilitate the control of prostheses. Earlier studies conducted to overcome this issue used computationally complex algorithms which were difficult to implement in real-time. The main aim here was to use a simple and efficient wrist independent algorithm. To verify this, an experiment was conducted on ten subjects performing six hand motions at three different wrist orientations. From the results, it is confirmed that DTW is robust against wrist orientation variation. For the real-time application, the possibility of using shorter windowing time of 200 ms is verified using DTW.

4.6.1 Performance of proposed method under different wrist orientation for the two training protocols

The performance of the DTW algorithm was tested using one of the wrist orientations as the training template and the remaining two wrist orientations as testing templates (*Training Protocol I*). From Figure 4.10, it can be observed that the classification accuracy remained the same at all wrist orientations. It can also be noted that the classification accuracy was low, which directs for the inclusion of more training data from the other wrist orientations. In this way, the *Training Protocol II* was implemented by training the DTW with data from all wrist orientations. From Figure 4.11, significant improvements in classification accuracy was seen. Compared to training the wrist at one single position, the classification accuracy was considerably increased through training at all wrist orientations. The main reason behind this is that the training data contained patterns which closely matched the test data. This leads us

to a conclusion of using the DTW method trained in all wrist orientations to develop a wrist independent PR scheme.

To check the classification accuracy of each movement individually, the confusion matrix is evaluated and presented in Figure 4.12. The movements C1 and C5 were classified with less accuracy when compared to the rest of the hand motions. This is because the wrist variation creates shortening and lengthening of limb muscles creating overlapping patterns across different classes of movements. The muscle shortening affects the time and frequency measure of EMG signal along with the amplitude (Roman-Liu and Bartuzi, 2013). To overcome this effect, further training is required with data generated from these scenarios.

It was also observed that the DTW algorithm can make an accurate prediction even while using shorter window length showing its suitability in real-time applications. The previously used methods in the literature were complex with high computational cost, which will introduce a delay into the system and affect the implementation of real-time control. The DTW method was compared with TD-PSD method proposed by Khushaba et al. (2016b). The results of the evaluation are given in Table 4.3. DTW also presented much lower processing time requirements than that of TD-PSD which additionally proves the impact of DTW method for overcoming wrist variation effect.

4.7 Conclusion

This work investigated the performance of the PR system for upper limb myoelectric control in the presence of force variation and wrist orientation variation separately. DTW is proposed as a computationally cheap and accurate method for the PR system in place of otherwise complex methods used previously in the literature. Thus the significance and novelty of the study lie in the affordable real-time solutions for upper limb prostheses. The study suggests a possible training strategy along with the DTW scheme to mitigate such movement artifacts. The study shows that the classification accuracy can be improved by including training data from multiple wrist orientations and force levels. These results are of significant interest in the biomedical signal processing domain since they help the amputees with functional wrist to control prosthesis efficiently. The DTW method achieved lower classification error with reduced computational time compared to the state-of-the-art TD-PSD method

and hence can be a possible alternative for the clinical implementation of PR based myoelectric prostheses.

Chapter 5

Summary and Future scope

This chapter provides the summary of the major findings of the thesis. Based on the research carried out in this thesis, the recommendations for future research are suggested.

5.1 Summary

In this thesis, two methods have been proposed for improvement of the performance of sEMG based MEC. This section gives a detailed summary of the thesis.

Novel Pre-processing method: In the analysis of sEMG signals, the challenge lies in the suppression of noise associated with the measurement and signal conditioning. The work presents a novel pre-processing step, namely Minimum Entropy Deconvolution Adjusted (MEDA), to enhance the signal for feature extraction resulting in better characterization of different upper limb motions. MEDA method is based on finding the set of filter coefficients under the condition of maximal kurtosis. The proposed method has been validated on sEMG dataset collected from seven subjects performing eight classes of hand movements with only two pairs of electrodes recorded from flexor carpi radialis and extensor carpi radialis on the forearm. The performance of the MEDA is then compared across four classifiers. Practical results indicate that MEDA can significantly enhance classification accuracy. The results demonstrate the effectiveness of the proposed method. The MEDA was compared against the traditional used pre-processing methods. It has been observed that the MEDA, in terms of the classification accuracy and processing time, can outperform such methods from the literature.

Method to overcome force level variation and wrist orientation: Regardless of the extensive research, attention towards the Pattern Recognition (PR) based myoelectric control of the upper limb prostheses, the factors which affect its clinical application has not received the same attention. The primary goal is to provide amputees with prostheses which have an accurate PR based myoelectric controller. In practice, the vital factors affecting the limited performance of the PR based Electromyography (EMG) controlled prostheses are changes in the force levels and wrist orientation. These effects create different sEMG patterns, even when the amputee makes the same movement. The main aim of the PR based myoelectric controller is to control the prostheses in a precise way, irrespective of the force level and wrist orientation at which the movement is made. In order to study the performance of the sEMG based PR classification accuracy under such variations, many methods have been proposed recently. The Time-Dependent Power Spectrum Descriptors (TD-PSD) method is seen to outperform the previous approaches regarding both classification accuracy and computational time. For decreasing the effect of force level and wrist variation on EMG pattern recognition, this work proposes to use a time domain implementation of the Dynamic Time Warping (DTW).

For force level variation, the DTW method is validated on two databases and compared with the previously used TD-PSD method to verify its improved performance in a real-life scenario. The first database, which has data from ten intact-limbed subjects, was used to test the usability of the DTW initially resulting in an average classification accuracy of more than 90%. With this encouraging result from the first database, the next database that has data from nine upper limb amputees recorded at three levels of forces (low, medium, and high) for six different hand grips has been used. The proposed scheme with the DTW achieved a significant 10% improvement in classification accuracy when trained at low force level when compared to the traditional TD-PSD method. This result is significant since for an amputee training at lower and medium force levels is comfortable when compared to training at a high force level. In the thesis, the DTW scheme has been deployed on data with varying wrist orientation to see its robustness. The first database with intact-bodied subjects used for force level studies also has data for varying wrist orientation and is utilized in this study. The performance of the DTW scheme as a PR system is validated using two training methods; with classification accuracy as a performance measure on data taken from the database of ten intact subjects for six hand motions carried out at

three different wrist orientations. On the database, an average classification accuracy of about 93.3% was obtained while trained using sEMG data from all possible wrist positions. The results from both the studies indicate that the performance of the DTW method has improved significantly when compared with the TD-PSD method in terms of classification accuracy and processing time.

5.2 Future scope

Based on the research carried out in this thesis, the recommendations for future research are as follows:

- Examine the online performance of PR systems with transradial amputees. The experiment carried out checked the performance of healthy subjects and used a database of amputees for PR. Further, there is a need for examination of PR with amputees
- The possibility of incorporating additional sensor data (say hand acceleration) as a surrogate for the sEMG sensor data should be investigated to bring down the cost of such systems. The cost of the sEMG sensor is high, by replacing some of the sEMG sensors with other sensors such as force or accelerometer will further reduce the cost of the system, thus making it affordable for amputees
- Investigation on the PR performance while both the force level and wrist orientation are changed simultaneously. The work performed in this thesis studied the effect individually. Future work needs to examine the impact on PR by taking the two variations together.
- Studying PR performance by examining the sEMG data recorded over many days. The investigation carried out in this work evaluated the performance of sEMG signal on a particular day. For reproducibility of the results, reiterating over many days is very important. The change in performance should be examined in the future

Appendix A

Definition of variables

- **Average amplitude change (AAC):** AAC is the mean value of the absolute difference between two consecutive samples.
- **Approximate entropy (ApEn):** ApEn is a method used to calculate the amount of regularity and the randomness of fluctuations over time-series data.
- **Difference absolute standard deviation value (DASDV):** DASDV looks similar to the RMS feature; it is a standard deviation value of the wavelength.
- **Integrated EMG (IEMG):** IEMG is used as a preliminary detection rate and is associated with the trigger point of the sEMG signal sequence. It is the sum of the absolute values of each sample of sEMG.
- **Kurtosis (Kurt):** Kurt is a statistical measure that is used to quantify the shape of the distribution.
- **Log detector (LOG):** This provides an approximation of the strength of muscle contraction force. However, its definition is changed based on the logarithm and log detector feature.
- **Mean absolute value (MAV):** MAV is an average of the absolute value of the sEMG signal amplitude in a segment.
- **Root mean square (RMS):** RMS is modeled as an amplitude modulated Gaussian random process, which is related to constant force and contraction without fatigue. It is similar to the calculation of the standard deviation method.

- **Sample entropy (SampEn)**: SampEn is the refinement of ApEn to reduce the bias induced by self-matching. It is independent of the length of the recording and displays relative consistency under various circumstances.
- **Simple square integral (SSI)**: SSI is a summation of square values of the sEMG signal amplitude. It uses the energy of the sEMG signal as a feature.
- **Variance (VAR)**: It is the average of square values of the deviation of that variable.
- **Waveform length (WL)**: It is simply the cumulative length of the EMG waveform over the time segment. It provides information about the complexity of the waveform in each segment.
- **Skewness (Skew)**: Skew is the measure of symmetry, or more precisely, the lack of symmetry.
- **Mean frequency (MNF)**: MNF is calculated as the sum of the product of the sEMG power spectrum and the frequency divided by the total sum of the spectrum intensity.
- **Median frequency (MDF)**: MDF is the frequency at which the spectrum is divided into two regions with equal amplitude. It is the total power average.
- **Mean power (MNP)**: MNP is the average power of the sEMG power spectrum.
- **Spectral moment (SM)**: SM is an alternative statistical analysis way to extract features from the sEMG power spectrum.
- **Total power (TTP)**: TTP is the total of the sEMG power spectrum.

Appendix B

Description of Dimensionality Reduction and Classification Methods

B.1 Wrapper based Dimensionality Reduction

The wrapper approach conducts a search in the space of possible parameters. A search requires a state space, an initial state, a termination condition, and a search engine. The goal of the search is to find the state with the highest evaluation. The evaluation function used is cross-validation repeated multiple times (Kohavi and John, 1997).

The following summary shows the instantiation of the search problem:

Initial state: The empty set of features (0,0,0.. ,0)

Evaluation: Five-fold cross-validation repeated multiple times with a small penalty (0.1%) for every feature

Search algorithm: Particle Swarm Optimisation (PSO), Best First, Linear Forward Selection and Greedy Step Wise search

Termination condition: Algorithm dependent

B.1.1 Greedy Step Wise

The algorithm expands on the current node and moves towards the child with the highest accuracy. The method terminates, when no child improves over the current node. The algorithm performs a greedy forward or backward search through the space

of attribute subsets. This may start with no/all attributes or from an arbitrary point in the space, stops when the addition/deletion of any remaining attributes results in a decrease in evaluation.

The algorithm is as follows (Kohavi and John, 1997):

1. Let $v \leftarrow$ initial state.
2. Expand v : apply all operators to v , giving v 's children.
3. Apply the evaluation function f to each child w of v .
4. Let $v' =$ the child w with highest evaluation $f(w)$.
5. If $f(v') > f(v)$ then $v \leftarrow v'$; goto 2.
6. Return v .

B.1.2 Best First Search

The algorithm selects the most promising node that has not already been expanded. Setting the number of consecutive non-improving nodes allowed controls the level of backtracking done. Best first may start with the empty set of attributes and search forward, or start with the full set of attributes and search backward, or start at any point and search in both directions (by considering all possible single attribute additions and deletions at a given point). In this research the forward setting was used.

In the last k expansion, if an improved node is not found then the search is terminated. An improved node is defined as a node with an accuracy estimation at least ϵ higher than the best one found so far. In the following experiments, k was set to five and ϵ was 0.1%.

The algorithm is as follows (Kohavi and John, 1997):

1. Put the initial state on the OPEN list, CLOSED list $\leftarrow \emptyset$, BEST \leftarrow initial state.
2. Let $v = \arg \max_{w \in OPEN} f(w)$ (get the state from OPEN with maximal $f(w)$).
3. Remove v from OPEN, add v to CLOSED.
4. If $f(v) - \epsilon > f(\text{BEST})$, then BEST $\leftarrow v$.
5. Expand v : apply all operators to v , giving v 's children.
6. For each child not in the CLOSED or OPEN list, evaluate and add to the OPEN list.
7. If BEST changed in the last k expansions, goto 2.
8. Return BEST.

B.1.3 Linear Forward Selection (LFS)

LFS is a technique to reduce the number of attributes expansions in each forward selection step. To reduce the number of subset evaluations, there are two steps 1) initially all attributes are ranked with the wrapper. 2) Algorithm builds N attribute subsets: the first set is the top-ranked attribute, followed by the two top-ranked attributes, the three top-ranked attributes, and so on. These subsets are evaluated using the wrapper.

Linear Forward Selection (D, R, k) denotes a forward selection with a limited number of k attributes, based on the ranking R, Linear Forward Selection To Size(...) uses a given subset size as termination criterion and outputs a subset of that size, evaluate (S, D_1, D_2) delivers the accuracy of the classifier on the data D_2 , trained on the data D_1 , using only the attributes in S .

The algorithm is as follows (Gutlein et al., 2009):

1. Perform m -fold cross-validation split on data D :
2. $D \rightarrow (D_{\text{Train}}^{(1)}, D_{\text{Test}}^{(1)}), (D_{\text{Train}}^{(2)}, D_{\text{Test}}^{(2)}), \dots, (D_{\text{Train}}^{(m)}, D_{\text{Test}}^{(m)})$
- 3.
4. STEP 1: COMPUTE OPT-SIZE
5. for all folds $i = 1$ to m do
6. Generate ranking $R_{D_{\text{Train}}^{(i)}}$ (a) on training data $D_{\text{Train}}^{(i)}$
7. $S_i = \text{Linear Forward Selection}(D_{\text{Train}}^{(i)}, R_{D_{\text{Train}}^{(i)}}, k)$
8. proceed all i forward selections until $|S_i| = \max_{1 \leq i \leq m} |S_i|$
- 9.
10. for all folds $i = 1$ to m do
11. for all subsets $S'_i = S_i$ and preceding subsets of S_i do
12. scores; = evaluate $(S'_i, D_{\text{Train}}^{(i)}, D_{\text{Test}}^{(i)})$
13. $\text{avgScore}_n = \text{mean score for subset size } n$
14. $\text{optSize} = \text{subset size } n \text{ with max avgScore}_n$
- 15.
16. STEP 2 : FORW.-SELECTION UP TO OPT.-SIZE
17. Generate ranking R_D on data D
18. $S = \text{Linear Forward Selection To Size}(D, \text{optSize}, R_D, k)$

19. return S

B.1.4 Particle Swarm Optimization (PSO)

PSO starts with the random initialization of a population of particles. Particles move in the search space to search for the optimal solution by updating the position of each particle based on the experience of its own and its neighboring particles. PSO searches for the optimal solution by updating the position and the velocity.

The algorithm is as follows (Moraglio et al., 2007):

1. for all particle i do
2. initialize position x_i and velocity v_i
3. end for
4. while stop criteria not met do
5. for all particle i do
6. set personal best \hat{x}_i as best position found so far by the particle
7. set global best \hat{g} as best position found so far by the whole swarm
8. end for
9. for all particle i do
10. update velocity using equation
$$v_i(t+1) = \omega v_i(t) + \phi_1 U(0,1) (\hat{g}(t) - x_i(t)) + \phi_2 U(0,1) (\hat{x}_i(t) - x_i(t))$$
where t denotes the iteration in the evolutionary process. ω is inertia weight. ϕ_1 and ϕ_2 are acceleration constants. U is the random variable distributed in $[0,1]$.
11. update position using equation
$$x_i(t+1) = x_i(t) + v_i(t+1)$$
12. end for
13. end while

B.2 Classifiers

B.2.1 Naive Bayes

The classifier works on Bayes theorem. Bayes Theorem finds the probability of an event occurring given the probability of another event that has already occurred. Bayes theorem is stated mathematically as the following equation (John and Langley, 1995):

$$P(A|B) = \frac{P(B|A)P(A)}{P(B)} \quad (\text{B.1})$$

From Bayes theorem, the probability of the occurrence of A can be calculated, given that B has occurred. A is the hypothesis and B is the evidence. The assumption made here is that presence of one particular feature does not affect the other.

Consider y is class variable and X is a dependent feature vector (of size n) where: $X = (x_1, x_2, x_3, \dots, x_n)$

Applying Bayes' theorem.

$$P(y|X) = \frac{P(X|y)P(y)}{P(X)} \quad (\text{B.2})$$

The joint distribution is decomposed as:

$$P(y|x_1, \dots, x_n) = \frac{P(x_1|y)P(x_2|y) \dots P(x_n|y)P(y)}{P(x_1)P(x_2) \dots P(x_n)} \quad (\text{B.3})$$

Which can be expressed as:

$$P(y|x_1, \dots, x_n) = \frac{P(y) \prod_{i=1}^n P(x_i|y)}{P(x_1)P(x_2) \dots P(x_n)} \quad (\text{B.4})$$

Since, the denominator remains constant for a given input:

$$P(y|x_1, \dots, x_n) \propto P(y) \prod_{i=1}^n P(x_i|y) \quad (\text{B.5})$$

In order to create a classification model, we find the probability of given set of inputs for all possible values of the class variable y and pick up the output with maximum probability. This can be expressed mathematically as:

$$y = \operatorname{argmax}_y P(y) \prod_{i=1}^n P(x_i|y) \quad (\text{B.6})$$

B.2.2 J-48

J-48 begins with a set of features, and create a tree data structure that can be used to classify new features. Each internal node of a decision tree contains a test, the result of which is used to decide what branch to follow from that node.

J-48 builds decision trees from a set of training data using the concept of informa-

tion entropy. The training data is a set $S = s_1, s_2, s_3, \dots$ of already classified samples. Each sample s_i consists of a p -dimensional vector $(x_1, x_2, x_3, \dots, x_j)$, where x_j represent attribute values or features of the sample.

At each node of the tree, J48 chooses the attribute of the data that most effectively splits its set of samples into subsets enriched in one class or the other. The splitting criterion is the normalized information gain (difference in entropy). The attribute with the highest normalized information gain is chosen to make the decision. The J48 algorithm then recurses on the partitioned sublists.

This algorithm has a few base cases:

- 1) All the samples in the list belong to the same class. When this happens, it simply creates a leaf node for the decision tree saying to choose that class.
- 2) None of the features provide any information gain. In this case, J-48 creates a decision node higher up the tree using the expected value of the class.
- 3) Instance of previously-unseen class encountered. Again, J-48 creates a decision node higher up the tree using the expected value.

The general algorithm for building decision trees is (Quinlan, 1993):

1. Check for the above base cases.
2. For each attribute a , find the normalized information gain ratio from splitting on a .
3. Let $abest$ be the attribute with the highest normalized information gain.
4. Create a decision node that splits on $abest$.
5. Recur on the sublists obtained by splitting on $abest$, and add those nodes as children of node.

B.2.3 Linear Discriminant Analysis (LDA)

This method projects a dataset onto a lower-dimensional space with good class-separability to avoid over-fitting, and to reduce computational costs. LDA is often to project a feature space (a dataset n -dimensional samples) into a smaller subspace (where $k \leq n-1$), while maintaining the class-discriminatory information. The goal of LDA as supervised algorithm is to find the feature subspace that optimizes class separability.

The general algorithm for LDA is (Quinlan, 1993):

1. Compute the d -dimensional mean vectors for the different classes from the dataset.
2. Compute the scatter matrices (in-between-class and within-class scatter matrix).
3. Compute the eigen vectors (e_1, e_2, \dots, e_d) and corresponding eigen values $(\lambda_1, \lambda_2, \dots, \lambda_d)$ for the scatter matrices.
4. Sort the eigenvectors by decreasing eigenvalues and choose k eigenvectors with the largest eigenvalues to form a $d \times k$ dimensional matrix W (where every column represents an eigenvector).
5. Use this $d \times k$ eigenvector matrix to transform the samples onto the new subspace. This can be summarized by the matrix multiplication: $Y = X \times W$, where X is a $d \times d$ dimensional matrix representing the n samples, and y are the transformed $n \times k$ dimensional samples in the new subspace.

B.2.4 k-Nearest Neighbors (kNN)

The kNN algorithm assumes similar things are near to each other. The algorithm captures the idea of similarity (sometimes called distance, proximity, or closeness) by calculating the distance between points on a graph.

The general algorithm for kNN is (Quinlan, 1993):

1. Load the data
2. Initialize the value of k
3. For getting the predicted class, iterate from 1 to total number of training data points
 - 3.1) Calculate the distance between test data and each row of training data. We have used Euclidean distance as our distance metric since it's the most popular method. The other metrics that can be used are Chebyshev, cosine, etc.
 - 3.2) Sort the calculated distances in ascending order based on distance values
 - 3.3) Get top k rows from the sorted array
 - 3.4) Get the most frequent class of these rows
 - 3.5) Return the predicted class

Bibliography

- AbdelMaseeh, M., Chen, T.-W., and Stashuk, D. W. (2015). Extraction and classification of multichannel electromyographic activation trajectories for hand movement recognition. *IEEE Transactions on Neural Systems and Rehabilitation Engineering*, 24(6):662–673.
- Adewuyi, A. A., Hargrove, L. J., and Kuiken, T. A. (2013). Towards improved partial-hand prostheses: the effect of wrist kinematics on pattern-recognition-based control. In *2013 6th International IEEE/EMBS Conference on Neural Engineering (NER)*, pages 1489–1492. IEEE.
- Adewuyi, A. A., Hargrove, L. J., and Kuiken, T. A. (2016). Evaluating EMG feature and classifier selection for application to partial-hand prosthesis control. *Frontiers in neurorobotics*, 10:15.
- Adewuyi, A. A., Hargrove, L. J., and Kuiken, T. A. (2017). Resolving the effect of wrist position on myoelectric pattern recognition control. *Journal of neuroengineering and rehabilitation*, 14(1):39.
- Ahmad Nasrul, N. and Mohd Hanafi, M. S. (2009). Surface electromyography signal processing and application: A review. In *Proceedings of the International Conference on Man-Machine Systems*. ICoMMS.
- Al-Timemy, A. H., Khushaba, R. N., Bugmann, G., and Escudero, J. (2015). Improving the performance against force variation of emg controlled multifunctional upper-limb prostheses for transradial amputees. *IEEE Transactions on Neural Systems and Rehabilitation Engineering*, 24(6):650–661.
- Amsuss, S., Paredes, L. P., Rudigkeit, N., Graimann, B., Herrmann, M. J., and Farina, D. (2013). Long term stability of surface EMG pattern classification

- for prosthetic control. In *Engineering in Medicine and Biology Society (EMBC), 2013 35th Annual International Conference of the IEEE*, pages 3622–3625. IEEE.
- Andrade, A. O., Nasuto, S., Kyberd, P., Sweeney-Reed, C. M., and Van Kanijn, F. (2006). EMG signal filtering based on empirical mode decomposition. *Biomedical Signal Processing and Control*, 1(1):44–55.
- Barişçi, N. (2008). The adaptive ARMA analysis of emg signals. *Journal of medical systems*, 32(1):43–50.
- Battye, C., Nightingale, A., and Whillis, J. (1955). The use of myo-electric currents in the operation of prostheses. *Bone & Joint Journal*, 37(3):506–510.
- Bhaskaranand, K., Bhat, A. K., and Acharya, K. N. (2003). Prosthetic rehabilitation in traumatic upper limb amputees (an indian perspective). *Archives of orthopaedic and trauma surgery*, 123(7):363–366.
- Bhuvaneshwar, C. G., Epstein, L. A., and Stern, T. A. (2007). Reactions to amputation: recognition and treatment. *Primary care companion to the Journal of clinical psychiatry*, 9(4):303.
- Boll, S. (1979). Suppression of acoustic noise in speech using spectral subtraction. *IEEE Transactions on acoustics, speech, and signal processing*, 27(2):113–120.
- Boostani, R. and Moradi, M. H. (2003). Evaluation of the forearm EMG signal features for the control of a prosthetic hand. *Physiological measurement*, 24(2):309.
- Brody, G., Scott, R., and Balasubramanian, R. (1974). A model for myoelectric signal generation. *Medical and Biological Engineering and Computing*, 12(1):29–41.
- Chan, A. D., Green, G. C., et al. (2007). Myoelectric control development toolbox. In *Proceedings of 30th conference of the Canadian medical & biological engineering society*, volume 1, pages M0100–1.
- Chowdhury, R. H., Reaz, M. B., Ali, M. A. B. M., Bakar, A. A., Chellappan, K., and Chang, T. G. (2013). Surface electromyography signal processing and classification techniques. *Sensors*, 13(9):12431–12466.

- Chu, J.-U., Moon, I., and Mun, M.-S. (2006). A real-time EMG pattern recognition system based on linear-nonlinear feature projection for a multifunction myoelectric hand. *IEEE Transactions on biomedical engineering*, 53(11):2232–2239.
- Conforto, S., D’Alessio, T., and Pignatelli, S. (1999). Optimal rejection of movement artefacts from myoelectric signals by means of a wavelet filtering procedure. *Journal of Electromyography and Kinesiology*, 9(1):47–57.
- Dellon, B. and Matsuoka, Y. (2007). Prosthetics, exoskeletons, and rehabilitation [grand challenges of robotics]. *IEEE robotics & automation magazine*, 14(1):30–34.
- Division, S. S. (2016). *Disabled Persons in India A statistical profile 2016*. Ministry of Statistics and Programme Implementation, Government of India.
- Doerschuk, P. C., Gustafon, D. E., and Willsky, A. S. (1983). Upper extremity limb function discrimination using EMG signal analysis. *IEEE Transactions on Biomedical Engineering*, (1):18–29.
- Earley, E. J. and Hargrove, L. J. (2016). The effect of wrist position and hand-grasp pattern on virtual prosthesis task performance. In *Biomedical Robotics and Biomechatronics (BioRob), 2016 6th IEEE International Conference on*, pages 542–547. IEEE.
- Edeer, D. and Martin, C. W. (2011). *Upper limb prostheses: A review of the literature: With a focus on myoelectric hands*. WorkSafeBC, Clinical Services, Worker and Employer Services.
- Endo, H. and Randall, R. (2007). Enhancement of autoregressive model based gear tooth fault detection technique by the use of minimum entropy deconvolution filter. *Mechanical Systems and Signal Processing*, 21(2):906–919.
- Englehart, K. and Hudgins, B. (2003). A robust, real-time control scheme for multifunction myoelectric control. *IEEE transactions on biomedical engineering*, 50(7):848–854.
- Englehart, K., Hudgins, B., Parker, P. A., and Stevenson, M. (1999). Classification of the myoelectric signal using time-frequency based representations. *Medical engineering & physics*, 21(6):431–438.

- Ephraim, Y. and Malah, D. (1984). Speech enhancement using a minimum-mean square error short-time spectral amplitude estimator. *IEEE Transactions on acoustics, speech, and signal processing*, 32(6):1109–1121.
- Farina, D., Vujaklija, I., Sartori, M., Kapelner, T., Negro, F., Jiang, N., Bergmeister, K., Andalib, A., Principe, J., and Aszmann, O. C. (2017). Man/machine interface based on the discharge timings of spinal motor neurons after targeted muscle reinnervation. *Nature Biomedical Engineering*, 1:0025.
- Farrell, T. R. and Weir, R. F. (2007). The optimal controller delay for myoelectric prostheses. *IEEE Transactions on neural systems and rehabilitation engineering*, 15(1):111–118.
- Finch, J. (2011). The ancient origins of prosthetic medicine. *The Lancet*, 377(9765):548–549.
- Fougner, A., Scheme, E., Chan, A. D., Englehart, K., and Stavdahl, Ø. (2011). Resolving the limb position effect in myoelectric pattern recognition. *IEEE Transactions on Neural Systems and Rehabilitation Engineering*, 19(6):644–651.
- Fougner, A., Stavdahl, Ø., Kyberd, P. J., Losier, Y. G., and Parker, P. A. (2012). Control of upper limb prostheses: terminology and proportional myoelectric control—a review. *IEEE Transactions on neural systems and rehabilitation engineering*, 20(5):663–677.
- Geethanjali, P. (2016). Myoelectric control of prosthetic hands: state-of-the-art review. *Medical Devices (Auckland, NZ)*, 9:247.
- Geng, Y., Zhou, P., and Li, G. (2012). Toward attenuating the impact of arm positions on electromyography pattern-recognition based motion classification in transradial amputees. *Journal of neuroengineering and rehabilitation*, 9(1):74.
- Graupe, D. and Cline, W. K. (1975). Functional separation of EMG signals via ARMA identification methods for prosthesis control purposes. *IEEE Transactions on Systems, Man, and Cybernetics*, (2):252–259.
- Graupe, D., Kohn, K. H., Kralj, A., and Basseas, S. (1983). Patient controlled electrical stimulation via EMG signature discrimination for providing certain

- paraplegics with primitive walking functions. *Journal of biomedical engineering*, 5(3):220–226.
- Graupe, D., Salahi, J., and Kohn, K. H. (1982). Multifunctional prosthesis and orthosis control via microcomputer identification of temporal pattern differences in single-site myoelectric signals. *Journal of Biomedical Engineering*, 4(1):17–22.
- Gutlein, M., Frank, E., Hall, M., and Karwath, A. (2009). Large-scale attribute selection using wrappers. In *2009 IEEE symposium on computational intelligence and data mining*, pages 332–339. IEEE.
- Hall, M. A. (1999). Correlation-based feature selection for machine learning.
- Hannaford, B. and Lehman, S. (1986). Short time Fourier analysis of the electromyogram: Fast movements and constant contraction. *IEEE Transactions on Biomedical Engineering*, (12):1173–1181.
- Hargrove, L., Englehart, K., and Hudgins, B. (2008). A training strategy to reduce classification degradation due to electrode displacements in pattern recognition based myoelectric control. *Biomedical signal processing and control*, 3(2):175–180.
- Hargrove, L. J., Englehart, K., and Hudgins, B. (2007). A comparison of surface and intramuscular myoelectric signal classification. *IEEE Transactions on Biomedical Engineering*, 54(5):847–853.
- Hargrove, L. J., Scheme, E. J., Englehart, K. B., and Hudgins, B. S. (2010). Multiple binary classifications via linear discriminant analysis for improved controllability of a powered prosthesis. *IEEE Transactions on Neural Systems and Rehabilitation Engineering*, 18(1):49–57.
- He, J., Zhang, D., Sheng, X., Li, S., and Zhu, X. (2015). Invariant surface EMG feature against varying contraction level for myoelectric control based on muscle coordination. *IEEE journal of biomedical and health informatics*, 19(3):874–882.
- Hefftner, G., Zucchini, W., and Jaros, G. G. (1988). The electromyogram (EMG) as a control signal for functional neuromuscular stimulation. I. autoregressive modeling as a means of emg signature discrimination. *IEEE Transactions on Biomedical Engineering*, 35(4):230–237.

- Herberts, P., Almström, C., Kadefors, R., and Lawrence, P. D. (1973). Hand prosthesis control via myoelectric patterns. *Acta Orthopaedica Scandinavica*, 44(4-5):389–409.
- Hoozemans, M. J. and Van Dieen, J. H. (2005). Prediction of handgrip forces using surface EMG of forearm muscles. *Journal of electromyography and kinesiology*, 15(4):358–366.
- Huang, G., Zhang, D., Zheng, X., and Zhu, X. (2010). An EMG-based handwriting recognition through dynamic time warping. In *2010 Annual International Conference of the IEEE Engineering in Medicine and Biology*, pages 4902–4905. IEEE.
- Hudgins, B., Parker, P., and Scott, R. N. (1993). A new strategy for multifunction myoelectric control. *IEEE Transactions on Biomedical Engineering*, 40(1):82–94.
- Hussain, M., Reaz, M. B. I., Mohd-Yasin, F., and Ibrahimy, M. I. (2009). Electromyography signal analysis using wavelet transform and higher order statistics to determine muscle contraction. *Expert Systems*, 26(1):35–48.
- Jiang, R., Chen, J., Dong, G., Liu, T., and Xiao, W. (2013). The weak fault diagnosis and condition monitoring of rolling element bearing using minimum entropy deconvolution and envelop spectrum. *Proceedings of the Institution of Mechanical Engineers, Part C: Journal of Mechanical Engineering Science*, 227(5):1116–1129.
- John, G. H. and Langley, P. (1995). Estimating continuous distributions in bayesian classifiers. In *Eleventh Conference on Uncertainty in Artificial Intelligence*, pages 338–345, San Mateo. Morgan Kaufmann.
- Jung, T.-P., Makeig, S., Lee, T.-W., McKeown, M. J., Brown, G., Bell, A. J., and Sejnowski, T. J. (2000). Independent component analysis of biomedical signals. In *Proc. Int. Workshop on Independent Component Analysis and Signal Separation*, pages 633–644. Citeseer.
- Kang, W.-J., Shiu, J.-R., Cheng, C.-K., Lai, J.-S., Tsao, H.-W., and Kuo, T.-S. (1995). The application of cepstral coefficients and maximum likelihood method

- in EMG pattern recognition [movements classification]. *IEEE Transactions on Biomedical Engineering*, 42(8):777–785.
- Kaplanis, P., Pattichis, C., Hadjileontiadis, L., and Panas, S. (2000). Bispectral analysis of surface EMG. In *2000 10th Mediterranean Electrotechnical Conference. Information Technology and Electrotechnology for the Mediterranean Countries. Proceedings. MeleCon 2000 (Cat. No. 00CH37099)*, volume 2, pages 770–773. IEEE.
- Karlsson, S., Yu, J., and Akay, M. (2000). Time-frequency analysis of myoelectric signals during dynamic contractions: a comparative study. *IEEE transactions on Biomedical Engineering*, 47(2):228–238.
- Karthick, P., Venugopal, G., and Ramakrishnan, S. (2016). Analysis of muscle fatigue progression using cyclostationary property of surface electromyography signals. *Journal of medical systems*, 40(1):28.
- Khezri, M. and Jahed, M. (2008). Surface electromyogram signal estimation based on wavelet thresholding technique. In *2008 30th Annual International Conference of the IEEE Engineering in Medicine and Biology Society*, pages 4752–4755. IEEE.
- Khushaba, R. N., Al-Ani, A., and Al-Jumaily, A. (2010). Orthogonal fuzzy neighborhood discriminant analysis for multifunction myoelectric hand control. *IEEE Transactions on Biomedical Engineering*, 57(6):1410–1419.
- Khushaba, R. N., Al-Ani, A., and Al-Jumaily, A. (2011). Feature subset selection using differential evolution and a statistical repair mechanism. *Expert Systems with Applications*, 38(9):11515–11526.
- Khushaba, R. N., Al-Ani, A., AlSukker, A., and Al-Jumaily, A. (2008). A combined ant colony and differential evolution feature selection algorithm. In *International Conference on Ant Colony Optimization and Swarm Intelligence*, pages 1–12. Springer.
- Khushaba, R. N., Al-Jumaily, A., and Al-Ani, A. (2009a). Evolutionary fuzzy discriminant analysis feature projection technique in myoelectric control. *Pattern Recognition Letters*, 30(7):699–707.

- Khushaba, R. N., Al-Timemy, A., Al-Ani, A., and Al-Jumaily, A. (2016a). Myoelectric feature extraction using temporal-spatial descriptors for multifunction prosthetic hand control. In *Engineering in Medicine and Biology Society (EMBC), 2016 IEEE 38th Annual International Conference of the*, pages 1696–1699. IEEE.
- Khushaba, R. N., Al-Timemy, A., Kodagoda, S., and Nazarpour, K. (2016b). Combined influence of forearm orientation and muscular contraction on EMG pattern recognition. *Expert Systems with Applications*, 61:154–161.
- Khushaba, R. N., AlSukker, A., Al-Ani, A., Al-Jumaily, A., and Zomaya, A. Y. (2009b). A novel swarm based feature selection algorithm in multifunction myoelectric control. *Journal of Intelligent & Fuzzy Systems*, 20(4, 5):175–185.
- Khushaba, R. N., Kodagoda, S., Takruri, M., and Dissanayake, G. (2012). Toward improved control of prosthetic fingers using surface electromyogram (EMG) signals. *Expert Systems with Applications*, 39(12):10731–10738.
- Khushaba, R. N., Takruri, M., Miro, J. V., and Kodagoda, S. (2014). Towards limb position invariant myoelectric pattern recognition using time-dependent spectral features. *Neural Networks*, 55:42–58.
- Kiryu, T., Saitoh, Y., and Ishioka, K. (1992). Investigation on parametric analysis of dynamic EMG signals by a muscle-structured simulation model. *IEEE transactions on biomedical engineering*, 39(3):280–288.
- Kohavi, R. and John, G. H. (1997). Wrappers for feature subset selection. *Artificial intelligence*, 97(1-2):273–324.
- Konrad, P. (2005). The ABC of EMG. *A practical introduction to kinesiological electromyography*, 1:30–35.
- Li, D., Pedrycz, W., and Pizzi, N. J. (2005). Fuzzy wavelet packet based feature extraction method and its application to biomedical signal classification. *IEEE Transactions on biomedical engineering*, 52(6):1132–1139.
- Li, G., Schultz, A. E., and Kuiken, T. A. (2010). Quantifying pattern recognition—based myoelectric control of multifunctional transradial prostheses. *IEEE transactions on neural systems and rehabilitation engineering: a publication of the IEEE Engineering in Medicine and Biology Society*, 18(2):185.

- Liu, J., Ying, D., and Zhou, P. (2014). Wiener filtering of surface emg with a priori snr estimation toward myoelectric control for neurological injury patients. *Medical Engineering and Physics*, 36(12):1711–1715.
- Maclsaac, D., Parker, P., Scott, R., Englehart, K., and Duffley, C. (2001). Influences of dynamic factors on myoelectric parameters. *IEEE engineering in medicine and biology magazine*, 20(6):82–89.
- Matsumura, Y., Fukumi, M., and Mitsukura, Y. (2006). Hybrid EMG recognition system by MDA and PCA. In *The 2006 IEEE International Joint Conference on Neural Network Proceedings*, pages 5294–5300. IEEE.
- Mayor, J. J. V., Costa, R. M., Frizera Neto, A., and Bastos, T. F. (2017). Dexterous hand gestures recognition based on low-density semg signals for upper-limb forearm amputees. *Research on Biomedical Engineering*, (AHEAD):0–0.
- Mazandarani, F. N. and Mohebbi, M. (2018). Wide complex tachycardia discrimination using dynamic time warping of ECG beats. *Computer methods and programs in biomedicine*.
- McCormick, A. and Nandi, A. (1998). Cyclostationarity in rotating machine vibrations. *Mechanical systems and signal processing*, 12(2):225–242.
- McDonald, G. L. and Zhao, Q. (2017). Multipoint optimal minimum entropy deconvolution and convolution fix: Application to vibration fault detection. *Mechanical Systems and Signal Processing*, 82:461–477.
- McKeown, M. J. and Radtke, R. (2001). Phasic and tonic coupling between EEG and EMG demonstrated with independent component analysis. *Journal of clinical neurophysiology*, 18(1):45–57.
- Moraglio, A., Di Chio, C., and Poli, R. (2007). Geometric particle swarm optimisation. *Genetic Programming*, pages 125–136.
- Muneer, A. and Pearce, I. (2016). An introduction to prosthetic devices. In *Prosthetic Surgery in Urology*, pages 1–4. Springer.
- Nagaraja, V. H., Bergmann, J. H., Sen, D., and Thompson, M. S. (2016). Examining the needs of affordable upper limb prosthetic users in india: A questionnaire-based survey. *Technology and Disability*, 28(3):101–110.

- Naik, G. R. and Kumar, D. K. (2012). Identification of hand and finger movements using multi run ICA of surface electromyogram. *Journal of medical systems*, 36(2):841–851.
- Naik, G. R., Kumar, D. K., and Weghorn, H. (2007). Performance comparison of ICA algorithms for isometric hand gesture identification using surface EMG. In *2007 3rd International Conference on Intelligent Sensors, Sensor Networks and Information*, pages 613–618. IEEE.
- National Academies of Sciences, E., Medicine, et al. (2017). *The promise of assistive technology to enhance activity and work participation*. National Academies Press.
- Nazarpour, K., Al-Timemy, A. H., Bugmann, G., and Jackson, A. (2013). A note on the probability distribution function of the surface electromyogram signal. *Brain research bulletin*, 90:88–91.
- Nishikawa, K. and Kuribayashi, K. (1991). Neural network application to a discrimination system for emg-controlled prostheses. In *Proceedings IROS'91: IEEE/RSJ International Workshop on Intelligent Robots and Systems' 91*, pages 231–236. IEEE.
- Norton, K. (2007). A brief history of prosthetics. *InMotion*, 17(7):11–13.
- Ortolan, R. L., Mori, R. N., Pereira, R. R., Cabral, C. M., Pereira, J. C., and Cliquet, A. (2003). Evaluation of adaptive/nonadaptive filtering and wavelet transform techniques for noise reduction in emg mobile acquisition equipment. *IEEE transactions on neural systems and rehabilitation engineering*, 11(1):60–69.
- Oskoei, M. A. and Hu, H. (2006). Ga-based feature subset selection for myoelectric classification. In *Robotics and Biomimetics, 2006. ROBIO'06. IEEE International Conference on*, pages 1465–1470. IEEE.
- Oskoei, M. A. and Hu, H. (2007). Myoelectric control systems — A survey. *Biomedical Signal Processing and Control*, 2(4):275–294.
- Paliwal, K., Wójcicki, K., and Schwerin, B. (2010). Single-channel speech enhancement using spectral subtraction in the short-time modulation domain. *Speech communication*, 52(5):450–475.

- Peng, L., Hou, Z., Chen, Y., Wang, W., Tong, L., and Li, P. (2013). Combined use of sEMG and accelerometer in hand motion classification considering forearm rotation. In *Engineering in Medicine and Biology Society (EMBC), 2013 35th Annual International Conference of the IEEE*, pages 4227–4230. IEEE.
- Phinyomark, A., Limsakul, C., and Phukpattaranont, P. (2009a). A comparative study of wavelet denoising for multifunction myoelectric control. In *2009 International Conference on Computer and Automation Engineering*, pages 21–25. IEEE.
- Phinyomark, A., Limsakul, C., and Phukpattaranont, P. (2009b). EMG denoising estimation based on adaptive wavelet thresholding for multifunction myoelectric control. In *2009 Innovative Technologies in Intelligent Systems and Industrial Applications*, pages 171–176. IEEE.
- Phinyomark, A., Limsakul, C., and Phukpattaranont, P. (2009c). A novel feature extraction for robust EMG pattern recognition. *arXiv preprint arXiv:0912.3973*.
- Phinyomark, A., Limsakul, C., and Phukpattaranont, P. (2009d). An optimal wavelet function based on wavelet denoising for multifunction myoelectric control. In *Electrical Engineering/Electronics, Computer, Telecommunications and Information Technology, 2009. ECTI-CON 2009. 6th International Conference on*, volume 2, pages 1098–1101. Ieee.
- Phinyomark, A., Phothisonothai, M., Limsakul, C., and Phukpattaranont, P. (2010). Effect of trends on detrended fluctuation analysis for surface electromyography (EMG) signal. In *Proceedings of 8th PSU-engineering conference*, pages 333–338.
- Phinyomark, A., Phukpattaranont, P., and Limsakul, C. (2011). Wavelet-based denoising algorithm for robust EMG pattern recognition. *Fluctuation and Noise Letters*, 10(02):157–167.
- Phinyomark, A., Phukpattaranont, P., and Limsakul, C. (2012a). Feature reduction and selection for EMG signal classification. *Expert Systems with Applications*, 39(8):7420–7431.
- Phinyomark, A., Phukpattaranont, P., and Limsakul, C. (2012b). Fractal analysis

- features for weak and single-channel upper-limb EMG signals. *Expert Systems with Applications*, 39(12):11156–11163.
- Phinyomark, A., Phukpattaranont, P., and Limsakul, C. (2012c). The usefulness of wavelet transform to reduce noise in the sEMG signal. In *EMG methods for evaluating muscle and nerve function*, pages 107–132. InTech.
- Phinyomark, A., Quaine, F., Charbonnier, S., Serviere, C., Tarpin-Bernard, F., and Laurillau, Y. (2013). EMG feature evaluation for improving myoelectric pattern recognition robustness. *Expert Systems with Applications*, 40(12):4832–4840.
- Popov, B. (1965). The bio-electrically controlled prosthesis. *J Bone Joint Surg Br*, 47:421–424.
- Powar, O. S. and Chemmangat, K. (2017). Feature selection for myoelectric pattern recognition using two channel surface electromyography signals. In *Region 10 Conference, TENCON 2017-2017 IEEE*, pages 1022–1026. IEEE.
- Powar, O. S., Chemmangat, K., and Figarado, S. (2018). A novel pre-processing procedure for enhanced feature extraction and characterization of electromyogram signals. *Biomedical Signal Processing and Control*, 42:277–286.
- Quinlan, R. (1993). *C4.5: Programs for Machine Learning*. Morgan Kaufmann Publishers, San Mateo, CA.
- Reaz, M. B. I., Hussain, M., and Mohd-Yasin, F. (2006). Techniques of EMG signal analysis: detection, processing, classification and applications. *Biological procedures online*, 8(1):11.
- Ren, X., Yan, Z., Wang, Z., and Hu, X. (2006). Noise reduction based on ICA decomposition and wavelet transform for the extraction of motor unit action potentials. *Journal of neuroscience methods*, 158(2):313–322.
- Roche, A. D., Rehbaum, H., Farina, D., and Aszmann, O. C. (2014). Prosthetic myoelectric control strategies: a clinical perspective. *Current Surgery Reports*, 2(3):44.
- Roman-Liu, D. and Bartuzi, P. (2013). The influence of wrist posture on the time and frequency EMG signal measures of forearm muscles. *Gait & posture*, 37(3):340–344.

- Roussel, J., Ravier, P., Haritopoulos, M., Farina, D., and Buttelli, O. (2017). Decomposition of multi-channel intramuscular EMG signals by cyclostationary-based blind source separation. *IEEE Transactions on Neural Systems and Rehabilitation Engineering*, 25(11):2035–2045.
- Sahu, A., Sagar, R., Sarkar, S., and Sagar, S. (2016). Psychological effects of amputation: A review of studies from india. *Industrial psychiatry journal*, 25(1):4.
- Scheme, E. and Englehart, K. (2011). Electromyogram pattern recognition for control of powered upper-limb prostheses: state of the art and challenges for clinical use. *Journal of Rehabilitation Research & Development*, 48(6).
- Scheme, E., Fougner, A., Stavadahl, Ø., Chan, A. D., and Englehart, K. (2010). Examining the adverse effects of limb position on pattern recognition based myoelectric control. In *Engineering in Medicine and Biology Society (EMBC), 2010 Annual International Conference of the IEEE*, pages 6337–6340. IEEE.
- Senin, P. (2008). Dynamic time warping algorithm review. *Information and Computer Science Department University of Hawaii at Manoa Honolulu, USA*, 855:1–23.
- Shahid, S. (2004). *Higher order statistics techniques applied to EMG signal analysis and characterization*. PhD thesis, University of Limerick.
- Shenoy, P., Miller, K. J., Crawford, B., and Rao, R. P. (2008). Online electromyographic control of a robotic prosthesis. *IEEE Transactions on Biomedical Engineering*, 55(3):1128–1135.
- Shin, S., Tafreshi, R., and Langari, R. (2016). Robustness of using dynamic motions and template matching to the limb position effect in myoelectric classification. *Journal of Dynamic Systems, Measurement, and Control*, 138(11):111009.
- Shokrollahi, M., Krishnan, S., Jewell, D., and Murray, B. (2009). Autoregressive and cepstral analysis of electromyogram in rapid movement sleep. In *World Congress on Medical Physics and Biomedical Engineering, September 7-12, 2009, Munich, Germany*, pages 1580–1583. Springer.
- Smith, L. H., Hargrove, L. J., Lock, B. A., and Kuiken, T. A. (2011). Determining the optimal window length for pattern recognition-based myoelectric control:

- balancing the competing effects of classification error and controller delay. *IEEE Transactions on Neural Systems and Rehabilitation Engineering*, 19(2):186–192.
- Staudenmann, D., Roeleveld, K., Stegeman, D. F., and Van Dieën, J. H. (2010). Methodological aspects of sEMG recordings for force estimation—a tutorial and review. *Journal of electromyography and kinesiology*, 20(3):375–387.
- Su, Y., Fisher, M. H., Wolczowski, A., Bell, G. D., Burn, D. J., and Gao, R. X. (2007). Towards an EMG-controlled prosthetic hand using a 3-d electromagnetic positioning system. *IEEE transactions on instrumentation and measurement*, 56(1):178–186.
- Subasi, A. and Kiyimik, M. K. (2010). Muscle fatigue detection in EMG using time–frequency methods, ica and neural networks. *Journal of medical systems*, 34(4):777–785.
- Tkach, D., Huang, H., and Kuiken, T. A. (2010). Study of stability of time-domain features for electromyographic pattern recognition. *Journal of neuroengineering and rehabilitation*, 7(1):21.
- Triolo, R. and Moskowitz, G. (1985). A multichannel time series myoprocessor for robust classification of limb function and estimation of muscle force. In *IEEE Transactions on Biomedical Engineering*, volume 32, pages 875–875. IEEE.
- Vial, J., Noçairi, H., Sassiati, P., Mallipatu, S., Cognon, G., Thiébaud, D., Teillet, B., and Rutledge, D. N. (2009). Combination of dynamic time warping and multivariate analysis for the comparison of comprehensive two-dimensional gas chromatograms: application to plant extracts. *Journal of Chromatography A*, 1216(14):2866–2872.
- Viswanathan, V. and Kumpatla, S. (2011). Pattern and causes of amputation in diabetic patients—a multicentric study from india. *J Assoc Physicians India*, 59(3):148–51.
- Vuskovic, M. and Du, S. (2005). Spectral moments for feature extraction from temporal signals. *International Journal of Information Technology*, 11(10):112–122.
- Weihe, W. (1999). In memoriam reinhold reiter-17 november 1920-24 september 1998.

- Westerink, J. H., Van Den Broek, E. L., Schut, M. H., Van Herk, J., and Tuinenbreijer, K. (2008). Computing emotion awareness through galvanic skin response and facial electromyography. In *Probing experience*, pages 149–162. Springer.
- Wiggins, R. A. (1978). Minimum entropy deconvolution. *Geoexploration*, 16(1-2):21–35.
- Willigenburg, N. W., Daffertshofer, A., Kingma, I., and Van Dieën, J. H. (2012). Removing ECG contamination from EMG recordings: A comparison of ICA-based and other filtering procedures. *Journal of electromyography and kinesiology*, 22(3):485–493.
- Xing, Z., Pei, J., and Keogh, E. (2010). A brief survey on sequence classification. *ACM Sigkdd Explorations Newsletter*, 12(1):40–48.
- Xue, B., Zhang, M., and Browne, W. N. (2013). Particle swarm optimization for feature selection in classification: A multi-objective approach. *IEEE transactions on cybernetics*, 43(6):1656–1671.
- Yana, K., Marushima, H., Mine, H., and Takeuchi, N. (1989). Bispectral analysis of filtered impulse processes with applications to the analysis of bioelectric phenomena. In *Workshop on Higher-Order Spectral Analysis*, pages 140–145. IEEE.
- Yang, D., Yang, W., Huang, Q., and Liu, H. (2017). Classification of multiple finger motions during dynamic upper limb movements. *IEEE journal of biomedical and health informatics*, 21(1):134–141.
- Yang, Z., Chen, Y., Tang, Z., and Wang, J. (2016). Surface EMG based handgrip force predictions using gene expression programming. *Neurocomputing*, 207:568–579.
- Yang, Z., Wu, Q., and Fu, S. (2014). Spectral analysis of surface EMG based on empirical mode decomposition. *Optik-International Journal for Light and Electron Optics*, 125(23):7045–7052.
- Young, A. J., Hargrove, L. J., and Kuiken, T. A. (2012). Improving myoelectric pattern recognition robustness to electrode shift by changing interelectrode distance and electrode configuration. *IEEE Transactions on Biomedical Engineering*, 59(3):645–652.

Zhang, X. and Zhou, P. (2012). Sample entropy analysis of surface emg for improved muscle activity onset detection against spurious background spikes. *Journal of Electromyography and Kinesiology*, 22(6):901–907.

Zhang, X. and Zhou, P. (2013). Filtering of surface EMG using ensemble empirical mode decomposition. *Medical engineering & physics*, 35(4):537–542.

PUBLICATIONS BASED ON THE RESEARCH WORK

Papers in refereed journals

1. **Omkar S Powar**, Krishnan Chemmangat, and Sheron Figarado., “A novel pre-processing procedure for enhanced feature extraction and characterization of electromyogram signals.”, *Biomedical Signal Processing and Control*,42 (2018): 277-286. [Publisher: Elsevier]
2. **Omkar S Powar**, and Krishnan Chemmangat., “Dynamic time warping for reducing the effect of force variation on myoelectric control of hand prostheses.”, *Journal of Electromyography and Kinesiology*,48 (2019): 152-160. [Publisher: Elsevier]
3. **Omkar S Powar**, and Krishnan Chemmangat., “Reducing the effect of wrist variation on pattern recognition of Myoelectric Hand Prostheses Control through Dynamic Time Warping.”, *Biomedical Signal Processing and Control*,55 (2020): 101626. [Publisher: Elsevier]

Papers published in referred conference proceedings

1. **Omkar S Powar**, and Krishnan Chemmangat., “Feature selection for myoelectric pattern recognition using two channel surface electromyography signals.” in Proc. *TENCON 2017-2017 IEEE Region 10 Conference. IEEE, 2017., 1022-1026.*
2. **Omkar S Powar**, and Krishnan Chemmangat., “Comparison of Pre-Processing Filters on the Performance of sEMG based Pattern Recognition.” in Proc. *International Conference on Power Electronics Applications and Technology in Present Energy Scenario (PETPES), Mangalore, India, 2019., 1-6.*

Bio-data

Name : Omkar S Powar

Date of birth: 04-07-1991

Marital status: Unmarried

E-mail: omkarpowar1991@gmail.com

Mobile: +91-8762114870

Address

Ganesh Kripa, 1N-34-3074,

Ashoknagar, Mangalore, 575006 , India.

Education

- **M.Tech.**, Energy Management and Climate Change Technology, Jain University , Bengaluru, Karnataka, 2015.
- **B.E.**, Electrical & Electronics Engineering, Canara Engineering College, Mangalore, Karnataka, 2013.